PL-TR-95-2154

# SEISMIC STUDIES OF THE CASPIAN BASIN AND SURROUNDING REGIONS

Keith Priestley
Stephen Mangino

University of Cambridge
Department of Earth Sciences
Madingley Rise, Madingley Road
Cambridge CB3 OEZ
UNITED KINGDOM



14 November 1995



Final Report
15 September 1993-14 November 1995

Approved for Public Release; Distribution Unlimited

PHILLIPS LABORATORY
Directorate of Geophysics
AIR FORCE MATERIEL COMMAND
HANSCOM AFB, MA 01731-3010

This technical report has been reviewed and is approved for publication.

JAMES F. LEWKOWICZ
Contract Manager

JAMES F. LEWKOWICZ, Director
Earth Sciences Division

This report has been reviewed by the ESC Public Affairs Office (PA) and is releasable to the National Technical Information Service (NTIS).

Qualified requestors may obtain additional copies from the Defense Technical Information Center. All others should apply to the National Technical Information Service.

If your address has changed, or if you wish to be removed from the mailing list, or if the addressee is no longer employed by your organization, please notify PL/TSI, 29 Randolph Road, Hanscom AFB, MA 01731-3010. This will assist us in maintaining a current mailing list.

Do not return copies of this report unless contractual obligations or notices on a specific document requires that it be returned.

# REPORT DOCUMENTATION PAGE

*Form Approved*
*OMB No 0704-0188*



**1. AGENCY USE ONLY** *(Leave blank)*

**2. REPORT DATE**
14 NOVEMBER 1995

**3. REPORT TYPE AND DATES COVERED**
FINAL REPORT(15 Sep 93-14 Nov 95)

**4. TITLE AND SUBTITLE**
SEISMIC STUDIES OF THE CASPIAN BASIN AND SURROUNDING REGIONS

**5. FUNDING NUMBERS**
PE 61102F
PR2309 TA G2 WU BM
Contract F49620-92-J-0475

**6. AUTHOR(S)**
KEITH PRIESTLEY
STEPHEN MANGINO

**7. PERFORMING ORGANIZATION NAME(S) AND ADDRESS(ES)**
University of Cambridge
Department of Earth Sciences
Madingley Rise, Madingley Road
Cambridge CB3 OEZ, UNITED KINGDOM

**8. PERFORMING ORGANIZATION REPORT NUMBER**

**9. SPONSORING/MONITORING AGENCY NAME(S) AND ADDRESS(ES)**
Phillips Laboratory
29 Randolph Road
Hanscom AFB, MA 01731-3010
Contract Manager: James Lewkowicz/GPEH

**10. SPONSORING/MONITORING AGENCY REPORT NUMBER**
PL-TR-95-2154

**11. SUPPLEMENTARY NOTES**

**12a. DISTRIBUTION/AVAILABILITY STATEMENT**
APPROVED FOR PUBLIC RELEASE DISTRIBUTION UNLIMITED

**12b. DISTRIBUTION CODE**

**13. ABSTRACT** *(Maximum 200 words)*

In order to investigate the anomalous crust and upper mantle structure of the south Caspian Basin, we installed a network of six three-component seismograph stations within the countries of Turkmenistan and Azerbaijan. Improved knowledge of the crust and upper mantle structure of the south Caspian Basin is important in a seismic verification context because of the anomalous effect it has on regional seismic waveforms. Our objective is to determine the velocity structure of this region using both body wave receiver function and surface wave modeling techniques. We present receiver function inversion results for four sites and fundamental mode Rayleigh wave observations for two great circle paths across this region. Also presented are results of a study of Russian deep seismic sounding data from a nuclear source recorded along a 2600km long profile in Siberia. This analysis supports the earlier observation that the 410km discontinunity beneath the Siberian Platform consists of a velocity increase over a 35km depth.

**14. SUBJECT TERMS**
Seismic studies
Caspian Basin
Upper mantle structure
Surface wave modeling techniques

**15. NUMBER OF PAGES**
84

**16. PRICE CODE**

| 17. SECURITY CLASSIFICATION OF REPORT | 18. SECURITY CLASSIFICATION OF THIS PAGE | 19. SECURITY CLASSIFICATION OF ABSTRACT | 20. LIMITATION OF ABSTRACT |
|---|---|---|---|
| unclassified | unclassified | unclassified | SAR |

# CONTENTS

## VELOCITY STRUCTURE OF UPPER MANTLE TRANSITION ZONES BENEATH CENTRAL EURASIA FROM SEISMIC INVERSION USING GENETIC ALGORITHMS

VELOCITY STRUCTURE IN THE REGION OF THE SOUTH CASPIAN BASIN FROM TELESEISMIC RECEIVER FUNCTION MODELING

## Velocity Structure of Upper Mantle Transition Zones beneath Central Eurasia from Seismic Inversion using Genetic Algorithms

Fernando A. Neves, Satish C. Singh and Keith F. Priestley

Bullard Laboratories, Madingley Rise, Madingley Road, Cambridge CB3 0EZ, UK

SUMMARY

We present velocity constraints for the upper mantle transition zones beneath Central Siberia based on observations of the 1982 "RIFT" Deep Seismic Sounding (DSS) profile. The data consist of seismic recordings of a nuclear explosion in northwestern Siberia along a 2600–km long seismic profile extending from the Yamal Peninsula to Lake Baikal. We invert seismic data from the mantle transition zones using a non–linear inversion scheme using a genetic algorithm for optimization and the WKBJ method to compute the synthetic seismograms. A statistical error analysis using a graph–binning technique was performed to provide uncertainty in the velocity models.

Our best model for the upper mantle velocity discontinuity near 410 km depth has a two–stage velocity gradient structure with velocities increasing from 8.65 to 9.30 km/s over a depth range of 400–415 km, a gradient of 0.043 $s^{-1}$, and from 9.30 to 9.65 km/s over a depth range of 415–435 km, a gradient of 0.0175 $s^{-1}$. This derived model is consistent with other seismological observations and mineral physics models. The model for the velocity discontinuity near 660 km depth is simple, sharp and includes velocities increasing from 10.10 km/s at 655 km depth to 10.65 km/s at 660 km depth, a gradient of 0.055 $s^{-1}$.

Key words: mantle transition zones, seismic inversion, genetic algorithm.

## INTRODUCTION

The size and sharpness of the 410–km and 660–km seismic discontinuities provide important constraints in assessing petrological models of upper mantle phase changes and chemical layering. Laboratory studies (Ito & Takahashi, 1989) suggest that the velocity discontinuity at 410 km depth corresponds to a phase change over 20 km from peridotite to $\beta$–spinel structure. This result contradicts seismological studies of P'P' precursors (Lees et al. 1983;

Benz & Vidale, 1993) that suggest a simple and sharp 410–km discontinuity. The velocity discontinuity at 660 km depth corresponds to a phase change over 5 km from $\delta$–spinel to perivoskite and magnesiowustite (Helffrich & Bina, 1994). Benz & Vidale (1993) have shown that the short–period frequency content of reflections from the 660–km discontinuity is sharp, corresponding to transition zones of 4 km or less.

Most of the previous seismic studies of the upper mantle transition zones have used low–frequency body wave or surface wave data, which results in poor resolution. Furthermore, a number of different source signatures are used in earthquake body wave studies, requiring a comparison of different waveforms or solving for the earthquake source, both resulting in possible ambiguities between velocities and earthquake source mechanism. Several recent upper mantle studies are based on very long refraction profiles in Asia (Mechie et al., 1993; Cipar et al., 1993; Priestley et al., 1994). The one–dimensional (1–D) model for the latter study, derived from travel–time forward modeling techniques and amplitude matching using reflectivity synthetic seismograms, has a 35–km thick transition zone (8.64–9.45 km/s) at 410 km depth and 4–km thick (10.25–10.62 km/s) at 660 km depth. As pointed out by Priestley et al. (1994) there is a clear evidence from the recorded section that lateral heterogeneity exists in the upper mantle along the profile.

In order to present seismic velocity models of upper mantle discontinuities that provide quantitative constraints on the petrology, error estimates on the velocity are necessary. Previous studies have used forward modeling techniques which give insight into the velocity structure, but they offer only qualitative estimates of the uncertainties associated with the velocity model features. Since the objective function which describes the goodness of fit between observed and synthetic seismograms is highly non–linear, a linear inversion scheme can provide neither a unique solution nor an error estimate. In this study we have used a non–linear global inversion scheme that can provide a statistical error analysis and model resolution. By obtaining the smallest structural details that are statistically resolvable, an inversion–derived velocity model can help discriminate between alternative seismic interpretations.

## NON–LINEAR GLOBAL INVERSION

Seismic inversion schemes consist of three steps: forward modeling, evaluation of an

objective function and optimization of the objective function. The main objective of an inversion analysis is to find a "best" model that explains the observations. The forward modeling is achieved by efficiently solving the wave equation. The objective function is a measure of goodness between data and synthetic seismograms. Depending upon the nature of the objective function, a local (linear) or a global (non–linear) method of optimization is used. Linearized methods of optimization depend strongly on the starting model, and hence are prone to being either trapped in local optima or becoming unstable. As a result, these methods fail if the initial model is too far from the most likely model. In addition, they may require derivative of the objective function, and the computation of, which could be difficult and costly. A non–linear global optimization avoids nearly all of the limitations of the linear methods. For instance, by using an initial population of many randomly chosen velocity models, one does not require a starting velocity model. Instead of trying to find a "best" model that explains the observations, the global methods search for a family of velocity models which explain the data to a desired level of confidence. It is also possible to quantify the degree of confidence on each of the final estimated velocity models. Non–linear global inversion methods are attractive for problems where efficient forward modeling schemes are available.

Misfit Function

There are many measures of goodness of fit, and the choice of a specific one depends on the problem and the kind of data being analyzed. In general, a least–squares misfit between the data and synthetic seismograms should be used. However due to the absence of true amplitude information in the data that are analyzed here, we have used the semblance functional $E(\mathbf{m})$ defined as (Landa et al., 1989)

$$E(\mathbf{m}) = \sum_{k=0}^{K} \frac{\left\{\sum_j U_j[kdt + \tau(\mathbf{m})]\right\}^2}{\sum_j \left\{U_j[kdt + \tau(\mathbf{m})]\right\}^2} \tag{1}$$

where $U_j$ represents the seismic trace for the $j^{th}$ receiver, $\tau$ is the traveltime calculated by raytracing through the model $\mathbf{m}$, $dt$ is the time sampling interval and $Kdt$ is the time window

for semblance calculation. Our goal is to find the model $\mathbf{m}$ which maximises the semblance functional $E(\mathbf{m})$ calculated for all seismic traces in a time window along the traveltime trajectory defined by a forward modeling scheme. A time window length of 2 s (K=20) was used for the analysis.

Our choice of the semblance function was motivated primarily to avoid traveltime picking of the data. This is important since the seismic phases we are analyzing are secondary arrivals and hence of low signal–to–noise ratio. Furthermore, since the true amplitude information on the data was not available, we could not use a norm based on the full wavefield.

In order to perform a global search, which is computationally time consuming when compared to local search methods, we need a fast forward modeling scheme. The WKBJ synthetic seismogram method (Chapman, 1978) provides such a solution. We have used the WKBJ seismogram algorithm extended to laterally inhomogeneous media using the Maslov asymptotic theory (Chapman & Drummond, 1982) as a 2–D forward modeling technique. For the traveltime calculation we have applied a dynamic raytracing algorithm, where non–geometrical signals caused by inhomogeneities in the Earth are modeled. This algorithm is an extension of geometrical ray theory and agrees with geometrical ray theory for high–frequency direct and turning rays (Chapman et al., 1988). The Maslov algorithm was chosen because it is a fast and accurate 2–D forward modeling scheme to evaluate the objective function for a large number of models. We have adopted the 2–D raytracing scheme in order to take into account propagation effects generated by lateral heterogeneities within the crust and upper mantle.

## Genetic Algorithms

The objective function $E(\mathbf{m})$ generally has many peaks and the methods based on local optimization often fail to find the largest value of the objective function if the starting model is not close enough to the final model. To avoid this problem, a global method, Genetic Algorithm (GA), is used. The GA works with a group of $M$ velocity models simultaneously, each represented by a bit–string (Goldberg, 1989). The initial search space for each velocity is divided into $2n$ parts described by $n$ bits. The initial population of $M$ velocity models is generated randomly within each velocity bound.

At each iteration the GA essentially consists of three operations (Fig. 1) : selection, crossover and mutation.

*Selection*: From the initial population of $M$-bit strings, an interim population of $M$ parents is generated by selecting models from the original group with likelihood of selection determined by a probability depending on the objective function. The probability of selecting the $k^{th}$ velocity model is written as (Sambridge & Drijkoningen, 1992)

$$P(\mathbf{m}_k) = \left[\sum_{j=1}^{M} \exp(BE_j)\right]^{-1} \exp(BE(\mathbf{m}_k)) \tag{2}$$

where $B = (E_\sigma)^{-1}$. $E_\sigma$ is the standard deviation of the objective function $E(\mathbf{m}_k)$ ($k = 1, ..., M$) within the population that is being evaluated by GA. $E_j$ ($j = 1, ..., M$) is the current value of the objective function $E(\mathbf{m}_k)$. Note in Fig. 1 that model 1 with the highest objective function was selected twice, model 2 and 3 once, model 4 with the lowest objective function was rejected.

*Crossover*: From the parent population of $M$-bit strings a new generation of $M$-strings is generated, each of which is obtained by mixing bit-strings from two parents. All the $M$ parents are randomly paired to produce $M/2$ couples. A probability for performing this step is assigned. The value designated for this probability is chosen by preliminary tests on the data. If this probability is greater than a generated random number between 0 and 1, then the current pair is to be crossed over. The location where the strings are cut is also determined randomly. Our GA algorithm uses a single-point crossover, with the cut position restricted to occur only at velocity boundaries (Fig. 1).

*Mutation*: This final process allows any bit in an individual string to flip between 0 and 1. The main goal of this process is to add some degree of local diversity (since only individual bits are affected) into the whole inversion process. Therefore, no genetic feature is permanently lost, something that would reduce the model space. A mutation probability (usually rather low) is used to control the likelihood of this process.

A Posteriori Probability Density (PPD) is assigned to each evaluated model, which is defined as (Basu & Frazer, 1990) :

$$\Psi(\mathbf{m}) = \frac{\exp(E(\mathbf{m})/\sigma)}{\sum \exp(E(\mathbf{m})/\sigma)} \tag{3}$$

where $E(\mathbf{m})$ is the semblance (objective) function value for model $\mathbf{m}$ and $\sigma$ is the variance in $E(\mathbf{m})$ for all the models sampled by the GA. Here we have assumed that the data are statistically independent. The square root of variance is a measure of uncertainty or standard error of the estimated parameter. The denominator $\sum \exp(E(\mathbf{m})/\sigma$ is summed and evaluated at the end of all the runs and is used to normalize the PPD. Since it is impossible to plot the PPD in the $M$–dimensional model space, we have used the graph–binning technique proposed by Frazer & Basu (1990) where each model parameter was assigned the model's PPD and summed into model parameter bins. Nolte & Frazer (1994) argue that there is no theoretical basis for using GA to compute the PPD. However, we agree with Stoffa & Sen (1991) that many independent GA runs with different initial populations followed by a graph–binning technique can provide an estimate of the PPD.

## APPLICATION TO DATA

### The Siberian RIFT Profile

During the past 30 years, the Soviet Ministry of Geology (now the Center of Regional Geophysical and Geological Research) has conducted an extensive seismic exploration program of the Eurasian crust and upper mantle. Many of these profiles used nuclear explosions as seismic sources for recording long–range profiles (up to 4000 km) and chemical explosives for recording short–range (up to 750 km) profiles ( Scheimer & Borg, 1984; Benz et al., 1992). Analysis of these data by Russian seismologists has largely been by forward modeling of the travel time data. Recently, data from several of these profiles have been analyzed by forward modeling of the waveform data (Cipar et al. 1993; Priestley et al. 1994).

The 1982 RIFT profile extends 2600 km across the Siberian platform from the Yamal Peninsula to Lake Baikal (Fig. 2). Seismic data were recorded from three nuclear explosions and thirty–four chemical explosions along this profile. The northernmost shot point (SP245) is located within the West Siberian rift on the northwest edge of the Siberian platform.

This aborted rift is buried beneath approximately 15 km of sediments (Cipar et al., 1993). The central section of the profile extends across the Tunguska basin (site of SP173), a region of widespread intraplate flood basalts. The southern portion of the profile crosses the presently active Baikal rift (site of SP35); this rift occurs within a recent regional uplift and is characterized by high heat flow and a low velocity upper mantle (Belousov et al. 1991).

We analyze the data from SP245 in this study. SP245 was located at 69.206°N 81.647°E, had a body wave magnitude of mb = 5.2, and was recorded in a SE–direction to a distance of 2400 km (Fig. 2). Analysis of the seismograms from the chemical explosions along this profile provides detailed crust and uppermost mantle velocity structure (Fig. 4) (Pavlenkova, personal communication).

SP245 was recorded at 182 sites, each equipped with three–component seismometers and a Taiga seismic recording system, (Chichinin et al., 1969). We analyze only the vertical component data in this study. The seismometers have a natural frequency of 1.5 Hz, and the recording system has a usable bandwidth between 0.5 and 20 Hz. The station locations are accurate to 0.1 km, which is lower than the accuracy of station locations for most modern crustal refraction studies. However, the source–receiver distances are much more accurate than in most mantle studies using earthquake data because the source location is accurately known. These data were commercially digitized and corrected for amplitude scaling to produce trace normalized record sections (Cipar et al., 1993). The seismic section for SP245 is shown in Fig. 3.

The nature of the wave field from these data have been discussed by Priestley et al. (1994). Crustal arrivals are prominent at short offsets, especially the crustal (Pg) phase. The uppermost mantle refracted arrival (Pn) is observed as a first arrival starting at a distance of $\sim$ 150 km. The Pn arrival is observed to about 600 km but has variable amplitude. Since this amplitude variation can be correlated over large distances, it is likely to be due to variations in the lithospheric structure. The upper mantle velocity is about 8.2 km/s (Priestley et al., 1994). In this study we concentrate our effort on reflected/refracted arrivals from the upper mantle transition zones. The phase from the 410–km discontinuity is a clear secondary arrival beginning at about 1600 km and 15 s reduced time with a reduction velocity of 8.2 km/s, and becomes the first arrival at about 2200 km. The phase from the 660–km discontinuity

starts at about 2100 km range and 13 s reduced time.

## Initial Models

Since we are interested in the details of the velocity discontinuities at 410 km and 660 km depths, we allow the velocity model to vary only in the vicinity of these zones and fix the model elsewhere. For the crust we include the 2–D velocity model determined from a study of refraction data recorded from the chemical explosions along the "RIFT" profile (Pavlenkova, personal communication). This crustal model is very complex, so instead of using this model for the crust, we have used a smoothed version (Fig. 4) of it. The smoothed crustal velocity model still contains significant lateral velocity variations which generate differential time delays at different ranges. These will certainly affect the depth and thickness estimates of mantle features. It is therefore important to use a 2–D raytracing technique for the crustal part of the profile. However, having only one line and one shot available, it is impossible to resolve lateral variations in upper mantle structures. Thus, we have used a hybrid method consisting of 2–D raytracing for the crust and a 1–D inversion scheme for the upper mantle transition zones. The 1–D upper mantle velocity model used in this study (Fig. 5, thin line) was derived by Priestley et al. (1994).

## Model Parameterization

The velocity model in the vicinity of the transition zone was parameterized as a function of depth V(z) at various node points with linear interpolation applied between the node points. This implies that velocity gradient is parameterized. The separation between nodes was determined by the dominant frequency content of the seismic data. The dominant frequency of the P–waves for the upper mantle arrivals is around 1.5 Hz, giving a resolution of 4–5 km. Therefore, we have parameterized the velocity model for the region with velocity nodes every 5 km. The structure in the vicinity of the 410–km discontinuity was parameterized by 8 nodes equally spaced at 5 km and in the vicinity of the 660–km discontinuity by 4 nodes. This was based on the maximum resolution of 5 km provided by the data and also by the maximum thickness of the transition zones given by previous studies (Priestley et al. 1994). Thus we restrict the thickness of the 410–km transition zone to be less than 35 km and the thickness

of the 660–km transition to be less than 15 km.

Inversion

The inversion was run for 200 iterations with an initial population of 50 models, and with probabilities of crossover and mutation equal to 0.6 and 0.05, respectively. These values were obtained from preliminary tests on the data and must be tuned for each particular problem or data set. This tuning represents an unsatisfactory aspect of the GA method (Sambridge & Drijkoningen, 1992). The initial population of models was chosen randomly within the velocity range defined from the model–T. The velocity range was defined as $V_T \pm 0.5$ km/s, where $V_T$ is the velocity of model–T. The velocity deviation in this range is greater than a typical accuracy of ± 0.1–0.2 km/s provided by a ordinary wide–angle seismological survey. A positive velocity gradient constraint was imposed to avoid the presence of low velocity zones.

The evaluation of the semblance functional (eq. (1)) requires knowledge of neither the source wavelet nor the instrument response. However, we have used the source function described in Evernden et al. (1986) to calculate the synthetic seismograms so that the synthetic seismograms can be visually compared to the data. Evernden et al. (1986) present an empirically determined formula for the far field amplitude spectrum generated by explosions. The attenuation model used in computing the synthetics seismograms was taken from Der et al. (1986) as used by Priestley et al. (1994). Due to the long extent of the seismic line (2400 km) we have also applied the Earth flattening transformation described by Chapman (1973). The final inversion results for the velocity model for the 410–km and 660–km discontinuities are shown in Figs. 6a and 7a, respectively. In order to evaluate the effect of the 2–D crustal velocity model and upper mantle velocity model on our final models, a 1–D crustal velocity model and a smoothed version of model–T (Fig. 5, thick line) were considered. The resulting velocity models for the 410–km and 660–km discontinuities with a 1–D crustal velocity model and a smoothed version of model–T are shown in Figs. 6a and 7a, respectively.

Merely fitting the data by an inversion scheme method is not sufficient for estimating model parameters; measurement of resolution and uncertainty are required. Therefore, we have evaluated the binned PPD function, where we have assumed a constant travel–time variance of $\sigma = 0.5$ s for all models. The binary coding requires that the number of velocity

intervals for each node is an integral power of two. Thus, during the GA optimization procedure we set a fixed velocity interval $\Delta V = 0.1$ km/s, which is within the expected accuracy. In Figs. 6b and 7b we have also plotted the PPD's (dashed lines), calculated using eq. (3), at each node depth point.

In Figs. 6b and 7b, we show the data (solid curve) and the synthetics for the final model (dashed curve) for the arrivals from the 410–km and 660–km discontinuities, respectively. Figure 6c shows the data (solid curve) and the synthetic waveforms for our "best–fit" preferred model, a two–step gradient (dotted–dashed curve), a simple (one step) gradient (dotted curve) and a simple sharp discontinuity (dashed curve), for the 410–km discontinuity for stations located at 1803 km and 1982 km away from SP245. In order to quantify the goodness of fit between observed and synthetic seismograms, we have used the misfit function $\phi(j)$ defined as

$$\phi(j) = \frac{\sum_{t=t_0}^{t_0 + Kdt} |U_{\mathrm{obs}}(j,t) - U_{\mathrm{syn}}(j,t)|^2}{\sum_{t=t_0}^{t_0 + Kdt} (U_{\mathrm{obs}}(j,t))^2} \qquad (4)$$

where $U_{\mathrm{obs}}(j,t)$ are the observed data, $U_{\mathrm{syn}}(j,t)$ are the synthetic seismograms for station $j$, and $t$ is the time. The computation of $\phi(j)$ is done within a time window $Kdt$ starting from the traveltime $t_0$ estimated from the inversion. For the 410–km discontinuity (Fig. 6(c)) the values of $\phi$(j=1803 km) for the sharp, one–step gradient and two–step are 0.33, 0.19 and 0.11, respectively. The values of $\phi$(j=1982 km) for the sharp, one–step gradient and two–step gradient are 0.38, 0.24 and 0.16, respectively. At both locations, the misfit is the lowest for the two–step gradient model.

## DISCUSSION

The synthetic seismograms obtained from our final velocity models for the 410–km and 660–km discontinuities adequately fit the general features of the observed data. Our model for the transition zone near 410 km depth (Fig. 6a) consists of a two–stage velocity gradient. This model has produced the best–fit (Fig. 6c). The first stage extends from 400 to 415 km depth with P–wave velocity increasing from 8.70 to 9.25 km/s with a high velocity gradient

of 0.0433 $s^{-1}$. The second stage extends from 415 to 435 km depth with P–wave velocity increasing from 9.25 to 9.60 km/s and a low velocity gradient of 0.0175 $s^{-1}$. The PPD's curves clearly show this bimodal velocity structure, which suggests that long period seismic data are more (or may be only) sensitive to this first step gradient, where there is a greater velocity variation at around 415 km depth. This may explain observations of Benz & Vidale (1993). In a mineral physics context, this would imply that the transformation from olivine to $\beta$–spinel is not linear in the 410–km transition zone, and it is faster for the first 15 km. For mineral physics models, a thickness of 35 km might be postulated when the transformation from olivine to $\beta$–spinel has taken place completely (Ita & Stixrude, 1992).

Although our model and the model–T for the 410–km discontinuity shows the same shape (two–step velocity gradient), our velocity model is faster (up to 0.2 km/s). However, Priestley et al. (1994) have adopted a broad transition region for the 410–km discontinuity.

The PPD plot in Fig. 6b shows clearly that model–T might result from a secondary optimum. With error analysis used here, we can distinguish various possible models.

Our model for the 660–km discontinuity (Fig. 7a) is consistent with previous seismological models, such as the model–T. We estimate this transition zone as 5 km thick over the depth range 655–660 km, with velocity ranging from 10.15 and 10.70 km/s and have a velocity gradient of 0.055 $s^{-1}$. The PPD plots are more complex than the one from Fig. 6b, which could be due to low signal–to–noise ratio for these later arrivals. It should be noted that we have assumed a 1–D model in the upper mantle although the earth is truly 3–D. For low frequency waves this is a good approximation, but this limits our power of spatial depth and lateral resolution, which means that lateral heterogeneity can be mapped into a 1–D velocity model (Kennett & Bowman, 1990). This may explain some small discrepancies between the data and synthetic seismograms.

## CONCLUSIONS

The main points of this study are :

(1) Our proposed inversion method approach which combines 2–D forward modeling with dynamic raytracing for the crust and 1–D inversion for the upper mantle is relevant. The

error–analysis using a graph–binning technique has shown the existence of local optima where solutions associated with previous velocity models derived from forward modeling schemes might get trapped.

(2) We presented a 1–D compressional velocity model for the 410–km and 660–km upper mantle discontinuities beneath the Siberian Platform that is derived from non–linear global inversion applied to the deep seismic data recorded along the RIFT profile. However, we still consider this a preliminary model since we have analyzed data from only one shot point of the RIFT profile.

The major features of our model are : (a) a two–stage velocity gradient for the transition zone near the 410 km depth. The first one is a high velocity gradient zone ranging from 400 to 415 km depth and the second one is a low velocity gradient zone ranging from 415 to 435 km depth, (b) a simple and narrow high gradient zone between 655 and 660 km depth.

(3) We also suggest that the phase transformation from olivine to $\beta$–spinel is not linear for the shallower transition zone, which in turn generates the two–step velocity gradient pattern observed for this region. This result is independently confirmed by Stixrude (1995)

REFERENCES


Basu, A. & Frazer, L. N., 1990. Rapid determination of the critical temperature in simulated annealing inversion, Science, 249, 1409–1412.

Belousov, B., Pavlenkova, N. I. & Kvyatkovskaya, G. N., 1991. Crustal structure of the territory of the USSR (in Russian), Nauka, Moscow.

Benz, H. M. & Vidale, J. E., 1993. Sharpness of upper–mantle discontinuities determined from high–frequency reflections, Nature, 365, 147–150.

Benz, H. M., Unger, J. D., Leith, W. S., Mooney, W. D., Solodilov, L., Egorkin, A. V. & Ryaboy, V. Z., 1992. Deep seismic sounding in Northern Eurasia, EOS, Trans. Am. geophys. Un., 73, 297–300.

Chapman, C. H., 1973. The Earth flattening transformation in body wave theory, Geophys.

J. R. astr. Soc., 35, 55–70.

Chapman, C. H., 1978. A new method for computing synthetic seismograms, Geophys. J. R. astr. Soc., 54, 481–518.

Chapman, C. H. & Drummond, R., 1982. Body wave seismograms in inhomogeneous media using Maslov asymptotic theory, Bull. seism. Soc. Am., 72, 277–317.

Chapman, C. H., Jen–Yi, C. & Lyness, D. G., 1988. The WKBJ seismogram algorithm, In Seismological Algorithms: Computational Methods and Computer programs, 47–74; Academic Press Ltd., London.

Chichinin, I. S., Yegorov, G. V., Yemelianov, A. V. & Bochanov, A. J., 1969. Portable Telemonitored Seismic Equipment Taiga, Methods of Seismic Research, 95–119; Nauka, Moscow.

Cipar, J. J., Priestley, K. F., Egorkin, A. V. & Pavlenkova, N. I., 1993. The Yamal Peninsula–Lake Baikal deep seismic sounding profile, Geophys. Res. Lett., 20, 1631–1634.

Der, Z., Lees, A. & Cormier, V., 1986. Frequency dependence of Q in the upper mantle underlying the shield areas of Eurasia, Part III: The Q model, Geophys. J. R. astr. Soc., 87, 1103–1112.

Evernden, J. F., Archambeau, C. B. & Cranswick, E., 1986. An evaluation of seismic decoupling and underground nuclear test monitoring using high–frequency seismic data, Rev. Geophysics, 24, 143–215.

Frazer, L. N. & Basu, A., 1990. Freeze–bath inversion, 60th Ann. Internat. Mtg., Soc. Expl. Geophys., Expanded Abstracts, 1123–1125.

Goldberg, D. E., 1989. Genetic Algorithms in Search, Optimization and Machine Learning, Addison–Wesley, Reading, MA.

Helffrich, G. & Bina, C. R., 1994. Frequency dependence of the visibility and depths of mantle seismic discontinuities, Geophys. Res. Lett., 24, 2613–2616.

Ita, J. & Stixrude, L., 1992. Petrology, elasticity, and composition of the mantle transition

zone, J. geophys. Res., 97, 6849–6866.

Ito, E. & Takahashi, E., 1989. Postspinel transformations in the system Mg2SiO4–Fe2SiO4 and some geophysical implications, J. geophys. Res., 94, 10637–10646.

Kennett, B. L. N. & Bowman, J. R., 1990. The velocity structure and heterogeneity of the upper mantle, Phys. Earth planet. Inter., 59, 134–144.

Lees, A. C., Bukowinski, M. S. T. & Jeanloz, R. J., 1983. Reflection properties of phase transition and compositional change models of the 670–km discontinuity, J. geophys. Res., 88, 8145–8159.

Landa, E., Beydoun, W. & Tarantola, A., 1989. Reference velocity model estimation from prestack waveforms : coherency optimization by simulated annealing, Geophysics, 54, 984–990.

Nolte, B. & Frazer, L. N., 1994. Vertical seismic profile inversion with genetic algorithms, Geophys. J. Int., 117, 162–178.

Mechie, J., Egorkin, A. V., Fuchs, K., Ryberg, T., Solodilov, L. & Wenzel, F., 1993. P–wave mantle velocity structure beneath northern Eurasia from long–range recordings along the profile Quartz, Phys. Earth planet. Inter., 33, 180–193.

Priestley, K. F., Cipar, J. J., Egorkin, A. V. & Pavlenkova, N.I., 1994. Upper–mantle velocity structure beneath the Siberian platform, Geophys. J. Int., 108, 369–378.

Sambridge, M. & Drijkoningen G., 1992. Genetic algorithms in seismic waveform inversion, Geophys. J. Int., 109, 323–342.

Scheimer, J. F. & Borg, I. Y., 1984. Deep seismic sounding with nuclear explosives in the Soviet Union, Science, 226, 787–792.

Stixrude, L., 1995. Mantle composition and structure of mantle discontinuities, IUGG XXI General Assembly, Abstract, B383.

Figure Captions

Figure 1. A schematic illustration of the operators employed by the genetic algorithm. The selection operator chooses the models from the initial population (in this example four models) with a probability of selection proportional to the maximum of the objective function ($E$). Model 1, with the highest $E$, was selected twice while model 4, with the lowest $E$, was rejected for the next generation. The crossover operator randomly chooses pairs of models and exchanges their portions (three parameter models in this example) at a point selected at random along the length of the model to produce two new off–spring. The mutation operator is shown operating on a single velocity of parameter 4. The colors represent different parameter values.

Figure 2. Simplified tectonic map of central Asia. The RIFT profile is the straight solid line and the large solid dots show the location of the nuclear explosion for the shot points 245, 173 and 35.

Figure 3. Recorded, unfiltered SP245 seismic section reduced at 8.2 km/s. The seismograms are trace normalized. The arrivals labeled are : (a) Pg, (b) Pn, (c) reflection/refraction from the 410–km discontinuity and (d) reflection/refraction from the 660–km discontinuity.

Figure 4. Smoothed 2–D crustal P–wave velocity model derived from chemical explosions along profile (Pavlenkova, personal communication). Numbers within the plot are velocities in km/s. Velocities vary linearly with distance and depth.

Figure 5. P–wave upper–mantle velocity–depth function (thin solid line) for SP245 model–T (Priestley et al., 1994). Thick solid line is a smoothed version of model–T.

Figure 6.(a) P–wave velocity–depth function for the 410–km discontinuity estimated from inversion with a 2–D crustal velocity structure (thick dark solid line), with a 1–D crustal velocity structure (thin solid line), with a smoothed model–T velocity structure (thick grey line) and model–T (dotted–dashed line). The crossed circles are the depth points where velocities were computed. The Posteriori Probability Density functions (PPDs) are shown by the dashed lines. (b) Comparison between synthetic seismograms (dashed

curve) filtered in the same frequency bandwidth and data (solid curve) for the 410–km discontinuity at reduced velocity of 8.2 km/s. The arrows show estimated traveltime from inversion and the dots those computed for model–T. (c) Comparison between data (solid curve) and the synthetic waveforms for a two–step gradient (dotted–dashed curve), a simple (one step) gradient (dotted curve) and a simple sharp discontinuity (dashed curve), for the 410–km discontinuity for the stations located at 1803 km and 1982 km away from SP245.

Figure 7. (a) P–wave velocity depth function for the 660–km discontinuity estimated from inversion with a 2–D crustal velocity structure (thick dark solid line), with a 1–D crustal velocity structure (thin solid line), with a smoothed model–T velocity structure (thick light solid line) and model–T (dotted–dashed line). The crossed circles are the depth points where velocities were computed. The Posteriori Probability Density functions (PPDs) are shown by the dashed lines.

(b) Comparison between synthetic seismograms (dashed curve) filtered in the same data frequency bandwidth and data (solid curve) for the 660–km discontinuity at reduced velocity of 8.2 km/s. The arrows show estimated traveltime from inversion and the dots those computed from model–T.

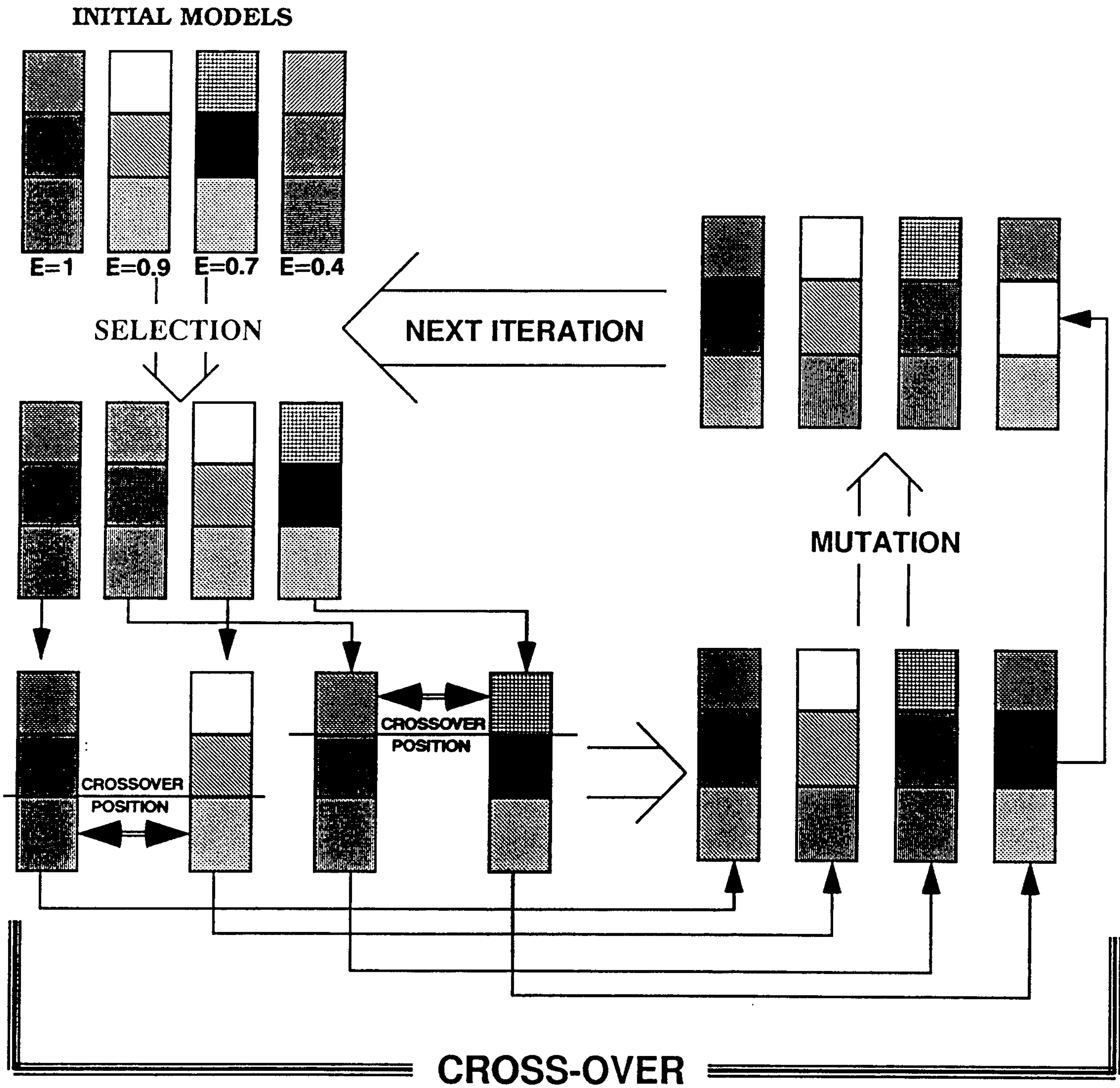
INITIAL MODELS
E=1
E=0.9
E=0.7
E=0.4
SELECTION
NEXT ITERATION
MUTATION
CROSSOVER
POSITION
CROSSOVER
POSITION
CROSS-OVER

FIGURE 1

FIGURE 2

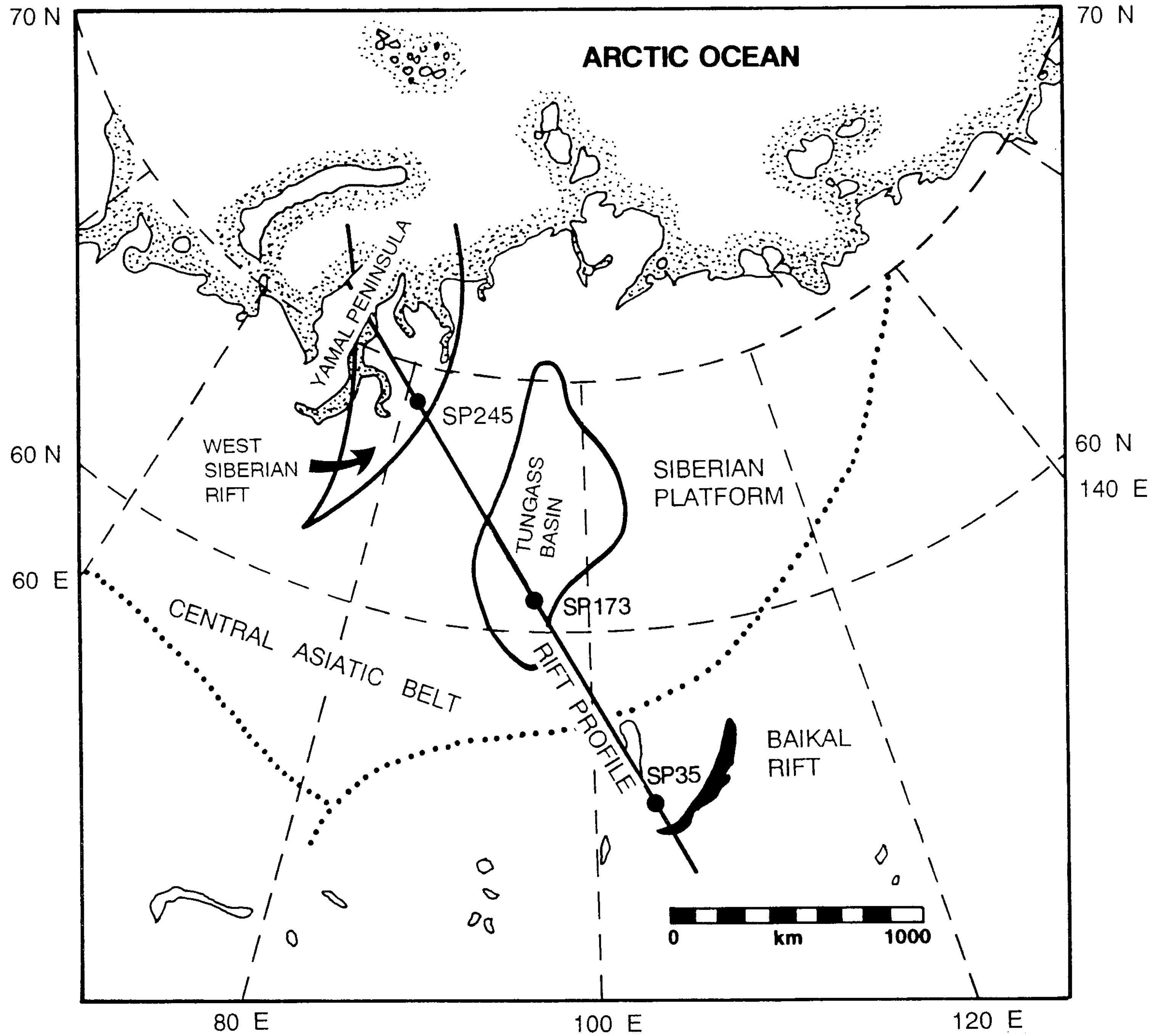
70 N
70 N
ARCTIC OCEAN
YAMAL PENINSULA
SP245
WEST
SIBERIAN
RIFT
60 N
60 N
140 E
60 E
TUNGASS
BASIN
SIBERIAN
PLATFORM
SP173
CENTRAL ASIATIC BELT
RIFT PROFILE
SP35
BAIKAL
RIFT
0
km
1000
80 E
100 E
120 E

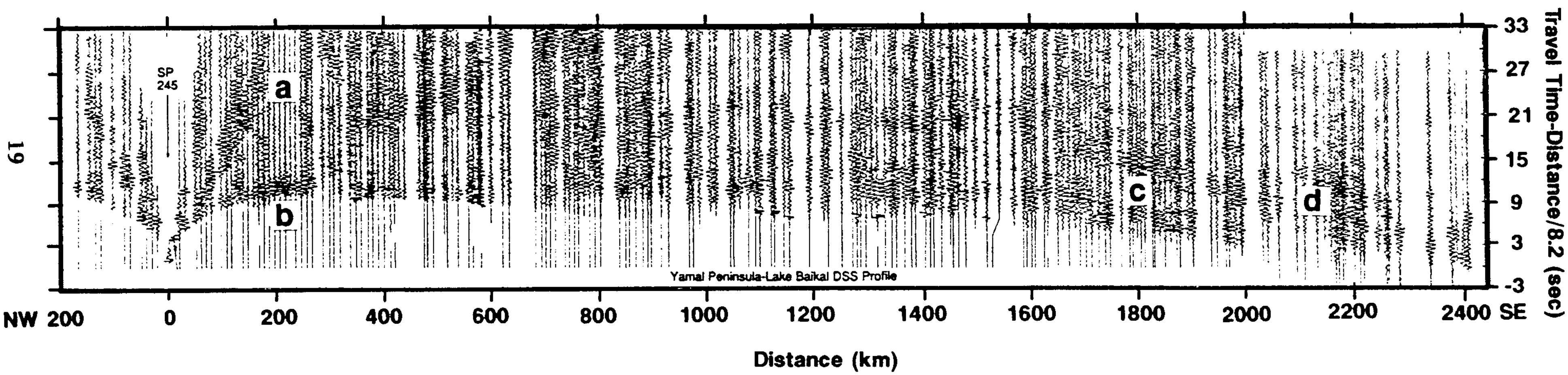
Travel Time-Distance/8.2 (sec)
33
27
21
15
9
3
-3
NW 200
0
200
400
600
800
1000
1200
1400
1600
1800
2000
2200
2400 SE
Distance (km)
SP
245
a
b
c
d
Yamal Peninsula-Lake Baikal DSS Profile

FIGURE 3

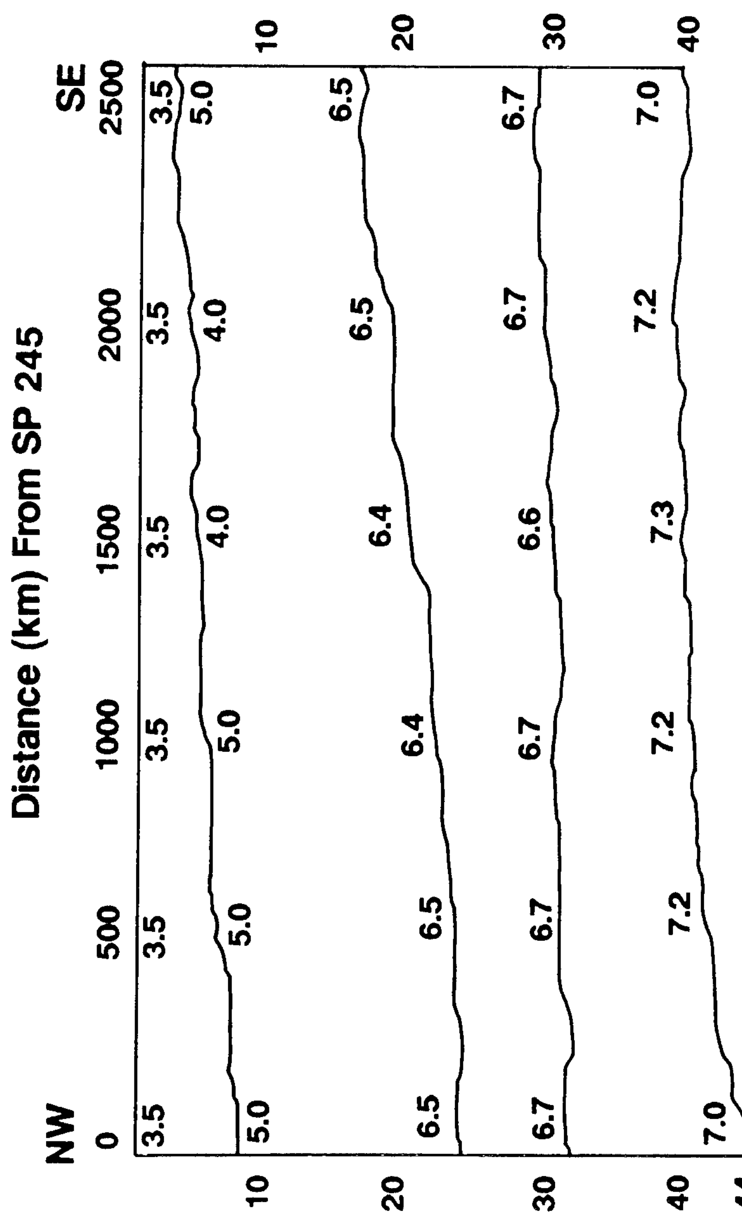
Distance (km) From SP 245
NW
SE
0
500
1000
1500
2000
2500
Depth (km)
10
20
30
40
44
3.5
5.0
4.0
6.5
6.4
6.7
6.6
7.0
7.2
7.3

FIGURE 4

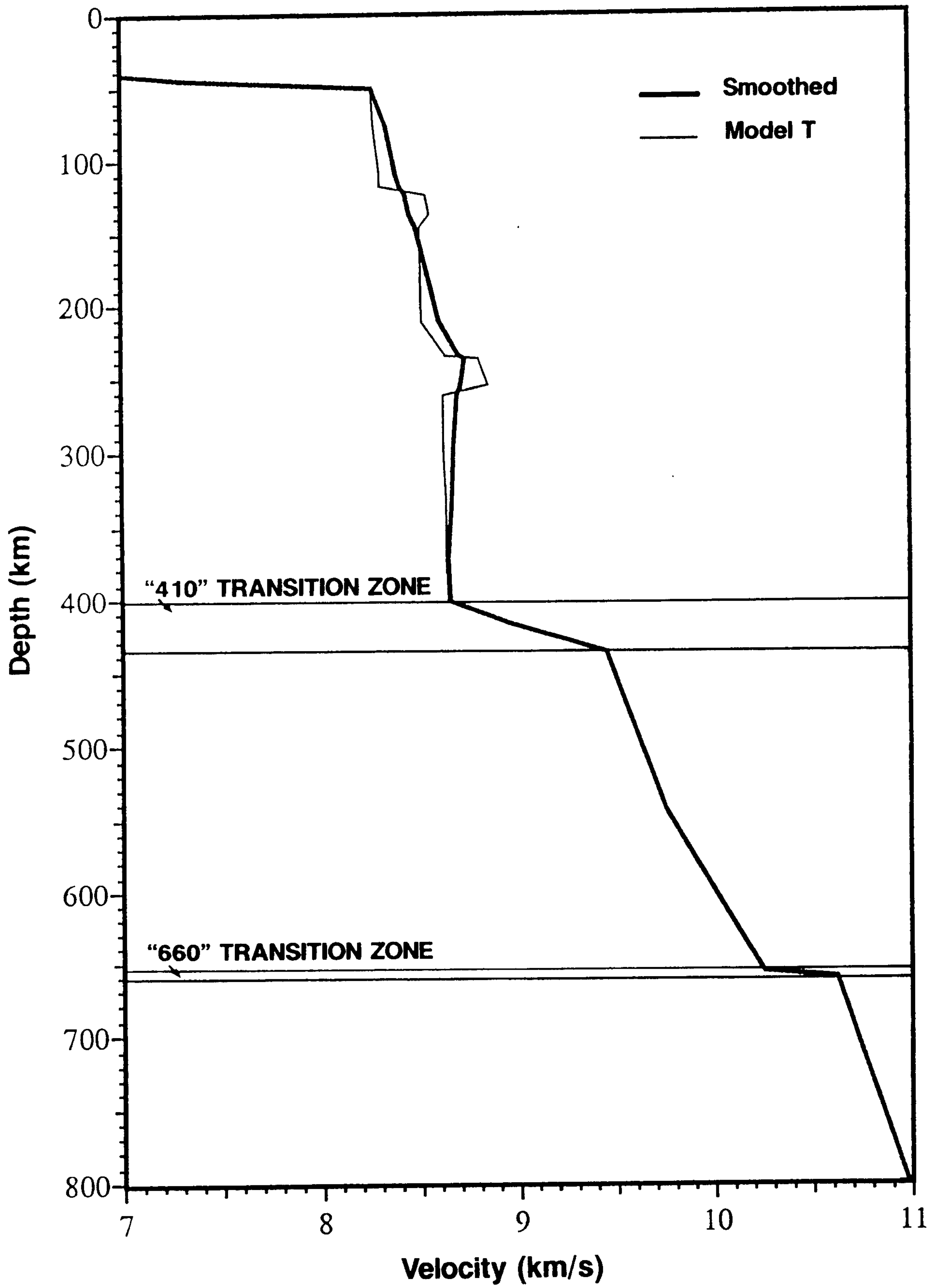
Smoothed
Model T
"410" TRANSITION ZONE
"660" TRANSITION ZONE
Depth (km)
Velocity (km/s)
0
100
200
300
400
500
600
700
800
7
8
9
10
11

FIGURE 5

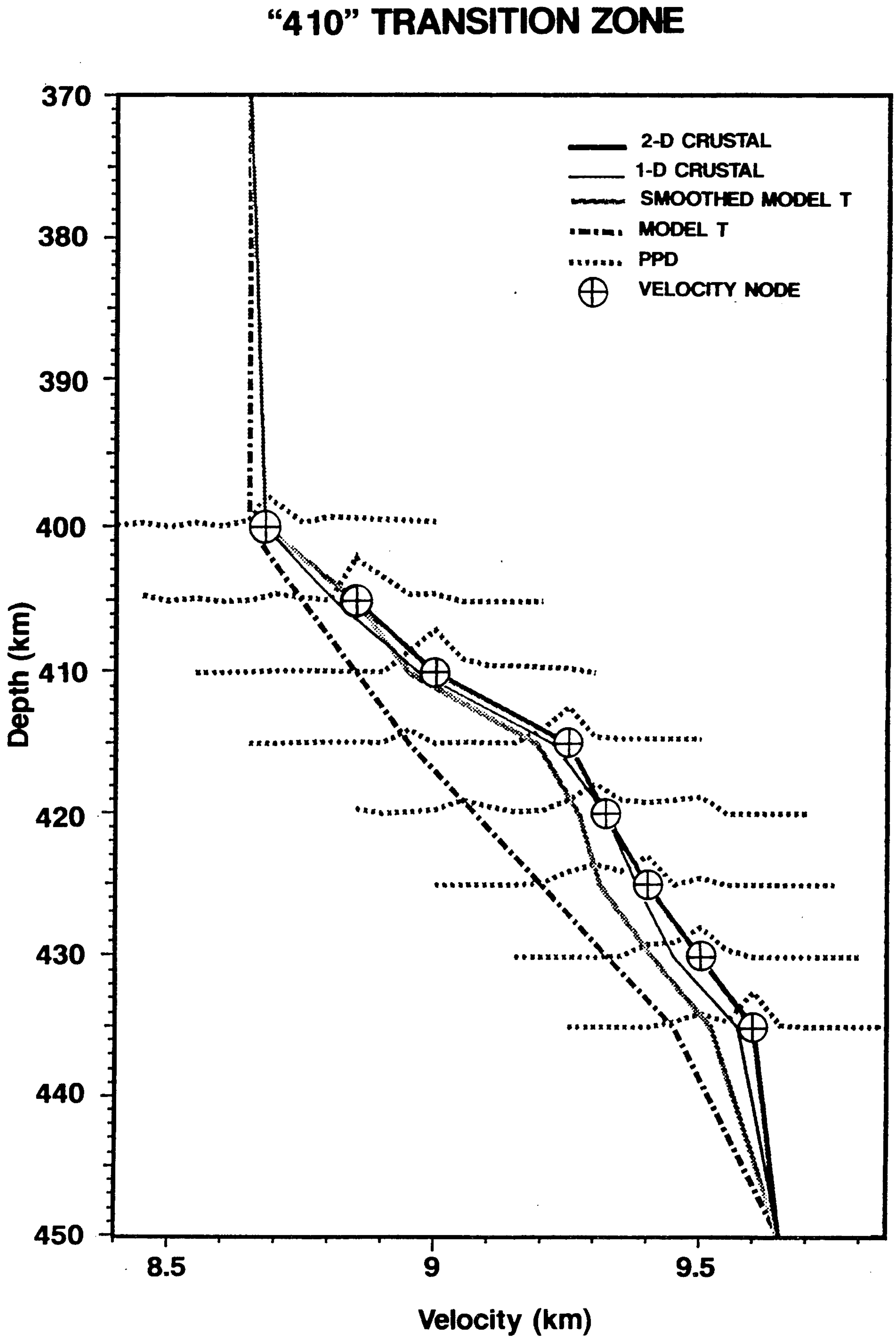
"410" TRANSITION ZONE
2-D CRUSTAL
1-D CRUSTAL
SMOOTHED MODEL T
MODEL T
PPD
VELOCITY NODE
Depth (km)
370
380
390
400
410
420
430
440
450
8.5
9
9.5
Velocity (km)

FIGURE 6a

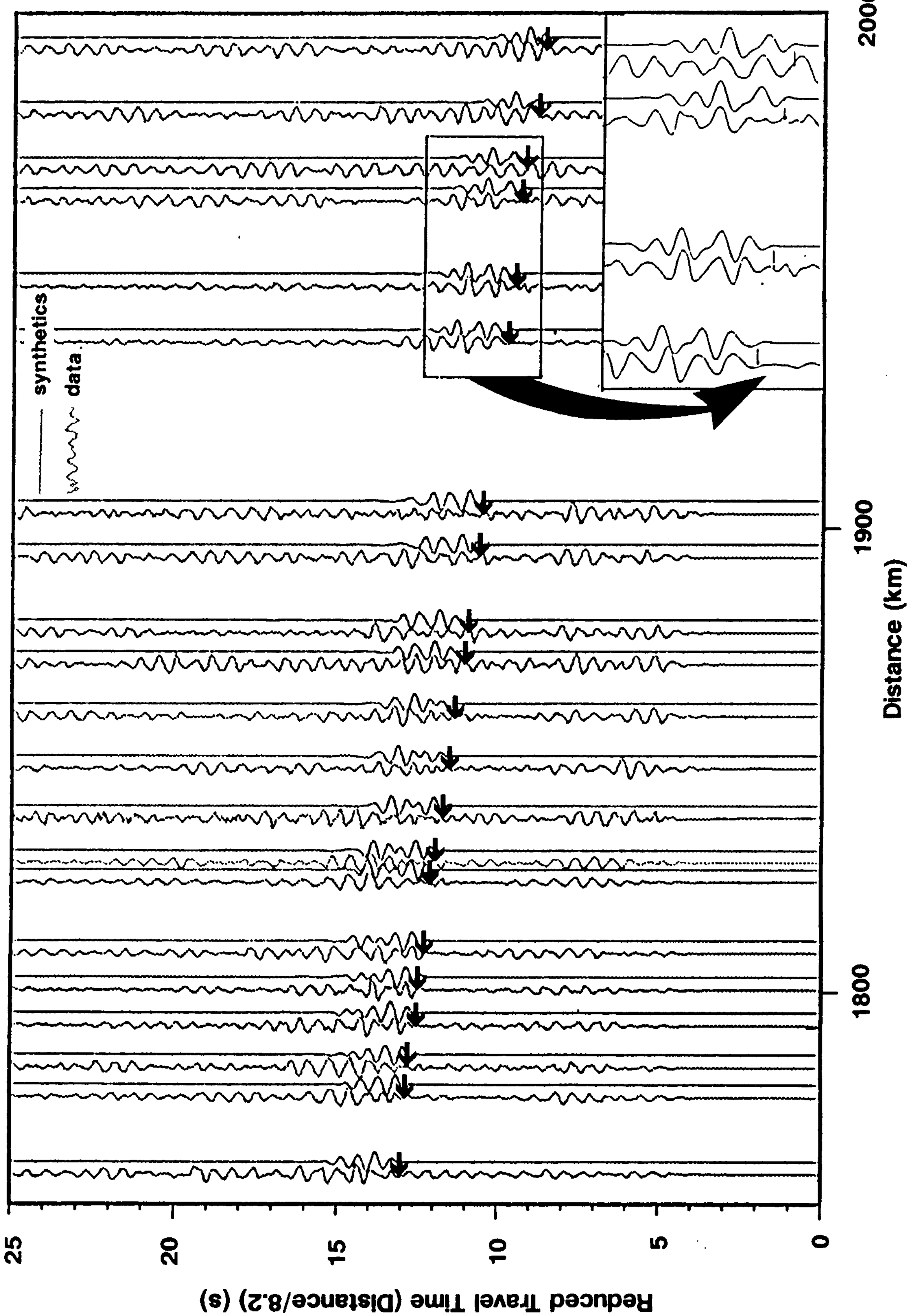
synthetics
data
25
20
15
10
5
0
Reduced Travel Time (Distance/8.2) (s)
1800
1900
2000
Distance (km)

FIGURE 6b

# 410 Km DISCONTINUITY

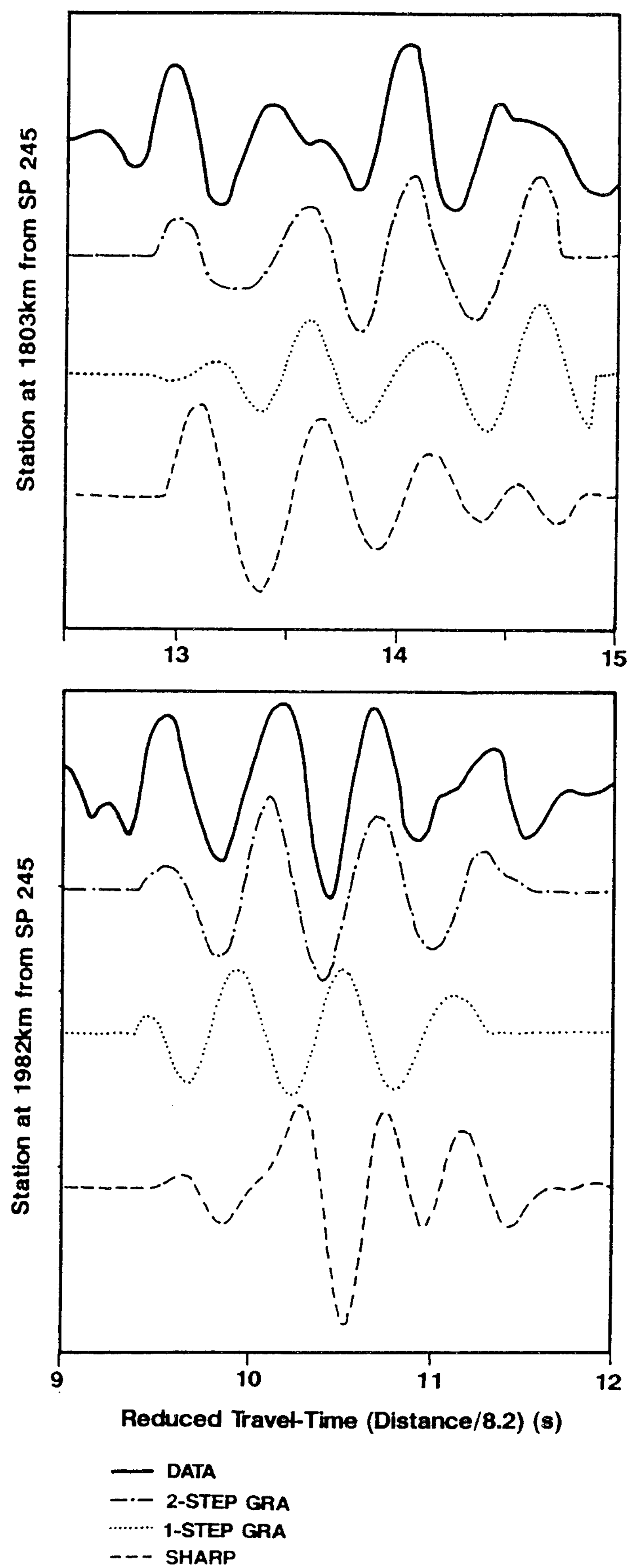


FIGURE 6c

# "660" TRANSITION ZONE

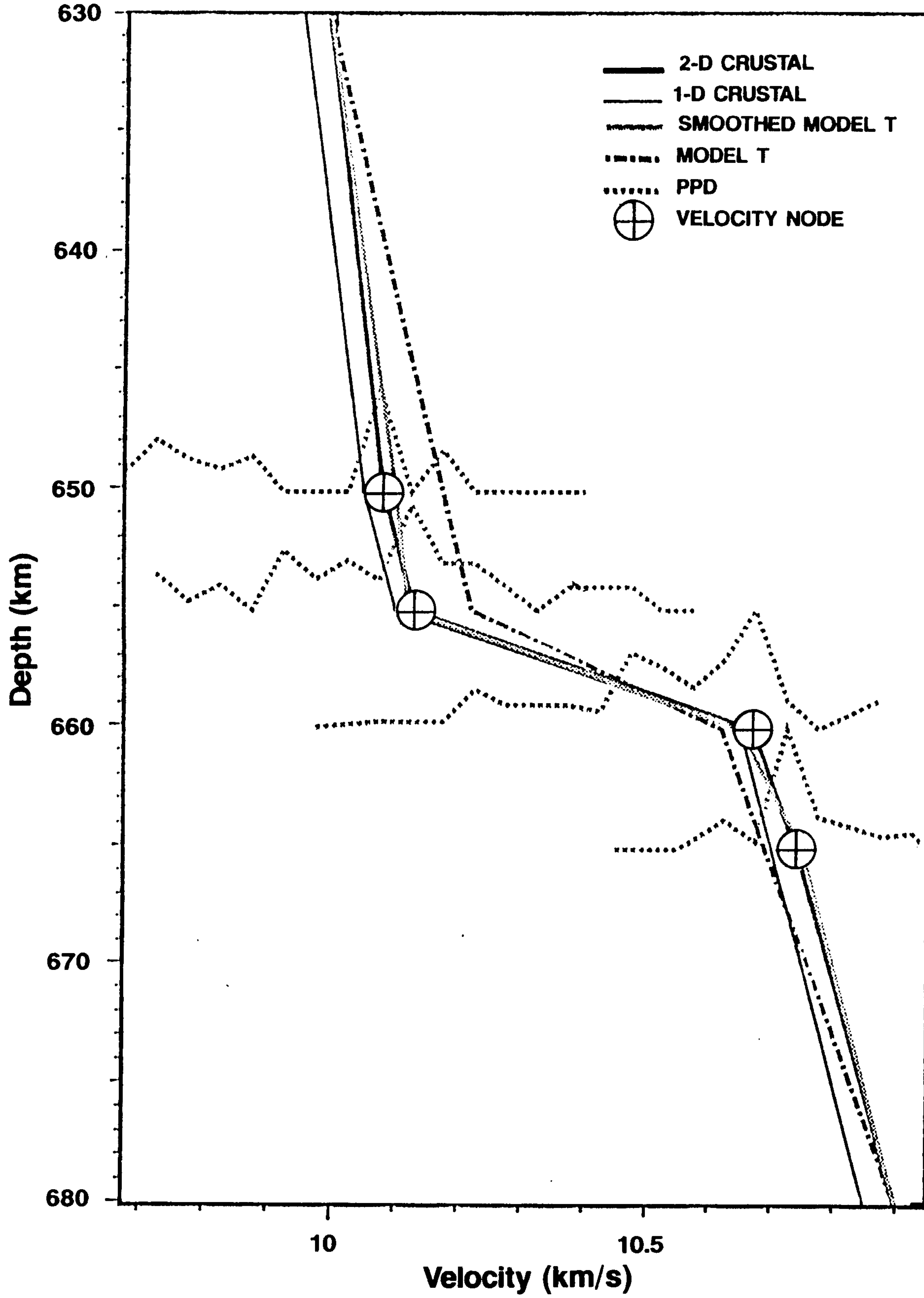


FIGURE 7a

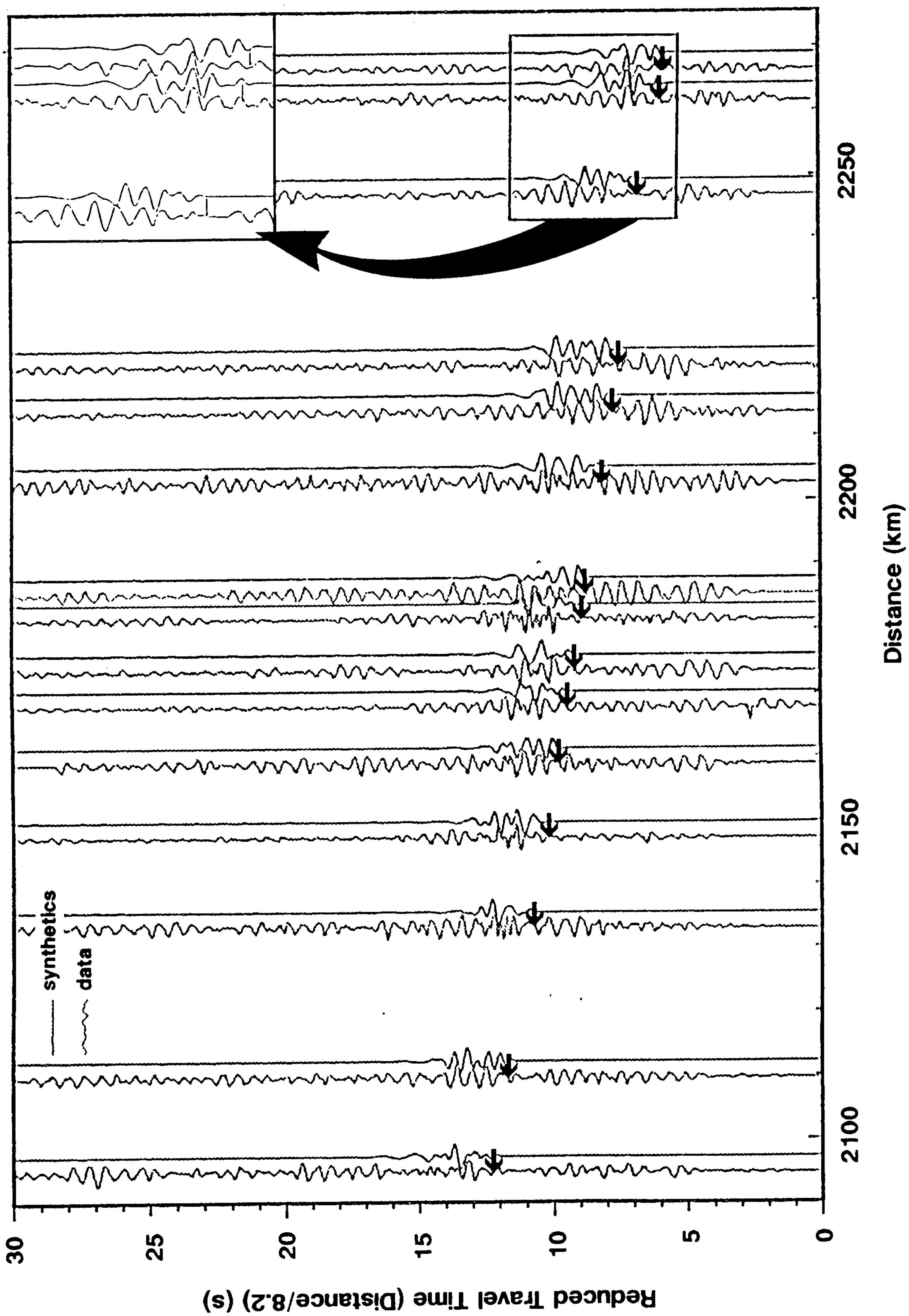
synthetics
data
Reduced Travel Time (Distance/8.2) (s)
0
5
10
15
20
25
30
2100
2150
2200
2250
Distance (km)

FIGURE 7b

# Velocity Structure in the Region of the South Caspian Basin from Teleseismic Receiver Function Modeling

Stephen Mangino and Keith Priestley

Bullard Laboratories, Madingley Rise, Madingley Road, Cambridge CB3 0EZ, UK

## SUMMARY

The crust and upper mantle structure of the south Caspian Basin and the Turkmenian Lowlands is enigmatic. From Soviet deep seismic sounding data collected in the 1960s, the crust appears to consist of two layers: a thick sedimentary section (15–25 km) with a low P–wave velocity (3.5–4.0 km/s) overlying a 12–18 km thick basaltic lower crust. It has been suggested that this basaltic lower crust is "oceanic–like" crust and that the south Caspian Basin represents a section of relic ocean from a Paleozoic – Triassic ocean or a Mesozoic – Paleogene marginal sea. Improved knowledge of the crust and upper mantle velocity structure of the south Caspian Basin is important in a seismic verification context because of the anomalous effect it has on regional seismic waveforms. To investigate the crust and upper mantle structure of the south Caspian Basin, we have installed six three–component seismograph stations within the former Soviet Republics of Turkmenia and Azerbaijan. Our objective is to determine the velocity structure of this region using both body wave receiver function and surface wave modeling techniques. We present receiver function inversion results for four sites and fundamental mode Rayleigh wave observations for two great circle paths across this region.

**Key Words**: South Caspian Basin, crust and upper mantle structure, receiver functions, surface wave dispersion

## INTRODUCTION

The south Caspian Basin and the Turkmenian Lowlands form an anomalous aseismic depression that is bounded to the north by the Apsheron–Balkhan Sill, a narrow seismogenic zone extending from the Caucasus Mountains in Azerbaijan to the Kopet Dagh Mountains of Turkmenia; and to the west in Azerbaijan and to the south along the Iranian border by the

active fold and thrust belts of the Talesh and Alborz Mountains, respectively. The northward movement of the Iranian plate with respect to the Eurasian plate is causing compressional deformation throughout the Caspian region (Jackson and McKenzie, 1984). Mechanisms of earthquakes occurring within the bounding seismic belts of the south Caspian Basin suggest that the crust of the south Caspian Basin is being overriden by the continental crust of the Iranian plateau in the south, and to a lesser extent, by the northern Caspian continental crust (Priestley et al, 1994).

The crust and upper mantle velocity structure of the south Caspian Basin is poorly known. Deep seismic sounding data collected in the early 1960s suggest that the crust of the south Caspian Basin and west Turkmenian Lowlands consists of two layers: a thick sedimentary layer (15–20 km) with a P–wave velocity of 3.5–4.0 km/s which overlies a 12–18 km thick "basaltic" layer with a P–wave velocity of 6.6–7.0 km/s (Neprochnov 1968; Rezanov and Chamo, 1969). It has been suggested that the south Caspian Basin represents a section of "ocean–like" crust that may be either a relic of an older Paleozoic–Triassic ocean or a marginal sea which developed behind a Mesozoic–Paleogene ocean (Berberian and King 1981; Berberian 1983). The south Caspian Basin strongly affects the propagation of regional seismic waves. For example, the seismic phase Lg is blocked for paths crossing the south Caspian Basin (Kadinsky–Cade et al, 1981). This has important ramifications for seismic monitoring in the Middle East.

To develop better velocity models for the crust and upper mantle for the south Caspian Basin and the surrounding region, we have installed and operated a network of digital three–component seismic stations in Turkmenia and Azerbaijan. In this report we present our preliminary results from the analysis of teleseismic P–wave: (1) travel time residuals, (2) P–wave azimuthal anomalies, and (3) velocity models of the crust and upper mantle from the analysis of receiver functions. We also discuss observations of fundamental mode Rayleigh waves for two great circle paths across this region.

## THE CASPIAN SEISMOGRAPH NETWORK

To better understand the crust and upper mantle structure in the south Caspian region and its effect on regional seismic wave propagation, we have installed a network of three–

component broadband digital seismographs around the south Caspian Sea in Turkmenia and Azerbaijan (Fig. 1). Not all stations have operated simultaneously. Five stations (BAK, KAT, KRV, LNK, and NBD) were installed in June, 1993. DTA was installed in December, 1993. BAK was found to be extremely noisy and was moved to SHE in June 1994. The highly unstable political climate in Azerbaijan due to war with Armenia coupled with the nearby fighting in Groznyy forced us to remove stations LNK and SHE in February, 1995. In June 1995 a new station was installed at KAR using the instruments previously deployed at LNK. Also shown in Figure 1 is the station ABKT which was installed in May, 1993 by the Incorporated Research Institutions for Seismology (IRIS).

Each of the Caspian Seismograph Network stations we operate consists of Refraction Technology 72a–02 16–bit data loggers with external hard disk drives and either Omega or GPS time code receivers. Stations DTA, KAR, KAT, KRV, and LNK have Guralp CMG–3T three–component broadband seismometers and stations BAK, NBD, and SHE have three–component Teledyne Geotech SL210/220 long period (15 sec free period) seismometers. Each seismograph was installed at a permanent seismograph site of either the Turkmenian Academy of Sciences or "Geoseism" (the equivalent Azerbaijan organization). The stations are permanently occupied by a station–keeper and family, which therefore contribute to the amount of noise generated at each site. All seismometers are installed on cement piers within vaults that are located either within a sub–basement or within a surface vault adjacent to the station keeper's house. To correct for seismometer drift we designed and installed a clock activated re–centering unit for each of the CMG–3T seismometers. This device issues a centering command to the CMG–3T at weekly intervals. The LP seismometers are manually re–centered by the station keeper. All stations record data continuously at 10 samples/sec. In addition, some stations have had a triggered data stream at 50 samples/sec. Every two months each stations' data is transferred from disk to either Exabyte or DAT tape and returned to the SYNAPSE Moscow Data Center (MDC). At the MDC an inspection of data quality is conducted and duplicate copies are made. The raw data files are then sent to the University of Cambridge, arriving between 5–8 months after initial collection. The IRIS station ABKT is equipped with Streckeisen STS–1 seismometers, a 24–bit Quantera digitizer, and a GPS clock. Data for ABKT is obtained from the IRIS Data Management Center in Seattle, Washington.

Parameters for each of these stations is given in Table 1.

We calibrate each station with a step function during each visit. More complete calibrations using a pseudo–random binary input and a sinusodial input are made on an annual basis. Analysis of the step calibrations indicate that the sensor characteristics have not deviated significantly during the deployment. Figure 2 shows the frequency response curves for the CMG–3T, the SL210/220, and STS–1 seismometers.

A catalogue of the recorded events recorded is given in Appendix 1.

## TELESEISMIC BODY WAVEFORM MODELING

To determine the velocity structure of the crust and upper mantle beneath the seismographs shown in Figure 1 we model the teleseismic P–waveform using receiver function analysis (Owens et al, 1984). However, before we apply the receiver function method we use other information contained within teleseismic P–wave to determine more gross properties of the crust and upper mantle structure beneath each site. We first determine P–wave travel time residuals for the stations in the immediate vicinity of the south Caspian Basin relative to IASP91 and station ABKT. We then estimate the affects of scattering by examining P–wave azimuth anomalies. Finally, we model the P–waveforms using the receiver function technique.

*P-wave Travel Time Residuals*: To determine relative differences in crust and upper mantle structure in the south Caspian region we computed absolute P–wave travel time residuals with respect to the IASP91 earth model and relative travel time residuals of the south Caspian Basin stations compared to station ABKT. The relative residual is defined as

$$\mathrm{T}_{\mathrm{resid}} = \left[\mathrm{T}_{\mathrm{CSN}} - \mathrm{T}_{\mathrm{IASP91(CSN)}}\right] - \left[\mathrm{T}_{\mathrm{ABKT}} - \mathrm{T}_{\mathrm{IASP91(ABKT)}}\right]$$

where $T_{CSN}$ is the arrival time at the CSN station, $T_{IASP91}$ is the predicted arrival time for the IASP91 model, and $T_{ABKT}$ is the observed arrival time at ABKT.

The observed residuals are plotted for each of the sites in Figures 3–5 and summarized in Table 2 and 3. Arrivals at all stations are late with respect to those predicted by the IASP91 earth model. Stations NBD and KAT, both located in the Turkmenian Lowlands, show mean delays of 0.9 sec with respect to ABKT. These large delays are likely due to

the thick sedimentary section in the south Caspian Basin. The KRV residuals are negative with respect to ABKT with a mean advance of -0.28 sec for events to the northeast and a mean advance of -0.70 sec for events to the southeast. The change of -0.5 sec occurs over a fairly narrow range at an azimuth of about N80°E. Negative residuals at KRV with respect to ABKT suggest either a faster mantle, a thinner crust, or a thinner sedimentary section beneath KRV compared to that beneath ABKT.

*P–wave azimuthal anomalies*: The frequency dependence of backazimuth anomalies and the polarization characteristics can be indicative of the level of scattering in the P–wavefield due to inhomogeneities in the crust and upper most mantle beneath the recording site. It is important to assess the level of scattering and its frequency dependence before attempting to extract information on the crust and upper mantle structure using the receiver function technique. We have measured the polarization using a technique discussed discussed in Kanasewich (1981) and implemented by Harris (1980). For this, the rectilinearity of the particle motion over a specified time window can be obtained from the ratio of the principal axes of the diagonalized covariance matrix from the three component time series. The degree of rectilinearity can be determined by comparing the relative magnitude of the two largest eigenvalues; and the direction of polarization can be determined by considering the components of the eigenvectors associated with the largest eigenvalue with respect to the coordinate directions (Fig. 6).

We use this procedure to examine the polarization of teleseismic P–waves in the 0.07–0.2 Hz and 0.3–2.0 Hz bands. Assuming an average crustal P–wave velocity of 6.4 km/s these bands correspond to wavelengths of about 96 to 32 km or crustal dimensions and about 21 to 3 km or subcrustal dimensions. Figure 7 shows an example of the measurement made on a teleseismic P–wave for the lower of these frequency bands, and the associated particle motion plots.

The results of the polarization analysis in the two frequency bands are shown in Figures 8–10 and summarized in Table 4. The results are complex however some conclusions can be drawn from these plots. With the exception of station KRV the differences between the low frequency observed and the theoretical backazimuths are small. However, the highpass backazimuth anomalies are large indicating significant scattering.

At ABKT the lowpass measurements are essentially on azimuth while a pattern is present at higher frequencies. Arrivals from teleseismic sources northeast of ABKT are deflected to the north while arrivals from the southeast are deflected to the south. The division between this frequency dependent scattering is roughly parallel to the trend of the Main Fault of the Kopet Dag Mountains. Although the bearing results at station DTA are sparse, this pattern is not present 200 km east of ABKT. At station KRV both the low and highpass bearings are inconsistent with the expected azimuth of arrival. The mean difference between the expected and observed azimuth of arrival is 17.5 degrees, counterclockwise about the station. These differences point to a mis–aligned seismometer. Stations NBD, KAT and LNK located within the Basin and all show significant scattering at higher frequencies while the lowpass bearings are variable.

*Receiver Functions*: We computed receiver function Caspian station we isolated the P to S converted phases in the 30 seconds following the P–wave arrival using the source equalization method (Langston, 1979; Ammon, 1991). Most of the source regions are along the Circum Pacific Seismogenic Zone, hence most of the receiver functions sample the lithosphere to the east of each station. Only the most stable deconvolutions (those with averaging functions that approximate a narrow band Gaussian pulse) are used to infer structure. Events from common source regions are then stacked and the variance of the stacked data is used as a measure of coherence of individual Ps arrivals. We examined the radial and tangential receiver functions as a function of azimuth and determined 1–D estimates of the receiver structure using the inversion method of Ammon et al. (1990).

Figure 11 presents the receiver function inversion results for the northeast backazimuth of CSN station KRV. The synthetic waveform fits are compared to the +/- 1 STD bounds obtained from the variance of the stacked data. Also shown are the stacked radial and tangential receiver functions and the range model space examined. We believe this range adequately covers most known rock types found in the earths crust. The KRV-NE radial receiver function is dominated by two Ps arrivals at 7s and 9.5s. These arrivals are well above the scattered wave field indicated by the amplitude of the tangential receiver function. Particle motion of these arrivals is consistent with P to S converted energy generated at a

near horizontal interface. Rotation of the KRV receiver functions by 17.5 degrees (the mean observed in the bearing analysis) yields a radial receiver function that does not significantly differ from the amplitude and phase of the unrotated data. The KRV-NE solution models indicate a 3-4 Km thick gradational shallow crust over a relatively constant upper crustal layer between 4-16 Km depth. A step in velocity of 1.5 Km/s is present between 16-18 Km. Beneath this step from 20 to 36 km depth the average P-wave velocity is between 6.5-7.0 km/s. From 36 to 46 km velocities range from 6.8-7.3 km/s. The crust-mantle boundary is gradational and velocities greater than 8 Km/s are first encountered at 52-54 Km depth.

Figure 12 presents a summary of the receiver function models obtained at the CSN stations and at station ABKT. Although these 1-D models represent only several data points across a complex region, some of the gross structural differences between the south Caspian Basin and adjacent Kopet Dag Mtns are clear. The models for stations KAT and LNK indicate the presence of a 10-12 km thick sedimentary layer in the upper crust. Both of these stations are located in the southern portion of the south Caspian Basin. The thickness of this layer is consistent with but less than the previously reported sedimentary thickness of 15-25 Km. It is important to note that our stations are located along the perimeter of the Basin and the previous DSS estimates are for the center of the Basin. Beneath the sedimentary layer at station LNK the mid-crustal velocities are high and are consistent with an ultra-mafic material, perhaps basalt, while at KAT a broad shallow low-velocity zone is present. The KRV-NE solutions and the ABKT-NE solutions both show a similar upper crustal velocity profile and include a step in velocity near 20 km depth. The crust-mantle boundary is gradational for all models and and occurs between 50-55 Km depth around the perimeter of the Basin and between 44-46 km depth beneath station ABKT. We are currently examining 1-D velocity estimates of the crust and upper mantle to depths approaching 150 km.

## SURFACE WAVE OBSERVATIONS

The study of Kadinsky–Cade et al. (1981) demonstrated that the seismic phase Lg is largely blocked for paths crossing the south Caspian Basin and this is also apparent in the data we have collected in the region immediately surrounding the Caspian. However, Figure

13 shows that the south Caspian Basin also severely disrupts low frequency fundamental mode surface wave trains. Figure 13a compares long period seismograms for a mid-Atlantic ridge earthquake propagating along a great circle path between LNK and KAT. The LNK seismogram shows a dispersed fundamental mode wave train ($\sim$ 2400–3000 seconds) followed by scattered surface wave arrivals. The lowest frequency fundamental mode surface wave arrival seen in the LNK seismogram is clear in the KAT seismogram ($\sim$2600–2700 seconds) but the dispersed wave train observed at LNK is largely missing from the KAT seismogram and the overall surface wave amplitude has decreased significantly. Figure 13b compares seismograms for a north Mulucca Sea earthquake propagating along a great circle path between KAT and LNK, i.e., reversing the path of the event in Figure 13a. These seismograms exhibit the same degradation of the surface wave train and show that this is not, for example, an instrumental effect. We have observed this phenomenon for all events propagating along great circle paths across the central portion of the south Caspian Basin.

Surface waves propagating along the KRV–KAT great circle path across the Turkmenian Lowlands do not show the same disruption (Fig. 14) as those propagating across the main part of the basin (Fig. 13). Russian earth scientists have suggested that this region is structurally part of the south Caspian Basin and that the crust in the region consists of 10–15 km of sediment lying on "ocean-like" crust. The deep thickness of sediments is verified from well logs (Sengor, personal communications, 1995). The two upper seismograms in Figure 14a show one of four great circle path Rayleigh wave pairs recorded at stations KRV and KAT that are used to determine the dispersion curve. The comparison of the two wave trains in the lower part of the upper plot shows the match of the original KAT Rayleigh wave with the KRV Rayleigh wave after being filtered with the dispersion transfer function.

Figure 14b shows the fundamental mode Rayleigh wave phase velocity dispersion curve for this path. This curve was computed from four seismogram pairs using a constrained least-squares algorithm (Gomberg et al, 1988). The KRV–KAT phase velocity curve is compared with observed dispersion curves for several other possibly analogous regions; an ocean basin structure (Kuo et al, 1962), a continental tectonic structure (Knopoff et al, 1966), and the Bay of Bengal [curves A to D] (Brune and Singh, 1986). The main difference between curves A to D is due to an increase of sedimentary layer thickness from south to north in the Bay

of Bengal as one gets closer to the mouth of the Ganges River. The dispersion curve for the western Turkmenian Lowlands is most similar to curve "D" for the Bay of Bengal observed by Brune and Singh (1986). They suggest that a thick sedimentary section introduces a blanketing effect which results in an increase in temperature causing in the serpentinization of oceanic crust into a more "continental-like" crust. A similar blanketing process might be affecting the crust in the south Caspian Basin.

## DISCUSSION AND CONCLUSIONS

This study has shown that the south Caspian has an anomalous crustal structure which has a pronounced effect on not only higher frequency regional seismic waveforms but also on lower frequency surface waves. The velocity structures from body wave modeling provide some insight into the effects of crustal structure on regional seismic waves propagating across the south Caspian Basin. It is clear from the Caspian data that both longer and shorter period surface wave trains are greatly scattered or attenuated for travel paths across the Caspian Sea, and to a lesser degree for paths across the Turkmenian Lowlands. The Lg phase is blocked for travel paths across the oceanic crust as well as in regions where the crustal structure includes rapid changes in thickness. If we consider the Lg phase to consist of multiple reflected S waves trapped within the crustal wave guide, then the receiver function modeling results suggest that the blockage is due to the abrupt change in crustal structure from a relatively simple model beneath ABKT to complex models beneath KAT and LNK. Although these are 1–D models and the basin is a 3–D structure, these observations support a scattering mechanism. Recent analysis of the logarithmic rms amplitude ratio of Sn/Lg (Zhang and Lay 1994) has shown that this ratio can be linearly related to changes in surface topography. The southern margins of the Basin and the eastern margin of the Turkmenian Lowlands range from below sea level at LNK up to 2 km in the Alborz Mountains. These features probably contribute to the Lg blockage, but these effects have not yet been examined.

*Acknowledgements*: Installation and the first year and a half of station operation in the Caspian was funded by the Phillips Laboratory. Operation of the stations in the second and third years was funded by USAF EOARD and INTAS grants. Station installation and main-

tenance in the Caspian region was made possible by the support of Drs. M. Roshkov and V. Kiseleivich, SYNAPSE Moscow Data Center; Drs. T Ashirov and B. Karryev, Institute of Seismology of Turkmenia; and Drs. A. Gasanov and S. Agamirzoev of the Geophysical Expedition of Azerbaijan. Throughout network operations indispensable technical support and software was obtained from the Program of Array Seismic Studies of the Continental Lithosphere (PASSCAL) Instrument Center at Lamont–Doherty Geological Observatory (LDGO) and from Refraction Technology.

References

Ammon, C. J., The isolation of receiver effects from teleseismic P waveforms, *Bull. Seism . Soc. Am.*, **81**, 2504–2510, 1991.

Ammon, C. J., G. E. Randall and G. Zandt, On the resolution and non–uniqueness of receiver function inversions, *J. Geophys. Res.*, **95**, 15303–15318, 1990.

Berberian, M., The southern Caspian: A compressional depression floored by trapped, modified oceanic crust, *Can. J. Earth Sci.*, **20**, 163–183, 1983.

Berberian, M. and G. C. P. King, Towards a paleogeography and tectonic evolution of Iran, *Can. J. Earth Sci.*, **18**, 210–265, 1981.

Gomberg, J.S., K.F. Priestley, T.G. Masters, and J.N. Brune, The structure of the crust and upper mantle of northern Mexico, *Geophys. J.*, **94**, 1–20.

Harris, D.B., Comparison of the direction estimation performance of high–frequency seismic arrays and three–component stations, *Bull. Seis. Soc. Am., 80*, 1951–1968, 1990.

Jackson, J. A., and D. McKenzie, Active tectonics of the Alpine–Himalayan Belt between western Turkey and Pakistan, *Geophys. J. R. Astr. Soc.*, **77**, 185–264, 1984.

Kadinsky–Cade, K., M. Barazangi, J. Oliver, and B. Isacks, Lateral variations of high–frequency seismic wave propagation at regional distances across the Turkish and Iranian Plateaus, *J. Geophys. Res.*, **86**, 9377–9369, 1981.

Knopoff, L., S. Mueller, and W.L. Pilant, Structure of the crust and upper mantle in the Alps

from the phase velocity of Rayleigh waves, *Bull. Seis. Soc. Am., 56*, 1009–1044, 1966.

Kuo, J., J. Brune, and M. Major, Rayleigh wave dispersion in the Pacific Ocean for the period range 20 to 140 seconds, *Bull. Seis. Soc. Am., 52*, 338–357, 1962.

Langston, C. A., Structure under Mount Rainier, Washington inferred from teleseismic body waves, *J. Geophys. Res.*, **84**, 4749–4762, 1979.

Neprochnov, Y. P., Structure of the earth's crust of epi–continental seas: Caspian, Black, and Mediterranean, *Can. J. Earth Sci.*, **5**, 1037–1043, 1968.

Park, J., F. Vernon and C. R. Lindberg, Frequency dependent polarization analysis of high–frequency seismograms, *J. Geophys. Res.*, **92**, 12,664–12,674, 1987.

Priestley, K., C. Baker and J. Jackson, Implications of earthquake focal mechanism data for the active tectonics of the south Caspian Basin and surrounding regions, *Geophys. J. Int.*, **118**, 111–141, 1994.

Rezanov, I. A. and S. S. Chamo, Reasons for absence of a granitic layer in basins of the South Caspian and Black Sea type, *Can. J. Earth Sci.*, **6**, 671–678, 1969.

Zhang, T., and T. Lay, Analysis of short period regional phase path effects associated with topography in Eurasia, *Bull. Seis. Soc. Am., 84*, 119–132, 1994.

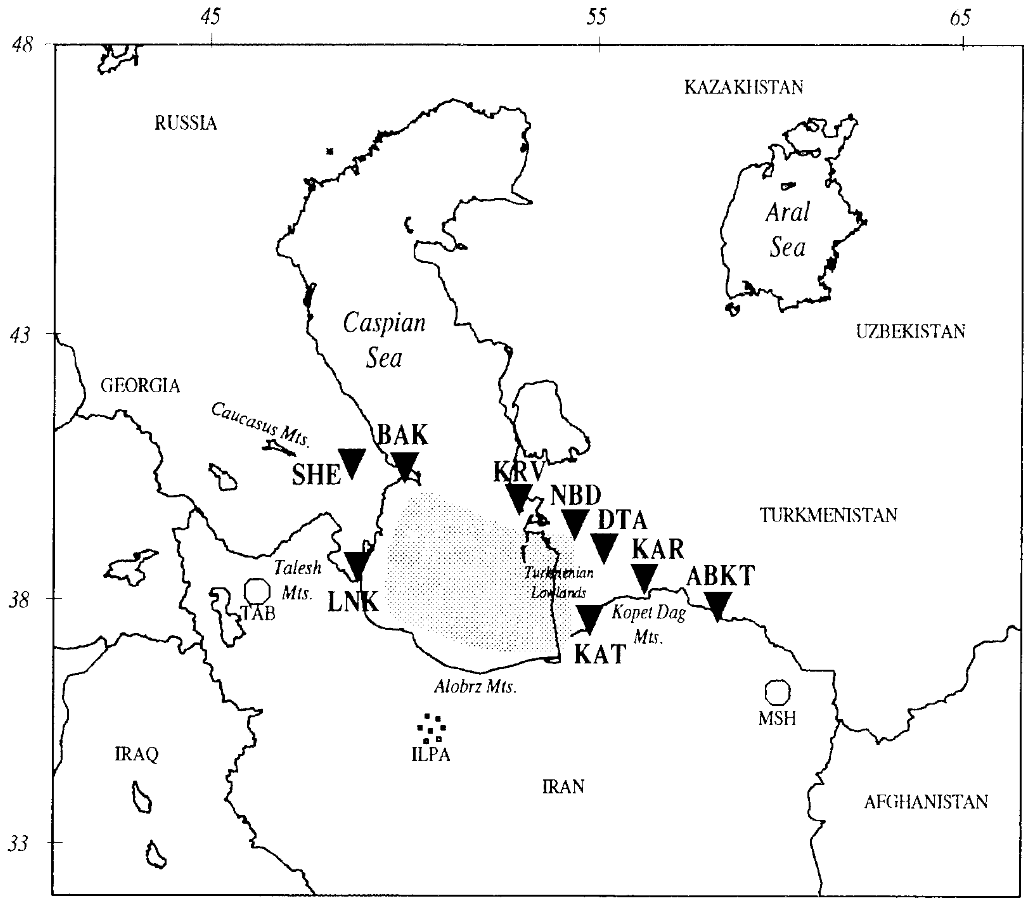


Figure 1. Map of the Caspian Sea and surrounding regions. Caspian Seismograph Network stations are located in Turkmenistan near Krasnovosdk (KRV), Nebit Dag (NBD), Kizyl Atrek (KAT), Dana Tag (DTA), Kala Kara (KAR), and in Azerbaijan near Lenkoran (LNK), Baku (BAK) and Shemaha (SHE). Also shown are WWSSN stations Tabriz (TAB) and Mashad (MSH), the Iranian Long Period Array (ILPA) and IRIS station Alibek (ABKT). The shaded region denotes the subsurface lateral extent of the suspected "oceanic" crust.

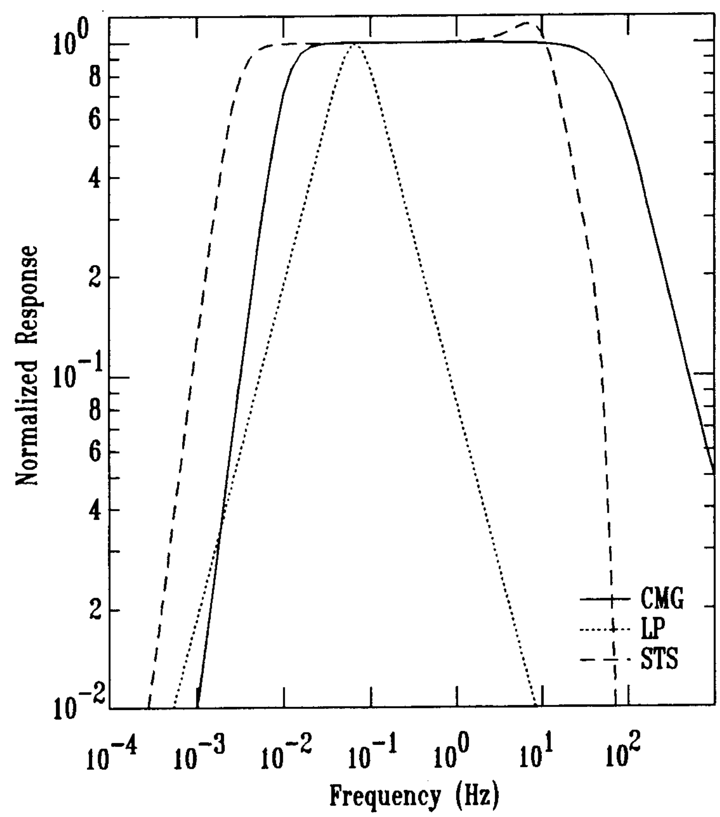


Figure 2. Instrument response characteristics for the CMG-3T, LP and STS-1 seismometers.

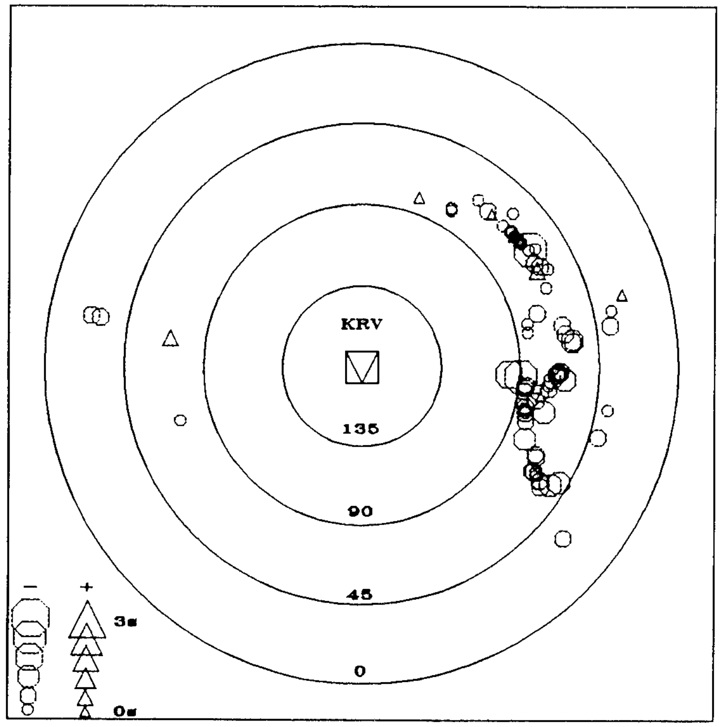


Figure 3. P-wave traveltime residuals for station KRV. Symbol size is scaled at 0.5s intervals, circles are fast and triangles are slow with respect to standard station ABKT. Concentric circles indicate epicentral distance in degrees and residuals are plotted as a function of azimuth.

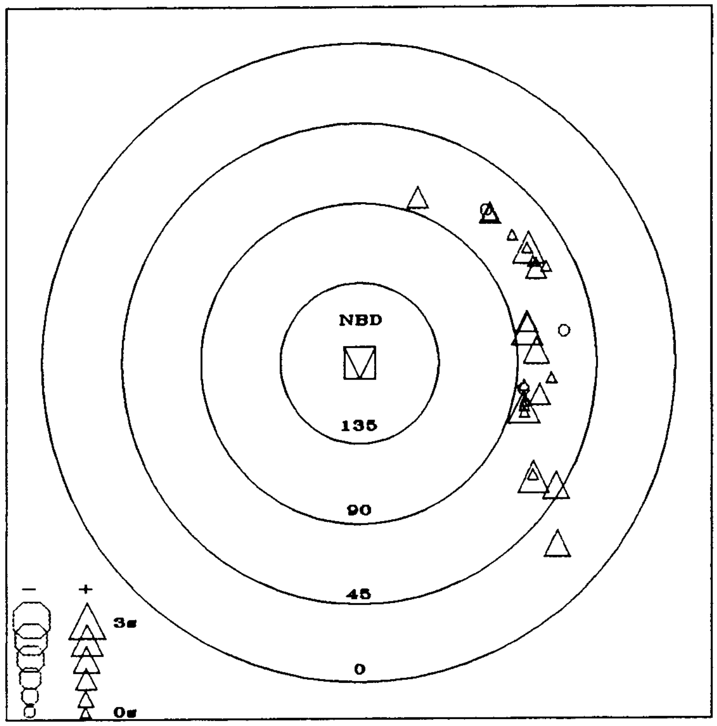


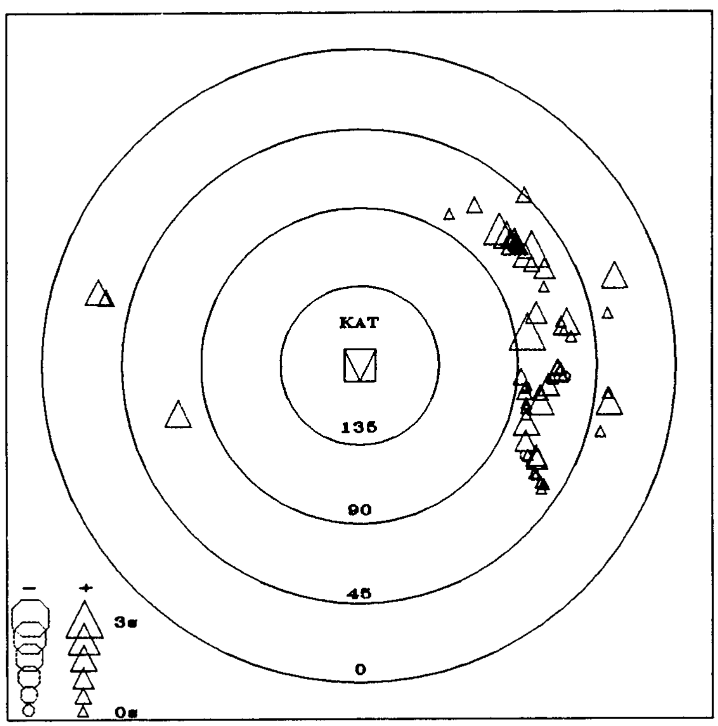


Figure 4. P-wave traveltime residuals for stations NBD (top) and KAT (bottom) relative to ABKT. Format is the same as in Figure 3.

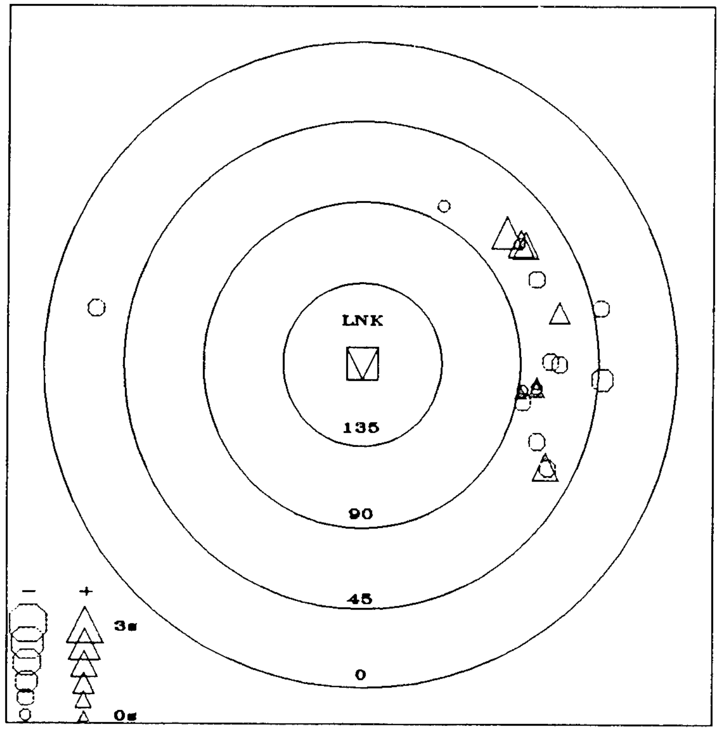


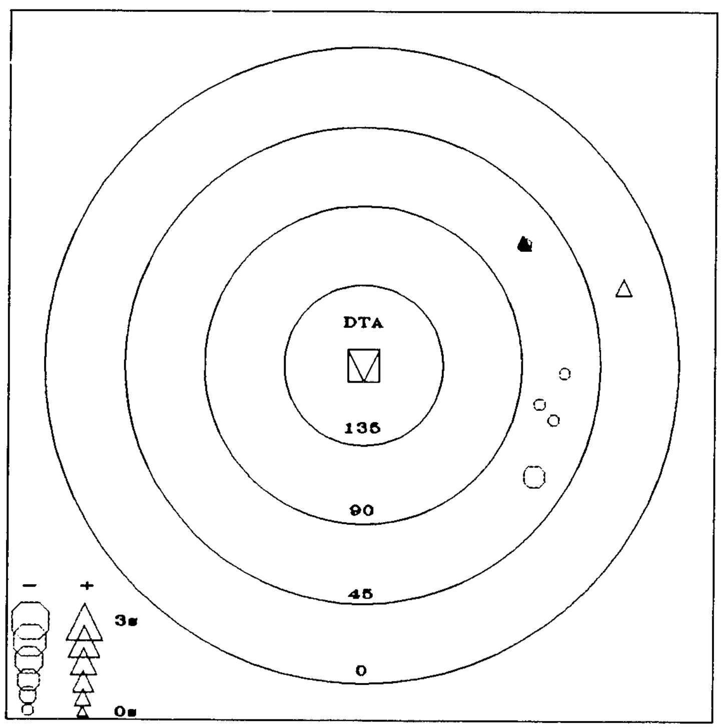


Figure 5. P-wave traveltime residuals for stations LNK (top) and DTA (bottom) relative to ABKT. Format is the same as in Figure 3.

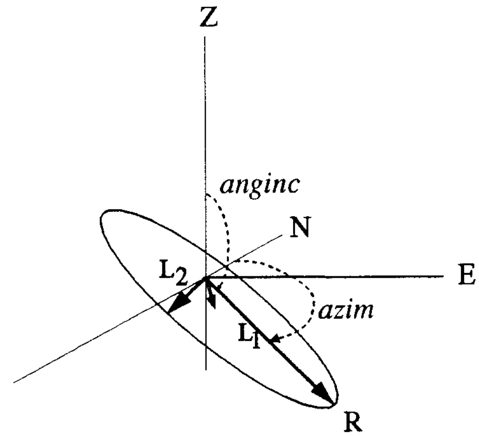


Figure 6. A perspective diagram of the three eigenvectors associated with the covariance matrix for a P-wave. The largest eigenvector extends through the center of the ellipse drawn above in 2 dimensions and defines the radial (R) direction.

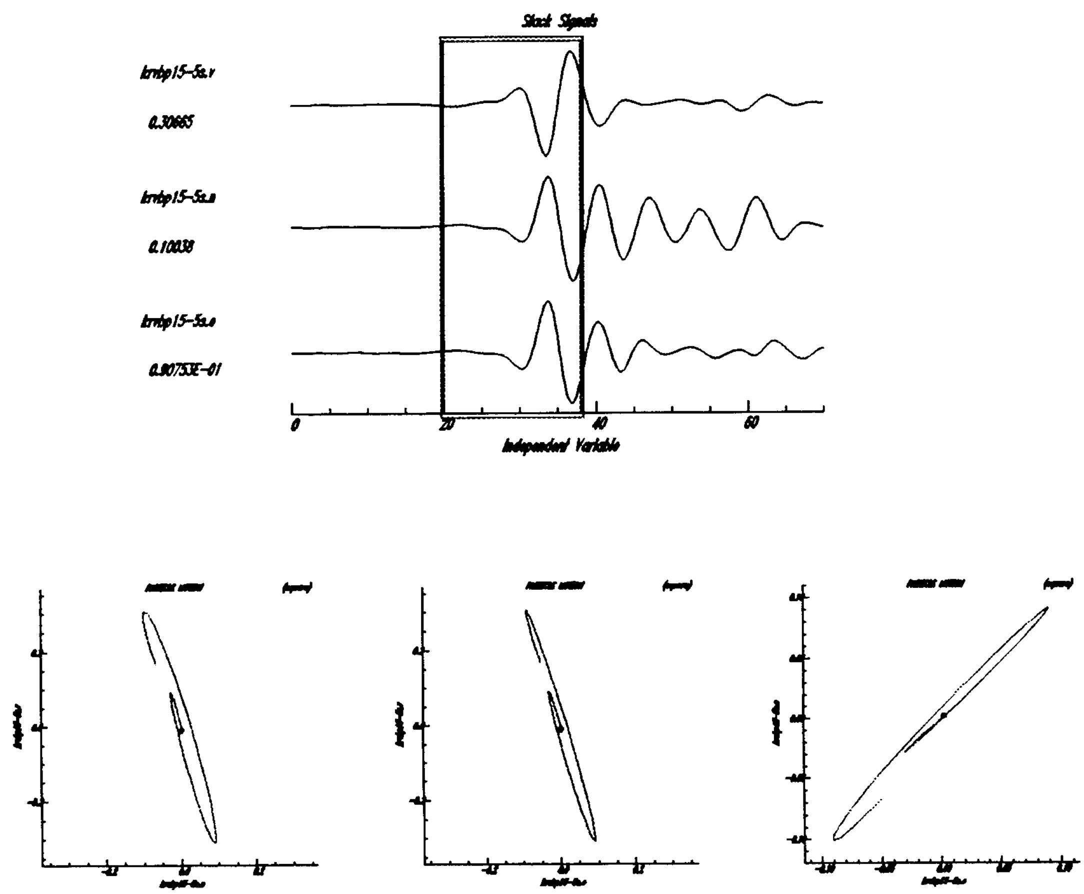


Figure 7. Sample P-wave polarization analysis window (top) and corresponding particle motion in the three orthogonal planes between the source and receiver.

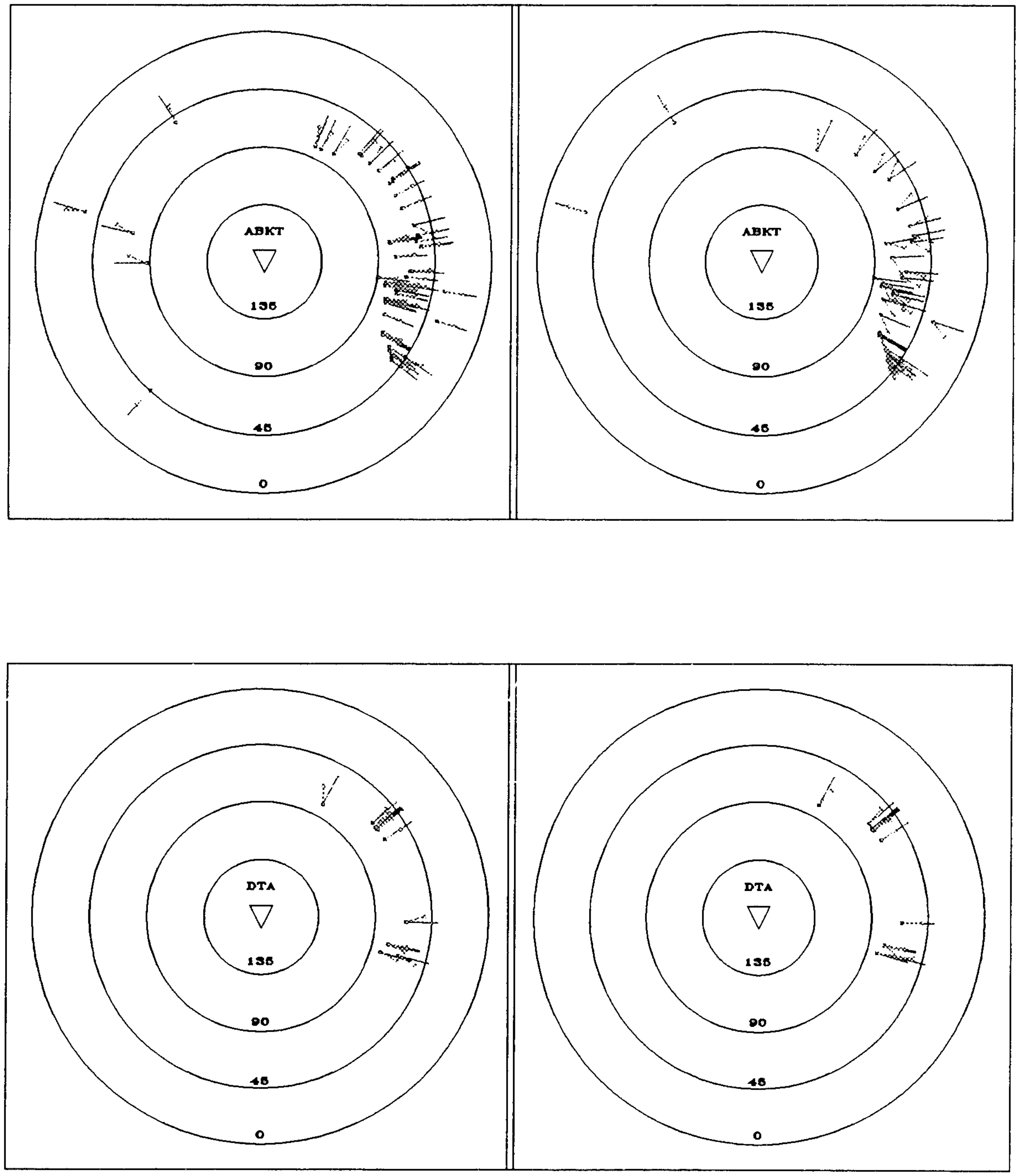


Figure 8. Stations ABKT (top) and DTA (bottom) expected (solid line) compared to the observed P-wave bearing (dashed line) for the lowpass 15s to 5s (left) and highpass 3s-2Hz filtered data (right). Concentric circles indicate epicentral distance from the station.

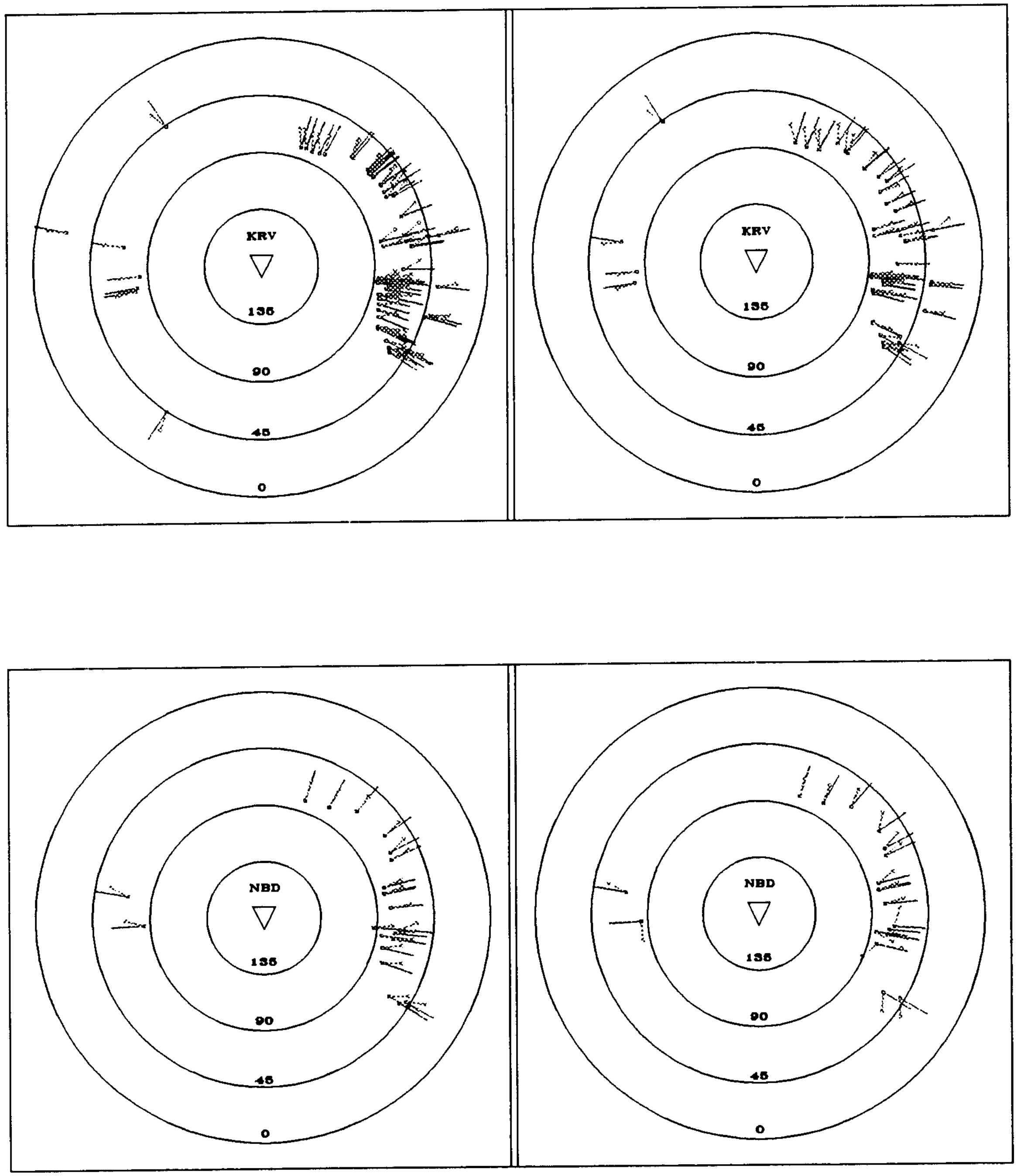


Figure 9. Stations KRV (top) and NBD (bottom) expected compared to the observed P-wave bearing . Format is the same as in Figure 8.

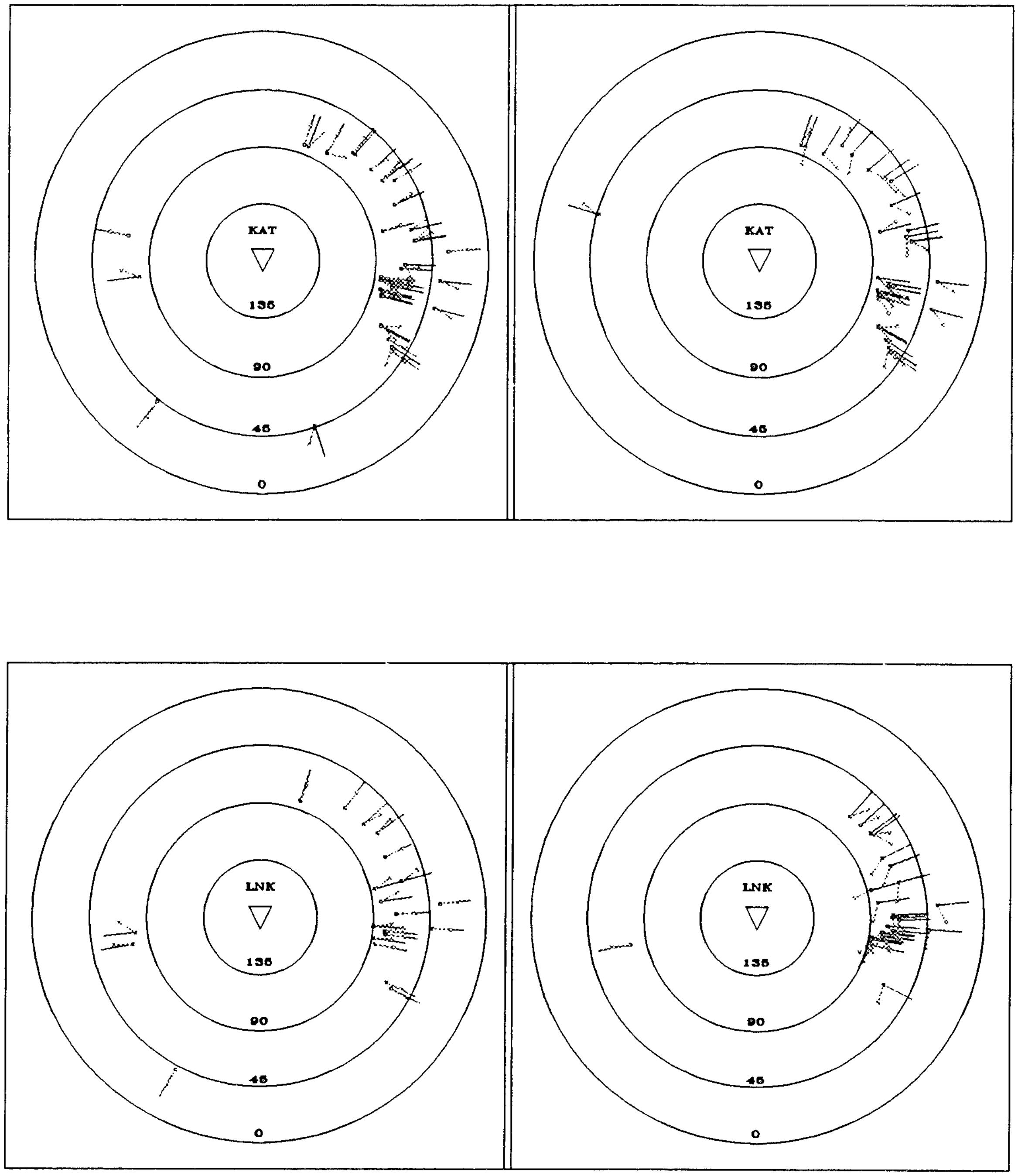


Figure 10. Stations KAT (top) and LNK (bottom) expected compared to the observed P-wave bearing . Format is the same as in Figure 8.

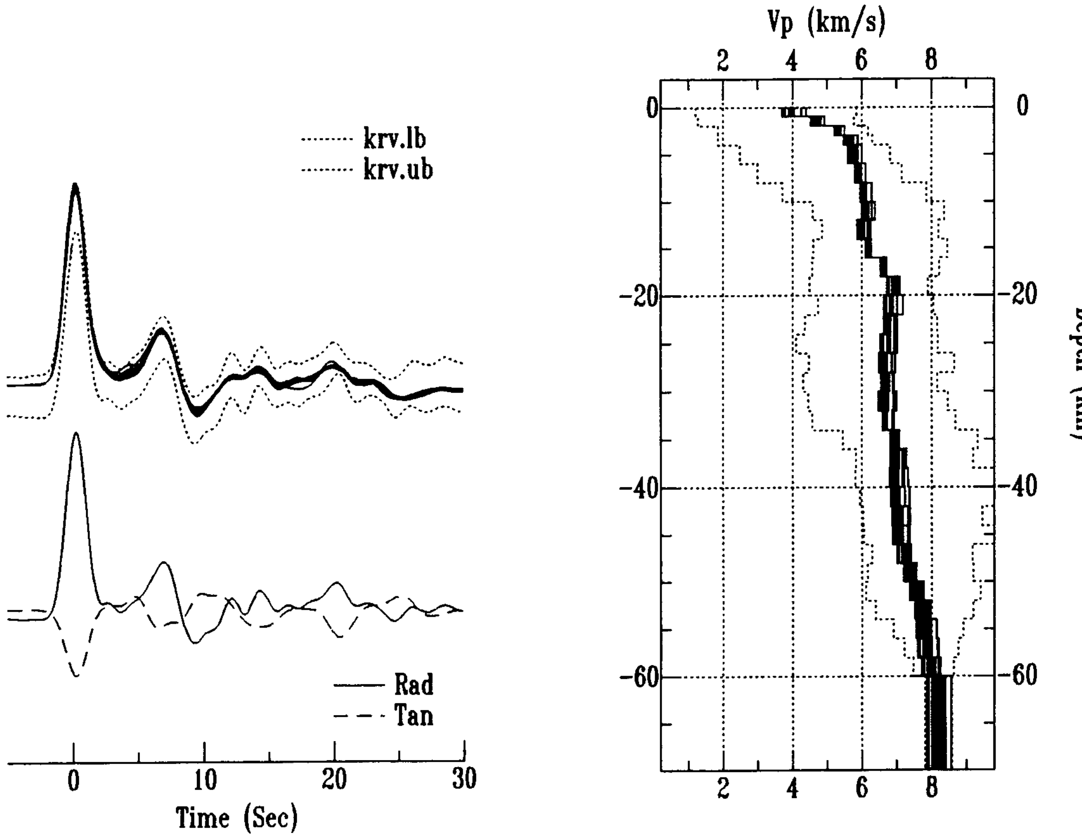


Figure 11. CSN station KRV-NE synthetic waveform fits compared to the +/- 1 STD bounds (top left), the stacked radial and tangential receiver functions (bottom left) and the corresponding solution models (right).

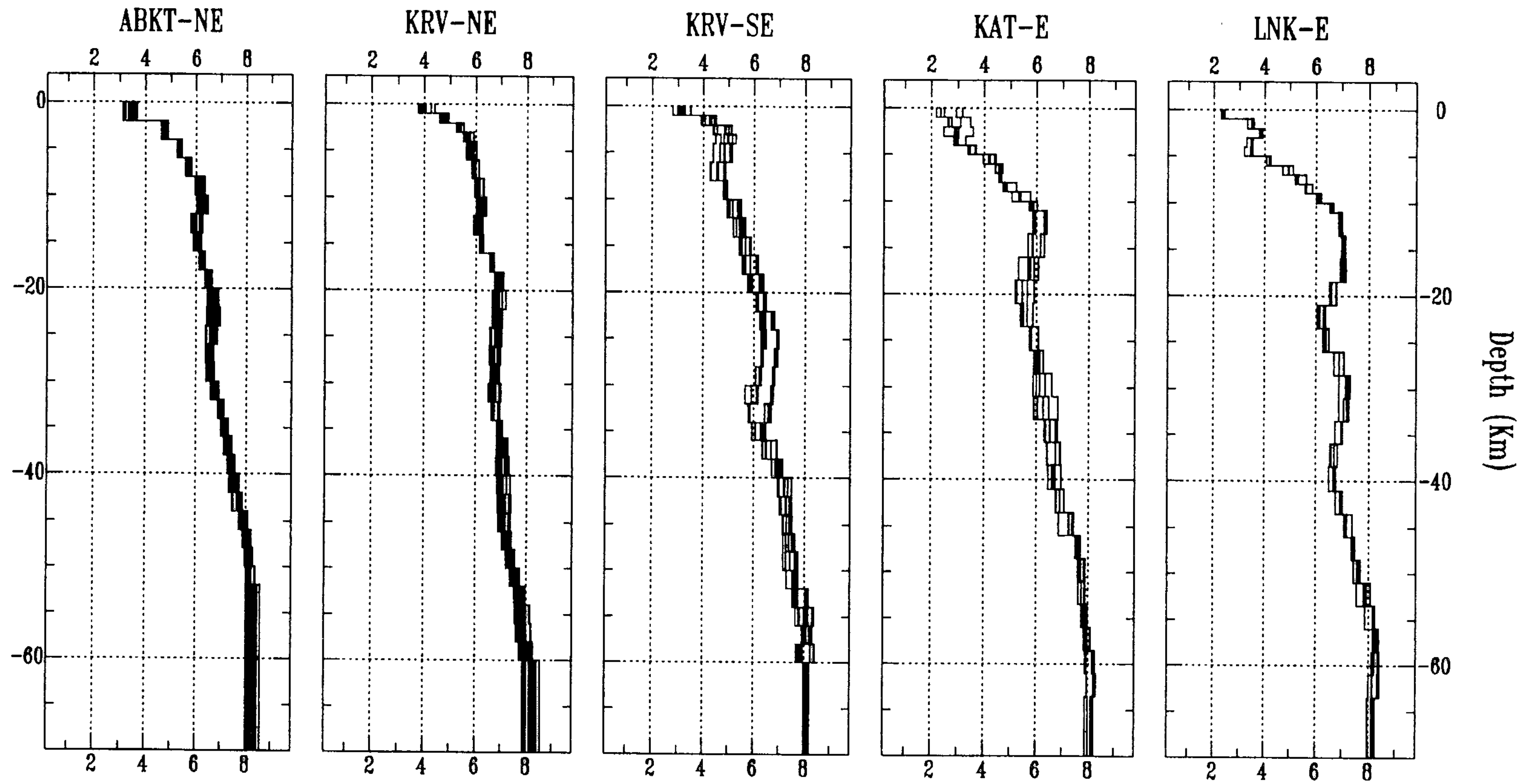


Figure 12. P-wave velocity receiver function modeling results for stations ABKT, KRV, KAT and LNK.

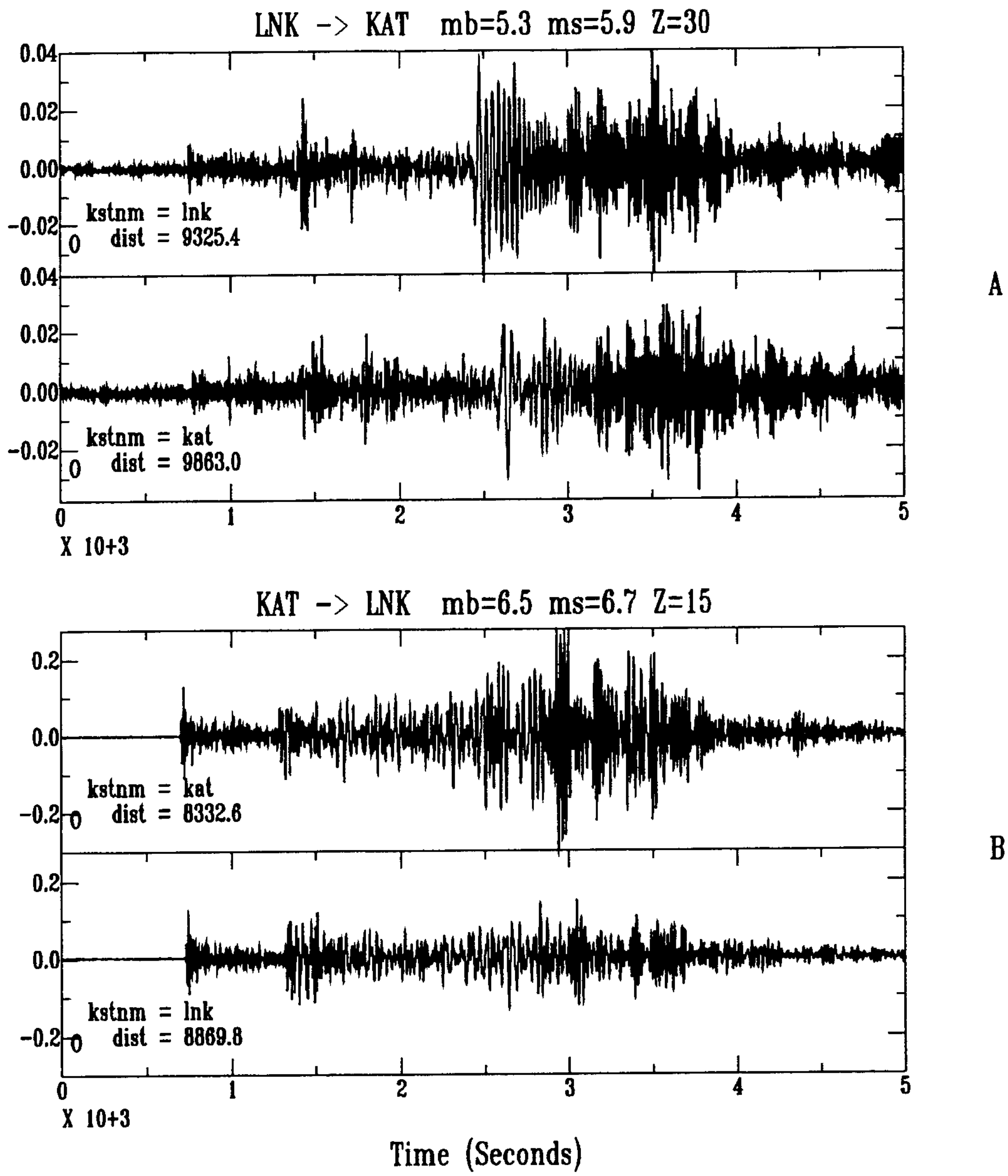


Figure 13. Reversed, great circle path vertical component seismograms recorded at CSN stations LNK and KAT. The upper pair (A) is a record of a mid-Atlantic ridge earthquake propagating from west to east across the south Caspian Basin, while the lower pair (B) is a larger event from the Mulucca Sea which propagates across the Basin from east to west. Both pairs show considerable degradation of the surface wave train after propagating across the south Caspian Basin. These seismograms are characteristic of all great circle path events across the central portion of the south Caspian Basin.

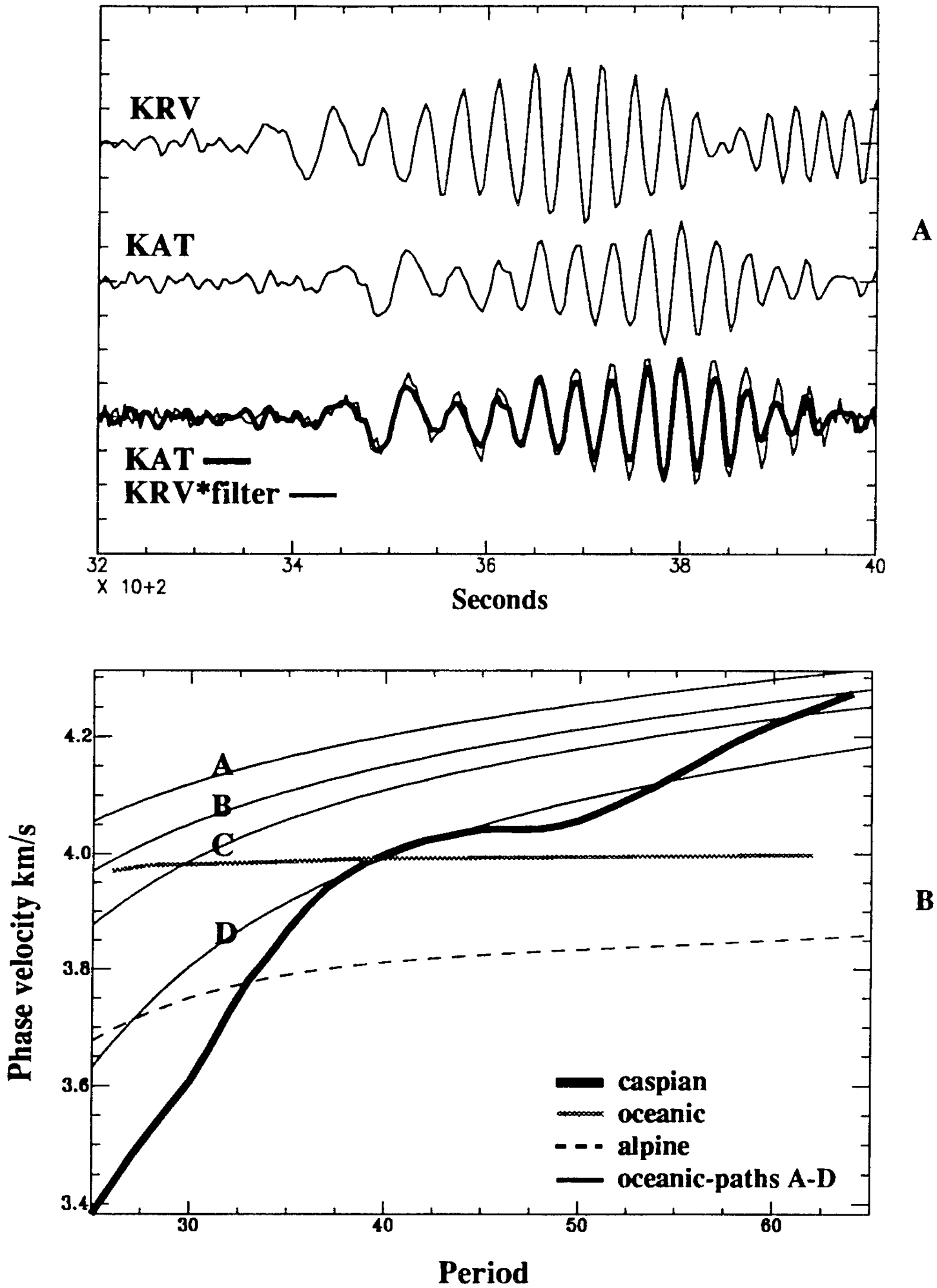


Figure 14. Fundamental mode Rayleigh wave phase velocity dispersion curve for the KRV-KAT path. This curve was computed from four seismogram pairs using a constrained least-squares alogrithm (Gomberg et al. 1988). The KRV-KAT phase velocity curve is compared with observed dispersion curves for an ocean basin (Kuo et al. 1962), a continental tectonic region (Knopoff et al. 1966), and the Bay of Bengal (Brune and Singh 1988) region. The primary differences in paths "A" to "D" is an increase in thickness of the near surface sedimentary layer and an increase in Moho depth from "A" to "D".

Table 1

Caspian Seismograph Network

| STATION ID # KEY | STATION LAT, LON ELEV | AZIMUTH +°N +°E | DAS# CLOCK SENSOR | FIELD NOTES |
|---|---|---|---|---|
| KRV #1 | 40.0063° N 52.9575° E +4 m | 184.8° 274.8° | 580 GPS CMG-3T | Installed 5/93 CMG#357, 3Km east of Caspian Sea sub-basement vault overlies bedrock. Topography varies up to 100m, Edge of Krasnovosdk Plateau, Turkmenistan. |
| NBD #2 | 39.5077° N 54.3872° E +18 m | 4.6° 94.6° | 458 Ω CMG-3T/ LP | Installed 5/93 CMG #360; 12/93-present: LPZ=186 LPN=048, LPE=050; Sub-basement vault overlies unconsolidated sands and clay; Relatively flat topography; Turkmenian Lowlands. |
| KAT #3 | 37.6697° N 54.7766° E +84 m | 4.1° 94.1° | 454 Ω CMG-3T | Installed 5/93 CMG#363; 12/93-present CMG#360 Sub-basement vault overlies alluvium. Topography is ±10m; Turkmenian Lowlands, 3 Km north of Iraian Border, 20 Km north of Alborz Mtns. |
| LNK #4 | 38.7100° N 48.7788° E -2 m | 4.4° 94.4° | 450 Ω CMG-3T | Installed 6/93 CMG #364; Removed 5/95. Surface vault overlies bedrock. Topography ±50m. Foothills of Talesh Mts., 10Km west of Caspian Sea; Azerbaijan. |
| BAK #5 | 40.5813° N 49.9869° E -27 m | 4.8° 94.8° | 456 Ω LP | Installed 6/93 LPZ=077 LPN=043 LPE=039 Removed 6/94; 1Km west of Caspian Sea. Surface vault overlies unconsolidated sands and clay. Apsheron Peninsula, Azerbaijan. |
| DTA #6 | 39.0755° N 55.1663° E +319 m | 4.5° 94.5° | 582 GPS CMG-3T | Installed 12/93 CMG #363; Surface vault overliies silt stone and shale, Topography ± 200m Kopet Dag Mtns., Turkmenistan |
| SHE #7 | 40.6433° N 48.6394° E +829 m | 184.8° 274.8° | 456 Ω LP | Installed 6/94 LPZ=077, LPN=043, LPE=039 Removed 5/95; Surface vault overlies carbonates. Topography ±100. Eastern Caucasus, Azerbaijan. |
| ABKT #8 | 37.9304° N 58.1189° E +678 m | 0° 90° | IRIS GPS STS-1 | Operated by IRIS, installed 4/93, Sensors in tunnel within silt stone and carbonates. Kopet Dag Mtns., Turkmenistan. |
| KAR #9 | 38.4357° N 56.2709° E +304 m | 184.3° 274.3° | 456 Ω CMG-3T | Installed 6/95 CMG #364, Sensors in sub-basement vault, Kopet Dag Mtns., Turkmenistan |

Table 2

Teleseismic P-wave residuals computed with respect to IASP91. BAZ= azimuthal search range, Mean= mean residual over the specified BAZ, STD= standard deviation and # Ev's= number of events used in calculation and all times are in seconds.

| STATION | BAZ | MEAN | STD | # EV'S |
|---|---|---|---|---|
| DTA | 0-360° | 1.78 | 0.523 | 36 |
| KRV | 0-360° | 1.38 | 0.807 | 113 |
| NBD | 0-360° | 2.80 | 1.289 | 29 |
| KAT | 0-360° | 2.96 | 0.888 | 99 |
| LNK | 0-360° | 1.94 | 0.870 | 25 |
| ABKT | 0-360° | 1.85 | 0.885 | 147 |

Table 3

Teleseismic P-wave residuals computed with respect to 'standard-station' ABKT. BAZ= azimuthal search range, Mean= mean residual over the specified BAZ, STD= standard deviation and # Ev's= number of events used in calculation, and all times are in seconds.

| STATION | BAZ | MEAN | STD | # EV'S |
|---|---|---|---|---|
| DTA | 0-360° | 0.06 | 0.433 | 17 |
| KRV | 0-360° | -0.51 | 0.472 | 94 |
| KRV | 0-70° | -0.28 | 0.411 | 39 |
| KRV | 70-180° | -0.70 | 0.412 | 51 |
| NBD | 0-360° | 0.89 | 0.825 | 26 |
| KAT | 0-360° | 0.87 | 0.691 | 72 |
| LNK | 0-360° | 0.06 | 0.998 | 22 |

Table 4

Summary of P-wave bearing analysis where BAZ is range of search, MEAN = average difference between observed and expected P-wave azimuth computed over the specified BAZ; STD=standard deviation; and # EV's = number of events.

| | Lowpass results | | | | Highpass results | | | |
|---|---|---|---|---|---|---|---|---|
| Station | BAZ | MEAN | STD | # EV's | BAZ | MEAN | STD | # EV's |
| ABKT | 0-360° | 1.89°N | 8.41 | 61 | 0-80°<br>80-180° | 22.66°N<br>31.85°S | 7.57<br>12.43 | 6<br>27 |
| DTA | 0-360° | 2.28°S | 11.56 | 17 | 0-80°<br>80-180° | 6.90°S<br>1.39°S | 7.92<br>13.64 | 10<br>6 |
| KRV | 0-360°<br>0-180° | 16.67°N<br>17.35°N | 7.51<br>7.17 | 69<br>64 | 0-360°<br>0-180° | 11.83°N<br>11.87°N | 10.6<br>10.89 | 52<br>48 |
| NBD | 0-360° | 8.26°N | 12.22 | 24 | 0-360° | 0.35°S | 48.76 | 20 |
| KAT | 0-360° | 7.74°S | 25.45 | 42 | 0-360° | 11.83°N | 10.6 | 52 |
| LNK | 0-360° | 1.74°N | 12.14 | 23 | 0-360° | 88.82°S | 41.61 | 27 |

Appendix 1

Caspian Seismograph Network Event Index

Events are indexed by YR:Day:HR:MN:SS according to the Preliminary Determination of Epicenter monthly (1993-1994) and weekly (1995) bulletins. The station lookup key is equal to 1 if archived, 0 if not, and the stations are numbered as: KRV=1, NBD=2, KAT=3, LNK=4, BAK=5, DTA=6, SHE=7, ABKT=8 and KAR=9.

| EventID | Lat | Lon | Z | Mb | Ms | Location | Key 123456789 |
|---|---|---|---|---|---|---|---|
| 93143161830 | 46.564 | 153.267 | 21 | 5.1 | 4.9 | KURIL ISLANDS | 011000010 |
| 93144235120 | -23.238 | -66.631 | 221 | 6.2 | | JUJUY PROVINCE, ARGENTINA | 111000010 |
| 93145183825 | 37.557 | 45.961 | 33 | 4.1 | | NORTHWESTERN IRAN | 111000000 |
| 93145231643 | 55.021 | -160.513 | 37 | 6.2 | 5.8 | ALASKA PENINSULA | 111000010 |
| 93148094903 | 62.354 | -147.732 | 51 | 4.0 | | CENTRAL ALASKA | 111000000 |
| 93148155527 | 55.862 | -155.171 | 33 | 5.0 | 5.0 | SOUTH OF ALASKA | 111000010 |
| 93148173110 | 37.031 | 68.067 | 33 | 4.4 | | AFGHANISTAN-USSR BORDER REGION | 111000000 |
| 93149065013 | 19.072 | -26.476 | 12 | 5.9 | 6.2 | NORTH ATLANTIC OCEAN | 111000010 |
| 93149105036 | 33.978 | 59.859 | 33 | 4.7 | | IRAN | 111000000 |
| 93150141220 | -3.674 | 142.703 | 6 | 5.9 | 5.6 | NEAR N COAST OF PAPUA NEW GUINEA | 111100000 |
| 93150170853 | 1.546 | 127.207 | 81 | 6.0 | | HALMAHERA | 111100010 |
| 93150223403 | -0.621 | 124.208 | 75 | 5.6 | | MOLUCCA SEA | 111100000 |
| 93151000527 | 28.713 | 55.561 | 33 | 4.1 | | SOUTHERN IRAN | 111100000 |
| 93151083422 | -72.448 | 174.838 | 10 | 5.3 | 5.1 | ROSS SEA | 111100010 |
| 93151133812 | 37.767 | 66.581 | 50 | 4.1 | | AFGHANISTAN-USSR BORDER REGION | 111100000 |
| 93151195329 | 36.599 | 71.626 | 33 | 4.8 | 3.4 | AFGHANISTAN-USSR BORDER REGION | 111000000 |
| 93152094529 | 34.352 | 26.184 | 47 | 4.9 | 4.2 | CRETE | 111000010 |
| 93152155347 | -45.711 | -77.211 | 33 | 5.3 | 5.4 | OFF COAST OF SOUTHERN CHILE | 111000010 |
| 93152195110 | 46.166 | 16.467 | 30 | 4.9 | | YUGOSLAVIA | 111000000 |
| 93153030018 | -46.471 | 33.954 | 10 | 5.6 | 5.5 | PRINCE EDWARD ISLANDS REGION | 111000010 |
| 93153082719 | 51.513 | -178.744 | 33 | 5.6 | 5.4 | ANDREANOF ISLANDS, ALEUTIAN IS. | 111000010 |
| 93153161512 | 32.407 | 48.669 | 53 | 4.2 | | WESTERN IRAN | 111000000 |
| 93153220148 | 28.940 | 47.606 | 10 | 4.7 | | EASTERN ARABIAN PENINSULA | 111000000 |
| 93154074647 | 40.896 | 35.964 | 10 | 4.3 | | TURKEY | 110000000 |
| 93154093825 | -14.841 | 167.299 | 152 | 5.9 | | VANUATU ISLANDS | 110000000 |
| 93155030635 | 11.799 | 142.493 | 25 | 5.6 | 5.5 | SOUTH OF MARIANA ISLANDS | 111000010 |
| 93155104933 | 3.734 | 128.497 | 20 | 5.9 | 5.8 | NORTH OF HALMAHERA | 111000010 |
| 93155215625 | 42.969 | 43.613 | 33 | 4.2 | | WESTERN CAUCASUS | 111000000 |
| 93157110500 | 36.377 | 71.333 | 33 | 4.6 | | AFGHANISTAN-USSR BORDER REGION | 111000000 |
| 93157132320 | 15.823 | 146.595 | 14 | 6.0 | 6.6 | MARIANA ISLANDS | 111000010 |
| 93158071427 | 39.924 | 46.273 | 36 | 4.4 | | N.W. IRAN-USSR BORDER REGION | 111000000 |
| 93158074935 | 35.972 | 141.529 | 36 | 5.6 | 5.5 | NEAR EAST COAST OF HONSHU, JAPAN | 111000010 |
| 93158131438 | 35.286 | 141.900 | 11 | 5.3 | 4.9 | NEAR EAST COAST OF HONSHU, JAPAN | 111000010 |
| 93159130336 | 51.218 | 157.829 | 71 | 6.4 | 7.3 | NEAR EAST COAST OF KAMCHATKA | 111000010 |
| 93159143037 | 33.585 | 72.746 | 33 | 4.8 | | PAKISTAN | 111000000 |
| 93159231741 | -31.560 | -69.234 | 113 | 6.5 | | SAN JUAN PROVINCE, ARGENTINA | 111000010 |
| 93160040740 | 32.026 | 49.278 | 33 | 4.4 | | WESTERN IRAN | 111000000 |
| 93160173336 | 34.763 | 53.276 | 30 | 5.0 | | IRAN | 111000010 |
| 93161054938 | 39.383 | 67.665 | 33 | 4.6 | | SOUTHEASTERN UZBEK SSR | 111000000 |
| 93161120456 | 51.170 | 159.097 | 21 | 5.5 | 5.2 | OFF EAST COAST OF KAMCHATKA | 111000010 |
| 93161125859 | 51.115 | 159.272 | 16 | 5.8 | 5.1 | OFF EAST COAST OF KAMCHATKA | 111000000 |
| 93161174838 | -24.353 | -176.082 | 34 | 5.7 | 5.4 | SOUTH OF FIJI ISLANDS | 111000000 |
| 93162095529 | 39.547 | 68.939 | 33 | 4.1 | | TAJIK SSR | 111000000 |
| 93162130903 | 35.508 | 26.603 | 28 | 4.5 | | CRETE | 111000000 |
| 93162132255 | 36.800 | 71.651 | 33 | 4.8 | | AFGHANISTAN-USSR BORDER REGION | 111000000 |
| 93163054521 | -11.140 | 162.937 | 15 | 5.5 | 6.1 | SOLOMON ISLANDS | 111000010 |
| 93163085826 | 40.624 | 35.792 | 10 | 4.6 | | TURKEY | 111000000 |
| 93163182642 | -4.375 | 135.118 | 10 | 5.8 | 6.1 | WEST IRIAN REGION | 111000010 |
| 93163203325 | 51.259 | 157.692 | 44 | 5.9 | 6.0 | NEAR EAST COAST OF KAMCHATKA | 111000010 |
| 93164232640 | 39.363 | 20.495 | 20 | 5.3 | 4.9 | GREECE-ALBANIA BORDER REGION | 111000010 |
| 93165073017 | 35.568 | 78.407 | 33 | 5.1 | 4.4 | EASTERN KASHMIR | 111000010 |
| 93165195942 | 39.624 | 38.410 | 26 | 5.0 | 4.5 | TURKEY | 111000010 |
| 93166044257 | 34.868 | 141.683 | 47 | 5.4 | 5.3 | OFF EAST COAST OF HONSHU, JAPAN | 111000010 |

Appendix 1 (continued)

| EventID | Lat | Lon | Z | Mb | Ms | Location | Key 123456789 |
|---|---|---|---|---|---|---|---|
| 93166231224 | 35.629 | 77.788 | 33 | 4.9 | | EASTERN KASHMIR | 111000000 |
| 93168204452 | 36.168 | 71.236 | 104 | 5.2 | | AFGHANISTAN-USSR BORDER REGION | 110000000 |
| 93169115251 | -29.053 | -176.753 | 16 | 6.2 | 6.7 | KERMADEC ISLANDS REGION | 110000000 |
| 93169175746 | -28.678 | -176.893 | 11 | 5.9 | 6.7 | KERMADEC ISLANDS REGION | 110000000 |
| 93170170156 | 36.807 | 54.904 | 33 | 4.6 | | IRAN | 110000000 |
| 93171020924 | -6.262 | 130.092 | 152 | 5.3 | | BANDA SEA | 110000000 |
| 93171172630 | -6.946 | 155.776 | 38 | 5.5 | 5.6 | SOLOMON ISLANDS | 110000000 |
| 93172003251 | 39.200 | 40.401 | 10 | 4.2 | | TURKEY | 110000000 |
| 93172161555 | 37.605 | 72.638 | 33 | 4.3 | | TAJIK SSR | 110000000 |
| 93173123345 | 64.624 | -17.543 | 5 | 5.1 | 4.8 | ICELAND | 110000000 |
| 93173163243 | 30.149 | 50.814 | 33 | 5.5 | 4.8 | IRAN | 110000000 |
| 93174112919 | -60.549 | -56.376 | 10 | 6.2 | 5.4 | SOUTH SHETLAND ISLANDS | 110000000 |
| 93175165339 | 38.911 | 71.230 | 33 | 4.5 | | AFGHANISTAN-USSR BORDER REGION | 110000000 |
| 93176100429 | 33.315 | 93.306 | 33 | 4.8 | 4.3 | QINGHAI PROVINCE, CHINA | 100000000 |
| 93186005241 | -24.886 | -112.393 | 10 | 5.2 | 5.6 | EASTER ISLAND REGION | 000100010 |
| 93186080221 | 37.164 | 71.379 | 33 | 4.5 | | AFGHANISTAN-USSR BORDER REGION | 000100000 |
| 93187194809 | 37.891 | 39.315 | 47 | 4.8 | | TURKEY | 100100000 |
| 93187025303 | -24.601 | -111.888 | 10 | 5.5 | 6.1 | EASTER ISLAND REGION | 000100010 |
| 93188111053 | 27.887 | 127.992 | 35 | 5.1 | 4.9 | RYUKYU ISLANDS | 100100010 |
| 93189103549 | -20.832 | 169.294 | 34 | 5.5 | 5.3 | VANUATU ISLANDS | 100100000 |
| 93189104625 | 51.218 | 159.151 | 36 | 5.4 | 5.3 | OFF EAST COAST OF KAMCHATKA | 100100010 |
| 93189182217 | -20.858 | 172.317 | 33 | 5.4 | 5.9 | VANUATU ISLANDS REGION | 101100010 |
| 93189233106 | 37.337 | 69.983 | 33 | 4.5 | | AFGHANISTAN-USSR BORDER REGION | 101100000 |
| 93190102921 | 28.416 | 55.369 | 23 | 5.3 | 4.8 | SOUTHERN IRAN | 101100010 |
| 93190153753 | -19.782 | -177.486 | 398 | 6.0 | | FIJI ISLANDS REGION | 101100010 |
| 93190230605 | 36.853 | 55.230 | 61 | 4.6 | | IRAN | 101100000 |
| 93192133621 | -25.304 | -70.166 | 48 | 6.2 | 6.1 | NEAR COAST OF NORTHERN CHILE | 101000010 |
| 93192174811 | 47.626 | 154.156 | 28 | 5.6 | 5.3 | KURIL ISLANDS | 101000010 |
| 93193050531 | 72.175 | 1.071 | 10 | 5.1 | 4.9 | NORWEGIAN SEA | 101000010 |
| 93193131711 | 42.851 | 139.197 | 17 | 6.6 | 7.6 | HOKKAIDO, JAPAN REGION | 101000010 |
| 93193144505 | 43.124 | 139.183 | 33 | 6.0 | 6.3 | EASTERN SEA OF JAPAN | 101000000 |
| 93194083553 | -3.372 | 145.633 | 24 | 5.3 | 5.6 | NEAR N COAST OF PAPUA NEW GUINEA | 101000010 |
| 93194142253 | 37.032 | 55.310 | 26 | 4.6 | | IRAN-USSR BORDER REGION | 101000010 |
| 93195123149 | 38.224 | 21.756 | 23 | 5.3 | 5.5 | GREECE | 101000000 |
| 93195173833 | 43.181 | 139.124 | 20 | 5.5 | | EASTERN SEA OF JAPAN | 101000000 |
| 93196005113 | 46.679 | 152.577 | 32 | 5.7 | 5.0 | KURIL ISLANDS | 101000000 |
| 93196193737 | 42.670 | 139.016 | 20 | 5.3 | 4.7 | HOKKAIDO, JAPAN REGION | 101000000 |
| 93198094634 | 28.011 | 99.636 | 31 | 5.3 | 4.8 | YUNNAN PROVINCE, CHINA | 101000000 |
| 93198184819 | 29.880 | 51.489 | 33 | 4.4 | | SOUTHERN IRAN | 101000000 |
| 93200193504 | 34.465 | 141.339 | 46 | 5.2 | 5.1 | OFF EAST COAST OF HONSHU, JAPAN | 101000000 |
| 93201132604 | 27.374 | 139.990 | 465 | 5.4 | | BONIN ISLANDS REGION | 101000000 |
| 93201165044 | -52.917 | 27.174 | 10 | 5.1 | 5.2 | SOUTH OF AFRICA | 101000000 |
| 93203015456 | 39.533 | 40.116 | 11 | 4.6 | | TURKEY | 101000000 |
| 93203045707 | 6.470 | -71.210 | 20 | 6.1 | 5.9 | NORTHERN COLOMBIA | 101000010 |
| 93203121536 | 21.760 | 144.261 | 127 | 5.6 | | MARIANA ISLANDS REGION | 101000010 |
| 93204115006 | 36.437 | 70.416 | 272 | 5.2 | | HINDU KUSH REGION | 101000000 |
| 93205020156 | 5.070 | 127.714 | 116 | 5.7 | | PHILIPPINE ISLANDS REGION | 101000000 |
| 93205102656 | 51.509 | -176.879 | 33 | 5.2 | 4.4 | ANDREANOF ISLANDS, ALEUTIAN IS. | 101000010 |
| 93205125603 | 39.087 | 138.636 | 14 | 5.1 | 4.6 | EASTERN SEA OF JAPAN | 101000000 |
| 93205202450 | -13.060 | 167.056 | 194 | 5.8 | | VANUATU ISLANDS | 101000000 |
| 93205213205 | 36.443 | 70.604 | 223 | 4.6 | | HINDU KUSH REGION | 101000000 |
| 93206150519 | -17.844 | -13.431 | 10 | 5.2 | 4.7 | SOUTH ATLANTIC RIDGE | 101000000 |
| 93207093130 | 29.960 | 66.626 | 33 | 4.1 | 4.9 | PAKISTAN | 101000000 |
| 93208194449 | 34.442 | 141.591 | 25 | 5.3 | 5.0 | OFF EAST COAST OF HONSHU, JAPAN | 001000000 |
| 93209031024 | 36.676 | 71.171 | 265 | 4.1 | | AFGHANISTAN-USSR BORDER REGION | 001000000 |
| 93209033238 | 36.639 | 70.785 | 33 | 4.1 | | HINDU KUSH REGION | 001000000 |
| 93209171640 | 46.361 | 150.971 | 86 | 5.0 | | KURIL ISLANDS | 001000000 |
| 93209180748 | -5.573 | 154.132 | 26 | 5.6 | 5.9 | SOLOMON ISLANDS | 001000000 |
| 93211142551 | 45.684 | 26.568 | 148 | 4.7 | | ROMANIA | 001000000 |
| 93211233410 | 28.864 | 34.821 | 18 | 4.7 | | ARAB REPUBLIC OF EGYPT | 001000000 |

Appendix 1 (continued)

| EventID | Lat | Lon | Z | Mb | Ms | Location | Key 123456789 |
|---|---|---|---|---|---|---|---|
| 93212023245 | -4.397 | 28.361 | 10 | 5.0 | | LAKE TANGANYIKA REGION | 001000000 |
| 93212175301 | 29.394 | 34.475 | 10 | 4.4 | | ARAB REPUBLIC OF EGYPT | 001000000 |
| 93212192921 | 27.976 | 91.944 | 33 | 4.4 | | BHUTAN | 001000000 |
| 93212231316 | 56.210 | 112.476 | 10 | 4.8 | | LAKE BAIKAL REGION | 001000010 |
| 93213002040 | 15.385 | 31.690 | 13 | 5.2 | 5.1 | SUDAN | 001000010 |
| 93213141928 | -43.824 | -16.235 | 10 | 5.0 | 4.9 | SOUTH ATLANTIC RIDGE | 001000000 |
| 93214031321 | 30.828 | 131.418 | 33 | 5.4 | 5.4 | KYUSHU, JAPAN | 001000010 |
| 93214160059 | 30.914 | 51.839 | 39 | 4.9 | 4.2 | IRAN | 001000000 |
| 93214164815 | 36.992 | 71.341 | 115 | 4.6 | | AFGHANISTAN-USSR BORDER REGION | 001000010 |
| 93214230455 | 37.482 | 70.947 | 33 | 4.7 | | AFGHANISTAN-USSR BORDER REGION | 001000000 |
| 93215061555 | 85.253 | 91.728 | 10 | 4.9 | 4.5 | NORTH OF SEVERNAYA ZEMLYA | 001000000 |
| 93215071959 | 51.188 | -130.797 | 10 | 5.5 | 6.1 | QUEEN CHARLOTTE ISLANDS REGION | 001000010 |
| 93215104327 | 85.294 | 91.440 | 10 | 4.8 | | NORTH OF SEVERNAYA ZEMLYA | 001100000 |
| 93215123120 | 28.549 | 34.608 | 10 | 4.5 | | ARAB REPUBLIC OF EGYPT | 001100000 |
| 93215124305 | 28.729 | 34.553 | 10 | 5.9 | 5.8 | ARAB REPUBLIC OF EGYPT | 001100010 |
| 93216075943 | 30.105 | 51.392 | 33 | 4.6 | | IRAN | 001100000 |
| 93216113118 | -1.629 | 99.615 | 32 | 5.9 | 6.3 | SOUTHERN SUMATERA | 001100010 |
| 93216194609 | 37.008 | 57.936 | 33 | 4.4 | | IRAN-USSR BORDER REGION | 001100000 |
| 93217070533 | 72.219 | 1.514 | 10 | 4.6 | 4.5 | NORWEGIAN SEA | 001100010 |
| 93217115319 | -5.430 | 151.700 | 61 | 5.2 | 5.1 | NEW BRITAIN REGION | 001100000 |
| 93219000037 | 26.585 | 125.612 | 155 | 6.0 | | NORTHEAST OF TAIWAN | 001100010 |
| 93219175324 | -23.866 | 179.846 | 523 | 6.0 | | SOUTH OF FIJI ISLANDS | 001100010 |
| 93219194241 | 41.985 | 139.839 | 14 | 6.2 | 6.1 | HOKKAIDO, JAPAN REGION | 001100010 |
| 93220083424 | 12.982 | 144.801 | 59 | 7.1 | 8.0 | SOUTH OF MARIANA ISLANDS | 001100000 |
| 93220200314 | 13.483 | 145.657 | 56 | 5.3 | 5.7 | MARIANA ISLANDS | 001100000 |
| 93220224143 | 38.662 | 70.447 | 16 | 5.1 | 4.8 | AFGHANISTAN-USSR BORDER REGION | 001100000 |
| 93221124248 | 36.379 | 70.868 | 215 | 6.2 | | HINDU KUSH REGION | 011000000 |
| 93221060503 | 28.737 | 34.704 | 10 | 4.6 | | ARAB REPUBLIC OF EGYPT | 001100000 |
| 93221113830 | 36.436 | 70.711 | 204 | 5.8 | | HINDU KUSH REGION | 001000000 |
| 93222005153 | -45.277 | 166.927 | 28 | 6.2 | 7.0 | OFF W. COAST OF S. ISLAND, N.Z. | 111000010 |
| 93222055822 | 40.201 | 22.978 | 15 | 4.6 | | GREECE | 111000010 |
| 93222094635 | -38.520 | 177.553 | 14 | 6.0 | 6.0 | NORTH ISLAND, NEW ZEALAND | 111000010 |
| 93222193620 | 83.066 | -27.533 | 10 | 5.4 | 5.0 | NEAR NORTH COAST OF GREENLAND | 111000010 |
| 93223141737 | 13.178 | 145.651 | 22 | 5.9 | 6.1 | MARIANA ISLANDS | 111000010 |
| 93225003143 | 28.561 | 34.716 | 9 | 4.7 | | ARAB REPUBLIC OF EGYPT | 111000000 |
| 93225004341 | 32.465 | 49.537 | 16 | 4.6 | | WESTERN IRAN | 111000000 |
| 93225110220 | -35.989 | 178.510 | 95 | 5.8 | | OFF E. COAST OF N. ISLAND, N.Z. | 111000010 |
| 93226035242 | 37.542 | 70.714 | 64 | 4.5 | | AFGHANISTAN-USSR BORDER REGION | 111000010 |
| 93226143004 | 25.440 | 101.545 | 33 | 4.9 | 4.8 | YUNNAN PROVINCE, CHINA | 111000010 |
| 93227031021 | 0.711 | -25.956 | 15 | 5.3 | 5.3 | CENTRAL MID-ATLANTIC RIDGE | 111000010 |
| 93228043348 | 12.966 | 144.972 | 18 | 5.6 | 6.0 | SOUTH OF MARIANA ISLANDS | 111000010 |
| 93230120921 | 34.969 | 26.016 | 29 | 4.5 | | CRETE | 110000000 |
| 93231080322 | 13.169 | 145.531 | 61 | 5.5 | | MARIANA ISLANDS | 110000010 |
| 93231100428 | 35.089 | 52.094 | 18 | 4.6 | | IRAN | 110000000 |
| 93231142656 | 33.204 | 71.983 | 33 | 4.7 | | PAKISTAN | 110000000 |
| 93231152138 | 7.197 | 126.807 | 31 | 5.4 | 5.5 | MINDANAO, PHILIPPINE ISLANDS | 110000010 |
| 93231215205 | 7.167 | 126.743 | 31 | 5.3 | 4.8 | MINDANAO, PHILIPPINE ISLANDS | 110000010 |
| 93232050653 | -5.997 | 142.743 | 15 | 6.0 | 6.0 | PAPUA NEW GUINEA | 110000010 |
| 93232101020 | 28.127 | 53.879 | 65 | 4.1 | | SOUTHERN IRAN | 110000000 |
| 93232115204 | 21.686 | 143.064 | 288 | 5.3 | | MARIANA ISLANDS REGION | 110000000 |
| 93232185710 | -25.991 | -175.261 | 22 | 5.5 | 5.1 | SOUTH OF TONGA ISLANDS | 110000000 |
| 93232231000 | 28.764 | 34.687 | 10 | 4.5 | | ARAB REPUBLIC OF EGYPT | 110000000 |
| 93233080749 | -46.404 | 96.032 | 10 | 5.2 | 5.5 | SOUTHEAST INDIAN RISE | 110000000 |
| 93233154114 | 27.359 | 55.922 | 33 | 4.3 | | SOUTHERN IRAN | 110000000 |
| 93234015304 | 14.255 | 56.262 | 10 | 4.8 | 3.8 | ARABIAN SEA | 110000000 |
| 93235052143 | 30.035 | 67.921 | 25 | 5.0 | 4.6 | PAKISTAN | 110000010 |
| 93235120740 | 36.401 | 141.994 | 35 | 5.1 | 4.7 | NEAR EAST COAST OF HONSHU, JAPAN | 110000000 |
| 93235195110 | 30.045 | 67.891 | 32 | 4.8 | | PAKISTAN | 110000000 |
| 93236174730 | 20.641 | 71.365 | 25 | 5.0 | 4.7 | INDIA | 110000010 |
| 93237052532 | -44.718 | -79.958 | 10 | 5.6 | 5.4 | OFF COAST OF SOUTHERN CHILE | 110000010 |

Appendix 1 (continued)

| EventID | Lat | Lon | Z | Mb | Ms | Location | Key 123456789 |
|---|---|---|---|---|---|---|---|
| 93237225704 | 36.070 | 31.018 | 66 | 4.4 | | TURKEY | 110000000 |
| 93238013000 | -35.899 | 178.265 | 33 | 5.5 | 5.4 | OFF E. COAST OF N. ISLAND, N.Z. | 110000010 |
| 93238100357 | 36.736 | 28.051 | 33 | 5.3 | 4.5 | DODECANESE ISLANDS | 110000010 |
| 93238213233 | 45.727 | 26.565 | 136 | 5.0 | | ROMANIA | 110000010 |
| 93240042623 | 17.173 | 73.672 | 5 | 4.9 | 4.5 | INDIA | 110000000 |
| 93240201445 | 6.571 | 94.668 | 133 | 5.8 | | NICOBAR ISLANDS REGION | 110000010 |
| 93241095754 | -7.005 | 129.560 | 147 | 5.8 | | BANDA SEA | 110000010 |
| 93242121231 | 48.508 | 143.326 | 18 | 5.2 | 4.3 | SAKHALIN ISLAND | 110000000 |
| 93243065532 | 41.878 | 49.466 | 85 | 5.3 | | CASPIAN SEA | 110000010 |
| 93244004123 | 31.712 | 141.611 | 46 | 5.4 | 5.7 | SOUTH OF HONSHU, JAPAN | 110000010 |
| 93244033527 | 31.859 | 141.641 | 44 | 5.1 | 4.9 | SOUTH OF HONSHU, JAPAN | 110000000 |
| 93244114838 | -4.331 | 102.567 | 71 | 5.8 | | SOUTHERN SUMATERA | 110000010 |
| 93244140319 | 2.986 | 96.122 | 34 | 5.9 | 6.2 | NORTHERN SUMATERA | 110000010 |
| 93246123500 | 14.523 | -92.713 | 27 | 5.8 | 6.8 | NEAR COAST OF CHIAPAS, MEXICO | 110000010 |
| 93247061137 | 13.862 | 145.003 | 26 | 5.5 | 4.6 | MARIANA ISLANDS | 110000000 |
| 93247113838 | 36.429 | 70.812 | 195 | 5.9 | | HINDU KUSH REGION | 110000010 |
| 93247172510 | 30.340 | 94.831 | 10 | 5.1 | | TIBET | 110000000 |
| 93247213933 | -9.571 | 122.528 | 33 | 5.8 | 5.8 | SAVU SEA | 110000010 |
| 93249035600 | -4.641 | 153.231 | 49 | 6.2 | 6.6 | NEW IRELAND REGION | 110000000 |
| 93250024850 | -31.635 | -179.440 | 10 | 5.9 | 6.5 | KERMADEC ISLANDS REGION | 110000010 |
| 93251113837 | 29.987 | 52.028 | 31 | 4.9 | 4.4 | SOUTHERN IRAN | 110100010 |
| 93251195441 | 40.191 | 52.490 | 82 | 4.5 | | TURKMEN SSR | 110100010 |
| 93253160232 | 35.039 | 12.366 | 10 | 5.0 | 4.9 | MEDITERRANEAN SEA | 110100000 |
| 93253191254 | 14.717 | -92.645 | 34 | 6.2 | 7.3 | NEAR COAST OF CHIAPAS, MEXICO | 110100010 |
| 93254045533 | 42.003 | 142.581 | 58 | 5.7 | | HOKKAIDO, JAPAN REGION | 110100010 |
| 93254173646 | 20.113 | 121.446 | 42 | 5.4 | 5.4 | PHILIPPINE ISLANDS REGION | 100100010 |
| 93255032238 | 13.826 | -90.429 | 68 | 5.4 | 5.5 | NEAR COAST OF GUATEMALA | 000100000 |
| 93255082234 | -29.608 | -177.279 | 33 | 5.6 | 5.8 | KERMADEC ISLANDS | 000100000 |
| 93256052207 | -6.072 | 149.908 | 30 | 5.3 | 5.4 | NEW BRITAIN REGION | 000100000 |
| 93256123751 | -29.492 | -177.136 | 20 | 5.8 | 6.2 | KERMADEC ISLANDS | 000100000 |
| 93257052112 | 14.410 | 53.566 | 10 | 4.7 | 4.3 | ARABIAN SEA | 000100000 |
| 93258150813 | 33.322 | 75.740 | 33 | 5.0 | | EASTERN KASHMIR | 100100000 |
| 93259005926 | 44.533 | 149.036 | 33 | 5.8 | 5.1 | KURIL ISLANDS | 100100010 |
| 93261002747 | 1.632 | 126.770 | 40 | 5.5 | 5.1 | MOLUCCA PASSAGE | 111100000 |
| 93261050227 | 36.421 | 71.592 | 113 | 6.1 | | AFGHANISTAN-USSR BORDER REGION | 111100000 |
| 93262041836 | -60.079 | -26.967 | 46 | 5.4 | 5.4 | SOUTH SANDWICH ISLANDS REGION | 110100010 |
| 93262141056 | 14.362 | -93.325 | 18 | 5.7 | 6.4 | NEAR COAST OF CHIAPAS, MEXICO | 110100010 |
| 93263101742 | 0.750 | -29.354 | 10 | 5.8 | 6.0 | CENTRAL MID-ATLANTIC RIDGE | 110100010 |
| 93264032855 | 42.314 | -122.012 | 11 | 5.7 | 5.8 | OREGON | 110100010 |
| 93264054533 | 42.358 | -122.045 | 5 | 5.6 | 5.8 | OREGON | 110100000 |
| 93264191135 | 11.478 | 39.638 | 15 | 5.4 | 5.0 | ETHIOPIA | 110100010 |
| 93265123703 | -6.470 | 154.901 | 28 | 6.1 | 6.0 | SOLOMON ISLANDS | 110100010 |
| 93268044419 | 38.167 | 73.002 | 103 | 4.4 | | TAJIK-XINJIANG BORDER REGION | 110100010 |
| 93269022934 | 36.253 | 71.219 | 106 | 4.6 | | AFGHANISTAN-USSR BORDER REGION | 110100000 |
| 93269033114 | 9.997 | 138.222 | 10 | 6.1 | 6.0 | WEST CAROLINE ISLANDS | 110100010 |
| 93269115552 | 13.009 | 145.016 | 64 | 5.8 | | MARIANA ISLANDS | 110100010 |
| 93270044355 | 30.678 | 132.121 | 38 | 5.5 | 5.3 | SOUTHEAST OF SHIKOKU, JAPAN | 110100010 |
| 93270133732 | -53.651 | -51.621 | 33 | 6.2 | 6.6 | SOUTH ATLANTIC OCEAN | 110100010 |
| 93272093920 | -18.966 | 167.667 | 35 | 5.5 | 5.2 | VANUATU ISLANDS | 110000000 |
| 93272111603 | 0.494 | 121.528 | 97 | 6.1 | | MINAHASSA PENINSULA | 110000010 |
| 93272141801 | 36.421 | 70.886 | 188 | 4.6 | | HINDU KUSH REGION | 110000010 |
| 93272182620 | -42.677 | -18.385 | 10 | 5.9 | 5.9 | SOUTH ATLANTIC RIDGE | 110000000 |
| 93272222548 | 18.066 | 76.451 | 7 | 6.3 | 6.2 | INDIA | 110000010 |
| 93273170445 | 11.815 | 92.529 | 23 | 5.4 | 4.7 | ANDAMAN ISLANDS REGION | 110000000 |
| 93273182750 | 15.417 | -94.698 | 19 | 5.8 | 6.4 | NEAR COAST OF OAXACA, MEXICO | 110000000 |
| 93274035933 | 36.637 | 23.967 | 88 | 4.9 | | SOUTHERN GREECE | 110000000 |
| 93275011730 | 39.066 | 69.966 | 14 | 5.0 | 4.4 | TAJIK SSR | 110000000 |
| 93275084232 | 38.190 | 88.663 | 14 | 6.2 | 6.3 | SOUTHERN XINJIANG, CHINA | 100000010 |
| 93275094319 | 38.169 | 88.605 | 14 | 5.8 | 5.3 | SOUTHERN XINJIANG, CHINA | 100000000 |
| 93275172333 | 38.171 | 88.690 | 14 | 5.6 | 5.0 | SOUTHERN XINJIANG, CHINA | 100000000 |

Appendix 1 (continued)

| EventID | Lat | Lon | Z | Mb | Ms | Location | Key 123456789 |
|---|---|---|---|---|---|---|---|
| 93277205438 | -21.437 | -174.301 | 34 | 5.8 | 5.7 | TONGA ISLANDS | 101000010 |
| 93278015956 | 41.667 | 88.695 | 0 | 5.9 | 4.7 | SOUTHERN XINJIANG, CHINA | 101000010 |
| 93278050945 | -6.130 | 128.965 | 13 | 5.9 | 6.1 | BANDA SEA | 101000010 |
| 93278183539 | 36.649 | 29.792 | 37 | 4.1 | | TURKEY | 101000000 |
| 93278212806 | 77.727 | 126.454 | 33 | 5.0 | | LAPTEV SEA | 101000010 |
| 93280032658 | 38.214 | 88.726 | 11 | 5.0 | | SOUTHERN XINJIANG, CHINA | 100000000 |
| 93280175938 | 36.443 | 70.628 | 216 | 4.9 | | HINDU KUSH REGION | 100000010 |
| 93281182347 | 46.505 | 150.037 | 172 | 5.5 | | KURIL ISLANDS | 100000010 |
| 93282222421 | 11.712 | 57.660 | 10 | 5.2 | 4.7 | ARABIAN SEA | 100000000 |
| 93284130729 | -17.845 | -178.726 | 555 | 5.8 | | FIJI ISLANDS REGION | 101100010 |
| 93284155421 | 32.020 | 137.832 | 351 | 6.4 | | SOUTH OF HONSHU, JAPAN | 101100010 |
| 93285023500 | -33.913 | 94.278 | 10 | 5.2 | 4.8 | SOUTH INDIAN OCEAN | 101100000 |
| 93285210452 | 13.048 | 51.063 | 10 | 5.0 | 4.8 | EASTERN GULF OF ADEN | 101110010 |
| 93286005233 | 7.576 | 121.484 | 44 | 5.3 | 4.8 | MINDANAO, PHILIPPINE ISLANDS | 101110010 |
| 93286020600 | -5.889 | 146.020 | 25 | 6.4 | 7.0 | EAST PAPUA NEW GUINEA REGION | 101110010 |
| 93286030730 | -5.932 | 146.153 | 33 | 6.1 | 6.7 | EAST PAPUA NEW GUINEA REGION | 101100000 |
| 93286233421 | 28.629 | 103.419 | 33 | 5.0 | | SICHUAN PROVINCE, CHINA | 101110010 |
| 93287120235 | -50.436 | 139.904 | 10 | 5.4 | 5.7 | SOUTH OF AUSTRALIA | 100110010 |
| 93288223719 | 40.744 | 48.105 | 56 | 4.8 | | EASTERN CAUCASUS | 100110000 |
| 93289030530 | -5.898 | 146.202 | 27 | 6.2 | 6.4 | EAST PAPUA NEW GUINEA REGION | 100110010 |
| 93289105225 | 7.472 | 123.447 | 31 | 5.5 | 5.4 | MINDANAO, PHILIPPINE ISLANDS | 100110010 |
| 93291012822 | 36.443 | 53.950 | 33 | 4.4 | | IRAN | 100110000 |
| 93291135714 | 22.133 | 62.861 | 10 | 5.2 | 4.7 | ARABIAN SEA | 100110010 |
| 93291205115 | 28.896 | 34.570 | 9 | 4.8 | | ARAB REPUBLIC OF EGYPT | 100110010 |
| 93292040221 | -22.378 | -65.971 | 272 | 5.9 | | JUJUY PROVINCE, ARGENTINA | 100110010 |
| 93292153137 | 38.791 | 73.242 | 33 | 4.8 | | TAJIK-XINJIANG BORDER REGION | 100110010 |
| 93292225038 | 35.140 | 25.888 | 83 | 4.3 | | CRETE | 100110000 |
| 93293101103 | 36.827 | 71.651 | 33 | 4.1 | | AFGHANISTAN-USSR BORDER REGION | 100110000 |
| 93294073655 | -56.497 | -138.909 | 10 | 5.4 | 5.4 | SOUTH PACIFIC CORDILLERA | 100110010 |
| 93294215220 | 30.154 | 51.235 | 15 | 5.2 | | IRAN | 101110010 |
| 93295084216 | -54.835 | -26.557 | 33 | 5.5 | 5.5 | SOUTH SANDWICH ISLANDS REGION | 101110010 |
| 93296132642 | 29.773 | 51.103 | 33 | 4.3 | | SOUTHERN IRAN | 100110000 |
| 93297055329 | 11.327 | 125.396 | 49 | 5.8 | 5.2 | SAMAR, PHILIPPINE ISLANDS | 100110010 |
| 93297075215 | 16.755 | -98.717 | 21 | 6.3 | 6.7 | NEAR COAST OF GUERRERO, MEXICO | 100110010 |
| 93298100711 | -5.882 | 145.933 | 18 | 5.7 | 5.6 | EAST PAPUA NEW GUINEA REGION | 100110010 |
| 93298102704 | -5.909 | 145.990 | 30 | 6.3 | 7.0 | EAST PAPUA NEW GUINEA REGION | 100110010 |
| 93298143319 | 41.336 | 49.478 | 33 | 4.7 | | CASPIAN SEA | 100110010 |
| 93299113821 | 38.477 | 98.655 | 8 | 5.9 | 5.4 | QINGHAI PROVINCE, CHINA | 100110010 |
| 93299202503 | 37.225 | 70.192 | 10 | 4.5 | | AFGHANISTAN-USSR BORDER REGION | 100110000 |
| 93301015206 | 41.604 | 142.024 | 67 | 5.2 | | HOKKAIDO, JAPAN REGION | 101110010 |
| 93301111357 | 34.390 | 26.203 | 47 | 4.6 | | CRETE | 101110000 |
| 93302040905 | 51.509 | -178.184 | 34 | 5.8 | 5.3 | ANDREANOF ISLANDS, ALEUTIAN IS. | 101110010 |
| 93303001607 | 11.249 | 57.597 | 10 | 4.7 | | ARABIAN SEA | 101110000 |
| 93303083033 | 15.437 | 121.785 | 39 | 5.3 | 5.1 | LUZON, PHILIPPINE ISLANDS | 101110010 |
| 93303175902 | -31.704 | -68.232 | 107 | 5.9 | | SAN JUAN PROVINCE, ARGENTINA | 101110010 |
| 93303230553 | 30.405 | 67.651 | 10 | 4.7 | 4.5 | PAKISTAN | 101110010 |
| 93305064631 | 28.244 | 57.569 | 10 | 4.7 | | SOUTHERN IRAN | 101110000 |
| 93305181722 | 38.950 | 29.947 | 13 | 4.7 | | TURKEY | 101110000 |
| 93306071450 | 42.812 | 131.129 | 546 | 4.9 | | E. USSR-N.E. CHINA BORDER REG. | 101110010 |
| 93307131810 | -7.123 | 67.916 | 10 | 5.4 | 5.4 | MID-INDIAN RISE | 101110010 |
| 93307183933 | 28.654 | 34.650 | 13 | 4.9 | 4.6 | ARAB REPUBLIC OF EGYPT | 101110010 |
| 93308003240 | 31.985 | 59.969 | 33 | 4.5 | | IRAN | 101110000 |
| 93308051837 | 38.372 | 22.002 | 17 | 5.0 | 5.2 | GREECE | 101110010 |
| 93309070206 | -7.033 | 106.101 | 75 | 5.4 | | JAVA | 101110010 |
| 93309223720 | -3.188 | 148.339 | 14 | 5.7 | 6.2 | BISMARCK SEA | 101110000 |
| 93311082951 | 34.494 | 70.671 | 33 | 4.7 | 3.9 | AFGHANISTAN | 101110000 |
| 93312010602 | 28.698 | 34.673 | 14 | 4.9 | 4.3 | ARAB REPUBLIC OF EGYPT | 101110010 |
| 93312204854 | 36.183 | 141.669 | 33 | 5.4 | 4.9 | NEAR EAST COAST OF HONSHU, JAPAN | 101110010 |
| 93313021403 | 14.353 | 53.744 | 10 | 5.3 | 5.1 | ARABIAN SEA | 101110010 |
| 93314214501 | -22.583 | 179.169 | 613 | 5.2 | | SOUTH OF FIJI ISLANDS | 101110010 |

Appendix 1 (continued)

| EventID | Lat | Lon | Z | Mb | Ms | Location | Key 123456789 |
|---|---|---|---|---|---|---|---|
| 93315002833 | 50.200 | -177.446 | 19 | 6.3 | 5.6 | ANDREANOF ISLANDS, ALEUTIAN IS. | 101110010 |
| 93315101355 | -4.543 | 153.147 | 46 | 5.7 | 5.5 | NEW IRELAND REGION | 101110010 |
| 93316111633 | 51.414 | -177.976 | 33 | 5.2 | 5.1 | ANDREANOF ISLANDS, ALEUTIAN IS. | 101110010 |
| 93316134923 | 40.929 | 51.907 | 33 | 4.4 | | CASPIAN SEA | 101110000 |
| 93317001649 | 16.288 | -98.638 | 20 | 5.7 | 5.3 | NEAR COAST OF GUERRERO, MEXICO | 101110010 |
| 93317011804 | 51.934 | 158.647 | 34 | 6.5 | 7.0 | NEAR EAST COAST OF KAMCHATKA | 101110010 |
| 93318082438 | 36.306 | 71.310 | 111 | 4.5 | | AFGHANISTAN-USSR BORDER REGION | 001110000 |
| 93319224519 | -18.559 | 167.637 | 48 | 5.2 | 4.8 | VANUATU ISLANDS | 101100000 |
| 93320155248 | 30.798 | 67.219 | 27 | 5.4 | 5.6 | PAKISTAN | 101100010 |
| 93321111851 | 51.816 | 158.659 | 33 | 6.1 | 5.6 | NEAR EAST COAST OF KAMCHATKA | 101100010 |
| 93323014323 | 54.287 | -164.164 | 30 | 6.1 | 6.4 | UNIMAK ISLAND REGION | 101100010 |
| 93323090539 | 7.317 | -34.703 | 10 | 5.7 | 5.6 | CENTRAL MID-ATLANTIC RIDGE | 101100010 |
| 93324192453 | 60.025 | -153.003 | 116 | 5.6 | | SOUTHERN ALASKA | 101100010 |
| 93326030055 | 5.877 | 126.229 | 38 | 5.7 | 5.1 | MINDANAO, PHILIPPINE ISLANDS | 101110010 |
| 93329083114 | -22.035 | 170.094 | 32 | 5.6 | 5.6 | LOYALTY ISLANDS REGION | 101110010 |
| 93329202400 | -0.963 | -13.264 | 10 | 5.7 | 5.5 | NORTH OF ASCENSION ISLAND | 101110010 |
| 93330232004 | -9.597 | 158.148 | 17 | 5.9 | 6.2 | SOLOMON ISLANDS | 101110010 |
| 93331061122 | 38.625 | 141.164 | 104 | 5.9 | | NEAR EAST COAST OF HONSHU, JAPAN | 101110010 |
| 93332105027 | -5.599 | 110.267 | 569 | 5.6 | | JAVA SEA | 101110010 |
| 93332205927 | 36.474 | 71.309 | 108 | 5.1 | | AFGHANISTAN-USSR BORDER REGION | 101110010 |
| 93334045926 | -59.047 | -18.158 | 33 | 5.2 | 5.5 | SOUTHWESTERN ATLANTIC OCEAN | 101110010 |
| 93334075830 | 36.537 | 71.050 | 170 | 4.3 | | AFGHANISTAN-USSR BORDER REGION | 101110000 |
| 93334203712 | 39.263 | 75.533 | 18 | 5.2 | 5.6 | SOUTHERN XINJIANG, CHINA | 101110010 |
| 93335005901 | -57.475 | -25.685 | 33 | 5.5 | 5.3 | SOUTH SANDWICH ISLANDS REGION | 101110010 |
| 93336143917 | 36.405 | 70.394 | 220 | 4.8 | | HINDU KUSH REGION | 101110010 |
| 93337054108 | 51.204 | 179.308 | 33 | 5.2 | 5.0 | RAT ISLANDS, ALEUTIAN ISLANDS | 101110010 |
| 93337123625 | -60.353 | -20.446 | 10 | 5.5 | 5.2 | SOUTHWESTERN ATLANTIC OCEAN | 101110010 |
| 93338233411 | 28.886 | 34.903 | 10 | 4.4 | 4.5 | ARAB REPUBLIC OF EGYPT | 101110000 |
| 93339001056 | 27.931 | 55.269 | 10 | 4.4 | | SOUTHERN IRAN | 101110000 |
| 93340025821 | 35.748 | 71.027 | 130 | 4.1 | | PAKISTAN | 101110000 |
| 93340104203 | -6.360 | 154.916 | 48 | 5.6 | 5.7 | SOLOMON ISLANDS | 101110010 |
| 93340125019 | 37.737 | 72.332 | 33 | 4.9 | | TAJIK SSR | 101110000 |
| 93340142535 | 39.201 | 30.189 | 33 | 4.1 | | TURKEY | 101110000 |
| 93340205445 | 6.818 | 78.301 | 10 | 5.2 | 4.7 | LACCADIVE SEA | 101110010 |
| 93343043219 | 0.486 | 125.995 | 15 | 6.5 | 6.7 | MOLUCCA PASSAGE | 101110010 |
| 93343113827 | 0.425 | 125.891 | 16 | 6.3 | 6.4 | MOLUCCA PASSAGE | 101110010 |
| 93344085935 | 20.912 | 121.282 | 12 | 5.8 | 5.8 | PHILIPPINE ISLANDS REGION | 101110010 |
| 93346170319 | 0.317 | 125.939 | 23 | 5.8 | 5.5 | MOLUCCA PASSAGE | 111110010 |
| 93346172126 | 41.514 | 28.823 | 28 | 4.8 | | TURKEY | 111110000 |
| 93346182628 | 0.344 | 125.925 | 33 | 5.6 | 5.5 | MOLUCCA PASSAGE | 111110010 |
| 93346204130 | 36.445 | 140.962 | 43 | 5.4 | 4.9 | NEAR EAST COAST OF HONSHU, JAPAN | 111110010 |
| 93347114344 | -20.422 | -173.839 | 33 | 5.8 | 5.9 | TONGA ISLANDS | 111110010 |
| 93348063119 | -20.704 | -173.451 | 31 | 5.5 | 6.1 | TONGA ISLANDS | 101110000 |
| 93348071214 | 37.963 | 72.732 | 134 | 5.0 | | TAJIK SSR | 101110000 |
| 93348074959 | -13.624 | 168.939 | 21 | 5.4 | 5.4 | VANUATU ISLANDS | 101110000 |
| 93349214942 | 23.184 | 120.574 | 17 | 5.5 | 5.2 | TAIWAN | 111110010 |
| 93350092215 | 41.473 | 23.079 | 10 | 4.5 | | GREECE-BULGARIA BORDER REGION | 111110000 |
| 93350114818 | 37.422 | 20.806 | 33 | 4.4 | | IONIAN SEA | 111110010 |
| 93350201121 | 53.804 | 171.382 | 9 | 5.8 | 5.7 | NEAR ISLANDS, ALEUTIAN ISLANDS | 111110010 |
| 93351031903 | 39.186 | 142.182 | 54 | 5.4 | | NEAR EAST COAST OF HONSHU, JAPAN | 111110010 |
| 93351174228 | 36.669 | 71.053 | 204 | 4.1 | | AFGHANISTAN-USSR BORDER REGION | 111110000 |
| 93352224420 | -20.477 | -173.883 | 33 | 5.7 | 5.7 | TONGA ISLANDS | 111110010 |
| 93353114530 | 25.210 | 62.603 | 24 | 5.1 | 5.0 | PAKISTAN | 111110010 |
| 93353175313 | 36.532 | 71.421 | 33 | 4.2 | | AFGHANISTAN-USSR BORDER REGION | 111110000 |
| 93354135614 | -6.876 | 131.340 | 8 | 6.4 | 5.7 | TANIMBAR ISLANDS REGION | 111110010 |
| 93354194538 | 36.330 | 71.086 | 33 | 4.6 | | AFGHANISTAN-USSR BORDER REGION | 111110000 |
| 93356103517 | -4.938 | 132.083 | 33 | 5.4 | | WEST IRIAN REGION | 111110010 |
| 93356194013 | 38.395 | 21.759 | 20 | 4.3 | | GREECE | 111110010 |
| 93357142235 | 36.756 | -2.937 | 27 | 5.0 | 4.9 | STRAIT OF GIBRALTAR | 111110010 |
| 93358051834 | -21.853 | -178.646 | 445 | 5.6 | | FIJI ISLANDS REGION | 111110010 |

Appendix 1 (continued)

| EventID | Lat | Lon | Z | Mb | Ms | Location | Key 123456789 |
|---|---|---|---|---|---|---|---|
| 93358215319 | 40.158 | 19.815 | 25 | 5.2 | 4.6 | ALBANIA | 111110010 |
| 93359100222 | 36.590 | 70.613 | 195 | 4.4 | | HINDU KUSH REGION | 111110010 |
| 93359101527 | 34.921 | 24.217 | 37 | 4.8 | | CRETE | 111110000 |
| 93359153335 | 37.467 | 68.253 | 33 | 4.5 | | AFGHANISTAN-USSR BORDER REGION | 111110000 |
| 93360084548 | 38.628 | 68.926 | 19 | 5.0 | | TAJIK SSR | 111110010 |
| 93362032943 | 12.519 | 125.267 | 40 | 5.6 | 5.6 | SAMAR, PHILIPPINE ISLANDS | 111110010 |
| 93362043521 | 12.470 | 125.288 | 24 | 5.3 | 4.8 | SAMAR, PHILIPPINE ISLANDS | 111110010 |
| 93363074814 | -20.230 | 169.789 | 33 | 6.1 | 6.7 | VANUATU ISLANDS | 111110010 |
| 93363083944 | -19.990 | 169.857 | 33 | 6.1 | 6.5 | VANUATU ISLANDS | 111110010 |
| 93363125719 | 32.003 | 49.029 | 79 | 4.2 | | WESTERN IRAN | 111110000 |
| 93364142404 | 44.735 | 78.793 | 15 | 5.7 | 5.2 | EASTERN KAZAKH SSR | 111110010 |
| 93365033030 | 40.169 | 63.304 | 33 | 4.3 | | UZBEK SSR | 111110000 |
| 94001051051 | 28.048 | 55.565 | 55 | 4.8 | | SOUTHERN IRAN | 111110000 |
| 94002041211 | 37.291 | 71.435 | 101 | 5.0 | | AFGHANISTAN-USSR BORDER REGION | 111110010 |
| 94003055227 | 36.028 | 100.104 | 8 | 5.8 | 5.5 | QINGHAI PROVINCE, CHINA | 111110010 |
| 94003132413 | -49.265 | 164.222 | 16 | 6.0 | 6.0 | AUCKLAND ISLANDS REGION | 111110010 |
| 94003210031 | 37.002 | 35.842 | 26 | 5.0 | 4.8 | TURKEY | 111110010 |
| 94004092938 | 29.188 | 51.442 | 30 | 4.8 | | SOUTHERN IRAN | 111110000 |
| 94004193159 | -4.301 | 135.145 | 11 | 5.8 | 6.0 | WEST IRIAN REGION | 111110010 |
| 94005132409 | 39.085 | 15.145 | 273 | 5.7 | | SOUTHERN ITALY | 111100010 |
| 94006022922 | 37.110 | 72.005 | 33 | 4.8 | | TAJIK SSR | 111100000 |
| 94007034242 | 52.028 | 159.019 | 55 | 5.6 | | OFF EAST COAST OF KAMCHATKA | 111100010 |
| 94007092546 | 34.761 | 71.211 | 37 | 4.7 | 4.0 | PAKISTAN | 111100000 |
| 94007192353 | -0.591 | 98.601 | 30 | 5.6 | 5.3 | SOUTHERN SUMATERA | 111100010 |
| 94008060411 | 36.006 | 70.712 | 98 | 4.8 | | HINDU KUSH REGION | 111100000 |
| 94009212901 | 48.482 | 154.491 | 65 | 5.9 | | KURIL ISLANDS | 111100010 |
| 94010155350 | -13.339 | -69.446 | 596 | 6.4 | | PERU-BOLIVIA BORDER REGION | 111100010 |
| 94011005156 | 25.231 | 97.203 | 10 | 6.0 | 5.9 | BURMA-CHINA BORDER REGION | 111100010 |
| 94011021805 | 25.223 | 97.128 | 32 | 4.6 | | BURMA-CHINA BORDER REGION | 111100000 |
| 94011072251 | 35.959 | 21.945 | 33 | 5.4 | 5.4 | MEDITERRANEAN SEA | 111100010 |
| 94012010024 | 30.511 | 131.637 | 45 | 5.0 | 4.6 | KYUSHU, JAPAN | 111100010 |
| 94012105045 | 34.797 | 23.099 | 10 | 4.6 | | CRETE | 111100010 |
| 94013094306 | -17.350 | -14.486 | 10 | 5.7 | | SOUTH ATLANTIC RIDGE | 111100010 |
| 94013235551 | 37.463 | 72.083 | 89 | 4.7 | | TAJIK SSR | 111100000 |
| 94014060748 | 37.571 | 20.942 | 31 | 4.8 | | IONIAN SEA | 111100000 |
| 94015165541 | 36.659 | 71.145 | 210 | 4.3 | | AFGHANISTAN-USSR BORDER REGION | 111110000 |
| 94015170331 | -20.849 | -173.926 | 36 | 5.5 | 5.6 | TONGA ISLANDS | 111110010 |
| 94016165813 | 49.106 | 103.276 | 12 | 4.8 | 4.7 | MONGOLIA | 111110010 |
| 94017123055 | 34.213 | -118.537 | 18 | 6.4 | 6.8 | SOUTHERN CALIFORNIA | 111110010 |
| 94017233330 | 34.326 | -118.698 | 10 | 5.7 | 5.9 | SOUTHERN CALIFORNIA | 111110010 |
| 94019015334 | -3.176 | 135.970 | 23 | 6.1 | 6.8 | WEST IRIAN REGION | 111110010 |
| 94019162648 | -17.584 | -178.495 | 533 | 5.4 | | FIJI ISLANDS REGION | 111110010 |
| 94020055010 | 23.976 | 121.811 | 36 | 5.4 | 5.3 | TAIWAN | 111110010 |
| 94020090652 | -6.002 | -77.052 | 123 | 5.8 | | NORTHERN PERU | 111110010 |
| 94021022429 | 1.015 | 127.733 | 20 | 6.2 | 7.2 | HALMAHERA | 111110010 |
| 94021180017 | -4.859 | 103.664 | 90 | 6.1 | | SOUTHERN SUMATERA | 111110010 |
| 94024195437 | 44.977 | 149.791 | 50 | 5.4 | | KURIL ISLANDS | 111100010 |
| 94025071244 | 10.601 | -41.715 | 30 | 5.3 | 5.9 | NORTH ATLANTIC RIDGE | 111100010 |
| 94025213148 | 36.421 | 71.111 | 223 | 4.9 | | AFGHANISTAN-USSR BORDER REGION | 111100010 |
| 94026100351 | 41.728 | 143.669 | 32 | 5.5 | 5.1 | HOKKAIDO, JAPAN REGION | 111100010 |
| 94028115209 | 38.719 | 38.688 | 17 | 4.4 | | TURKEY | 111100000 |
| 94028154524 | 38.693 | 27.493 | 5 | 5.2 | 5.1 | TURKEY | 111100010 |
| 94030205743 | -29.184 | -177.589 | 61 | 5.6 | | KERMADEC ISLANDS | 111110010 |
| 94031095735 | -37.132 | 52.395 | 10 | 5.2 | 4.8 | SOUTH INDIAN OCEAN | 111110010 |
| 94032093055 | 17.228 | 73.523 | 10 | 5.0 | | INDIA | 111110010 |
| 94032224428 | 24.778 | 122.525 | 133 | 5.4 | | TAIWAN REGION | 111100010 |
| 94033162011 | 36.363 | 71.349 | 75 | 4.6 | | AFGHANISTAN-USSR BORDER REGION | 111100010 |
| 94034102330 | -15.413 | 166.961 | 23 | 5.6 | 5.2 | VANUATU ISLANDS | 111110010 |
| 94034154343 | -41.886 | 84.490 | 10 | 5.4 | 5.4 | SOUTHEAST INDIAN RISE | 111110010 |
| 94036233409 | 0.593 | 30.037 | 14 | 5.8 | 6.0 | UGANDA | 111100010 |

Appendix 1 (continued)

| EventID | Lat | Lon | Z | Mb | Ms | Location | Key 123456789 |
|---|---|---|---|---|---|---|---|
| 94039032754 | 66.512 | -19.220 | 10 | 5.3 | 5.3 | ICELAND REGION | 111100010 |
| 94040192708 | -21.126 | -174.091 | 26 | 5.7 | 5.2 | TONGA ISLANDS | 111100010 |
| 94041022435 | 39.121 | 71.580 | 24 | 4.7 | 4.1 | TAJIK SSR | 111100010 |
| 94041061518 | 36.969 | 35.828 | 17 | 4.9 | 4.3 | TURKEY | 111100010 |
| 94042174007 | 42.478 | 43.726 | 16 | 4.5 | | WESTERN CAUCASUS | 111100000 |
| 94042211731 | -18.773 | 169.169 | 206 | 6.4 | | VANUATU ISLANDS | 111100010 |
| 94043041626 | -10.786 | -128.798 | 15 | 6.3 | 6.6 | SOUTH PACIFIC OCEAN | 111100010 |
| 94043175823 | -20.553 | 169.361 | 28 | 6.4 | 7.1 | VANUATU ISLANDS | 111100010 |
| 94045111427 | 51.920 | 158.894 | 51 | 5.6 | 5.5 | NEAR EAST COAST OF KAMCHATKA | 111100010 |
| 94046150817 | -20.563 | 169.393 | 30 | 5.8 | 5.7 | VANUATU ISLANDS | 111110010 |
| 94046170743 | -4.967 | 104.302 | 23 | 5.9 | 7.0 | SOUTHERN SUMATERA | 111110010 |
| 94046210939 | 36.104 | 100.164 | 20 | 5.6 | 5.5 | QINGHAI PROVINCE, CHINA | 111110010 |
| 94046222927 | 44.208 | 39.427 | 33 | 4.6 | | WESTERN CAUCASUS | 111110000 |
| 94047064657 | -20.094 | 168.906 | 13 | 5.7 | 6.3 | LOYALTY ISLANDS | 111110010 |
| 94047220308 | -20.230 | 168.925 | 11 | 5.7 | 5.8 | LOYALTY ISLANDS | 111110010 |
| 94048215247 | -9.506 | 152.083 | 20 | 5.5 | 5.6 | DENTRECASTEAUX ISLANDS REGION | 111110010 |
| 94048194156 | 9.891 | 125.838 | 35 | 5.4 | 5.0 | MINDANAO, PHILIPPINE ISLANDS | 011110000 |
| 94049041907 | -45.330 | 96.232 | 10 | 5.6 | 6.1 | SOUTHEAST INDIAN RISE | 111110010 |
| 94049125332 | 14.290 | 56.233 | 10 | 5.0 | 4.5 | ARABIAN SEA | 111110000 |
| 94049161940 | 14.133 | 56.248 | 10 | 5.2 | 4.8 | ARABIAN SEA | 111110010 |
| 94050031308 | 29.991 | 67.845 | 33 | 4.6 | | PAKISTAN | 111110010 |
| 94051015435 | 2.059 | 126.475 | 28 | 5.6 | 5.6 | MOLUCCA PASSAGE | 111110010 |
| 94051214812 | 13.691 | 120.787 | 207 | 5.6 | | MINDORO, PHILIPPINE ISLANDS | 111110010 |
| 94054080204 | 30.853 | 60.596 | 6 | 6.1 | 6.1 | IRAN | 111110010 |
| 94054115433 | 30.765 | 60.519 | 10 | 5.3 | 4.9 | IRAN | 111110010 |
| 94054224517 | 30.767 | 60.480 | 10 | 5.4 | | IRAN | 111110010 |
| 94055001112 | 30.775 | 60.495 | 10 | 6.1 | 6.1 | IRAN | 111110010 |
| 94055004500 | 30.869 | 60.510 | 10 | 4.5 | | IRAN | 111110000 |
| 94055100922 | 36.488 | 70.014 | 193 | 4.8 | | HINDU KUSH REGION | 111110010 |
| 94055152535 | -17.421 | -174.287 | 124 | 5.7 | | TONGA ISLANDS | 111110000 |
| 94055205131 | 30.924 | 60.446 | 10 | 4.7 | 4.4 | IRAN | 111110010 |
| 94056004029 | -17.420 | -174.271 | 121 | 5.6 | | TONGA ISLANDS | 111110000 |
| 94056023051 | 38.854 | 20.532 | 36 | 5.3 | 5.1 | GREECE | 111110010 |
| 94057023111 | 30.897 | 60.549 | 9 | 5.8 | 6.0 | IRAN | 111110010 |
| 94057180228 | 30.825 | 60.376 | 10 | 4.5 | | IRAN | 111110000 |
| 94058090427 | 30.832 | 131.427 | 40 | 4.9 | 5.0 | KYUSHU, JAPAN | 111110010 |
| 94059111354 | 30.805 | 60.562 | 10 | 5.5 | 5.5 | IRAN | 111110010 |
| 94060034900 | 29.096 | 52.617 | 13 | 5.8 | 6.0 | SOUTHERN IRAN | 111110010 |
| 94060190132 | 28.941 | 52.855 | 33 | 4.4 | | SOUTHERN IRAN | 111110000 |
| 94061130009 | 36.434 | 69.826 | 24 | 4.8 | 4.2 | HINDU KUSH REGION | 111110010 |
| 94061145722 | 30.844 | 60.460 | 33 | 4.6 | | IRAN | 111110000 |
| 94062145648 | 27.920 | 57.234 | 33 | 4.7 | | SOUTHERN IRAN | 111110000 |
| 94062151048 | 33.134 | 48.394 | 33 | 4.3 | 4.1 | WESTERN IRAN | 111110000 |
| 94062235401 | 28.900 | 52.465 | 33 | 4.9 | 3.9 | SOUTHERN IRAN | 111110000 |
| 94064040352 | 36.579 | 68.659 | 27 | 5.1 | 4.4 | HINDU KUSH REGION | 111110010 |
| 94065080143 | -21.556 | -113.701 | 10 | 5.6 | 5.7 | EASTER ISLAND CORDILLERA | 111110010 |
| 94066105457 | 33.146 | 48.033 | 26 | 4.8 | 4.2 | WESTERN IRAN | 111110000 |
| 94066172900 | 36.475 | 71.075 | 194 | 4.4 | | AFGHANISTAN-USSR BORDER REGION | 111110010 |
| 94068061337 | 32.625 | 47.150 | 10 | 4.5 | | IRAN-IRAQ BORDER REGION | 111110000 |
| 94068120834 | -9.580 | 154.986 | 38 | 5.7 | 5.6 | DENTRECASTEAUX ISLANDS REGION | 111110010 |
| 94068165837 | -9.444 | 159.604 | 10 | 5.6 | 5.4 | SOLOMON ISLANDS | 111110000 |
| 94068232806 | -18.039 | -178.413 | 563 | 6.6 | | FIJI ISLANDS REGION | 111110010 |
| 94069122543 | -18.058 | -178.260 | 600 | 5.2 | | FIJI ISLANDS REGION | 111110000 |
| 94072031128 | 51.343 | -178.231 | 33 | 5.3 | 4.4 | ANDREANOF ISLANDS, ALEUTIAN IS. | 111110010 |
| 94073043007 | -1.083 | -23.929 | 10 | 6.0 | | CENTRAL MID-ATLANTIC RIDGE | 111110000 |
| 94073205124 | 15.994 | -92.428 | 164 | 5.8 | 6.2 | MEXICO-GUATEMALA BORDER REGION | 111110010 |
| 94074033619 | 11.110 | -88.083 | 15 | 5.8 | 5.6 | OFF COAST OF CENTRAL AMERICA | 111110010 |
| 94074214615 | 36.800 | 54.780 | 33 | 4.4 | | IRAN | 111010000 |
| 94076080616 | 28.941 | 52.536 | 33 | 4.8 | | SOUTHERN IRAN | 111010000 |
| 94077035110 | 29.035 | 52.491 | 33 | 4.4 | | SOUTHERN IRAN | 111010000 |

Appendix 1 (continued)

| EventID | Lat | Lon | Z | Mb | Ms | Location | Key 123456789 |
|---|---|---|---|---|---|---|---|
| 94078012444 | 51.500 | 159.290 | 33 | 5.3 | 5.2 | OFF EAST COAST OF KAMCHATKA | 111010010 |
| 94078045400 | 28.633 | 53.129 | 33 | 4.4 | | SOUTHERN IRAN | 111010000 |
| 94078055704 | 28.727 | 52.588 | 33 | 4.4 | | SOUTHERN IRAN | 111010000 |
| 94082171445 | 28.874 | 52.596 | 33 | 4.7 | | SOUTHERN IRAN | 111010010 |
| 94085152224 | 39.506 | 55.155 | 33 | 4.3 | | TURKMEN SSR | 111010000 |
| 94085215101 | 33.437 | 141.289 | 38 | 5.4 | | OFF EAST COAST OF HONSHU, JAPAN | 111010000 |
| 94086134512 | -10.326 | 161.153 | 54 | 5.4 | 5.2 | SOLOMON ISLANDS | 111010000 |
| 94088075653 | 29.096 | 51.256 | 33 | 5.4 | | SOUTHERN IRAN | 111010010 |
| 94088112041 | 30.695 | 70.385 | 33 | 4.6 | | PAKISTAN | 111010000 |
| 94089132911 | 9.003 | 126.254 | 40 | 5.9 | 5.3 | MINDANAO, PHILIPPINE ISLANDS | 111010010 |
| 94089195546 | 28.994 | 52.745 | 54 | 5.5 | | SOUTHERN IRAN | 111010010 |
| 94090224052 | -22.057 | -179.533 | 580 | 6.1 | | SOUTH OF FIJI ISLANDS | 101010010 |
| 94091142459 | 28.823 | 52.650 | 33 | 4.6 | | SOUTHERN IRAN | 101010000 |
| 94093065157 | 28.821 | 52.745 | 23 | 5.2 | 4.8 | SOUTHERN IRAN | 101010010 |
| 94093071936 | 28.887 | 52.705 | 33 | 4.7 | | SOUTHERN IRAN | 101010000 |
| 94093130351 | 30.134 | 68.015 | 33 | 4.4 | | PAKISTAN | 101010000 |
| 94093224937 | 36.420 | 67.212 | 21 | 4.8 | 4.7 | HINDU KUSH REGION | 101010010 |
| 94094013702 | -15.468 | -173.014 | 24 | 5.7 | 5.5 | TONGA ISLANDS | 101010010 |
| 94094152833 | 36.194 | 66.826 | 33 | 4.5 | | HINDU KUSH REGION | 101010010 |
| 94094183547 | 37.017 | 71.382 | 80 | 4.7 | | AFGHANISTAN-USSR BORDER REGION | 101010000 |
| 94095093544 | 51.296 | -178.152 | 20 | 5.8 | 6.0 | ANDREANOF ISLANDS, ALEUTIAN IS. | 101010010 |
| 94096070327 | 26.188 | 96.867 | 33 | 5.6 | 5.6 | BURMA | 101010010 |
| 94096121344 | -17.371 | 167.816 | 17 | 5.6 | 5.9 | VANUATU ISLANDS | 101010010 |
| 94096211832 | 28.740 | 34.645 | 10 | 4.6 | | ARAB REPUBLIC OF EGYPT | 101010000 |
| 94098011040 | 40.608 | 143.683 | 13 | 6.0 | 6.3 | OFF EAST COAST OF HONSHU, JAPAN | 101010010 |
| 94100134047 | 43.049 | 46.180 | 86 | 4.7 | | EASTERN CAUCASUS | 101010010 |
| 94100194620 | 39.982 | 23.620 | 20 | 4.7 | 4.6 | AEGEAN SEA | 101010010 |
| 94100234555 | 23.710 | 126.852 | 10 | 5.9 | 5.8 | RYUKYU ISLANDS REGION | 101010010 |
| 94101112021 | 11.735 | 42.859 | 16 | 5.6 | 5.7 | ETHIOPIA | 101010010 |
| 94102001717 | 44.515 | 146.612 | 123 | 5.4 | | KURIL ISLANDS | 101010010 |
| 94102111442 | 34.956 | 24.074 | 13 | 4.7 | | CRETE | 101010000 |
| 94103040047 | 22.775 | 123.628 | 10 | 5.7 | 5.6 | SOUTHEAST OF TAIWAN | 101010010 |
| 94103141923 | -33.975 | -108.801 | 10 | 5.0 | 5.5 | EASTER ISLAND CORDILLERA | 101010010 |
| 94103222229 | -3.136 | 135.968 | 29 | 6.0 | 6.3 | WEST IRIAN REGION | 101010010 |
| 94104032826 | -6.587 | 129.771 | 166 | 5.8 | | BANDA SEA | 101010010 |
| 94104100805 | 29.158 | 51.592 | 33 | 4.5 | | SOUTHERN IRAN | 111010000 |
| 94104110340 | 28.290 | 55.340 | 22 | 5.2 | | SOUTHERN IRAN | 111010010 |
| 94104112637 | 28.237 | 55.288 | 20 | 4.6 | | SOUTHERN IRAN | 111010000 |
| 94104201539 | -7.015 | 155.885 | 40 | 5.7 | 5.1 | SOLOMON ISLANDS | 111010000 |
| 94107054651 | 37.042 | 71.485 | 129 | 4.5 | | AFGHANISTAN-USSR BORDER REGION | 111010010 |
| 94107080232 | 41.948 | 46.317 | 33 | 5.0 | 4.6 | EASTERN CAUCASUS | 111010010 |
| 94108162955 | -34.531 | -71.897 | 5 | 0.0 | | NEAR COAST OF CENTRAL CHILE | 111010000 |
| 94108172954 | -6.470 | 154.934 | 26 | 6.6 | 6.7 | SOLOMON ISLANDS | 111010010 |
| 94108200735 | 36.319 | 70.922 | 134 | 5.0 | | HINDU KUSH REGION | 111010010 |
| 94109161455 | 31.432 | 49.536 | 17 | 4.8 | 4.4 | WESTERN IRAN | 111010000 |
| 94110000508 | 28.294 | 55.326 | 24 | 4.8 | | SOUTHERN IRAN | 111010010 |
| 94110233530 | -17.800 | -178.404 | 543 | 5.6 | | FIJI ISLANDS REGION | 111010010 |
| 94111024215 | -5.617 | 154.067 | 38 | 5.5 | 5.5 | SOLOMON ISLANDS | 111010010 |
| 94111035144 | -5.702 | 154.120 | 28 | 5.9 | 6.6 | SOLOMON ISLANDS | 111010010 |
| 94111115032 | 27.477 | 54.385 | 33 | 4.6 | | SOUTHERN IRAN | 111010000 |
| 94113150052 | -14.175 | 167.537 | 11 | 6.0 | 6.0 | VANUATU ISLANDS | 111010000 |
| 94114025710 | 11.604 | 43.014 | 10 | 5.3 | 4.9 | ETHIOPIA | 111010000 |
| 94115001905 | 60.899 | -151.142 | 68 | 5.4 | | KENAI PENINSULA, ALASKA | 111010000 |
| 94116185927 | 56.727 | 117.867 | 18 | 5.3 | 5.4 | EAST OF LAKE BAIKAL | 111010010 |
| 94117092326 | -21.515 | -173.667 | 28 | 6.2 | 6.1 | TONGA ISLANDS | 111010010 |
| 94117141145 | 13.074 | 119.545 | 10 | 5.8 | 5.8 | PHILIPPINE ISLANDS REGION | 111010010 |
| 94118164454 | -39.312 | -74.756 | 27 | 5.7 | 5.0 | OFF COAST OF CENTRAL CHILE | 111010010 |
| 94119071129 | -28.299 | -63.252 | 562 | 6.3 | | SANTIAGO DEL ESTERO PROV., ARG. | 111010010 |
| 94120032838 | 31.420 | 131.292 | 26 | 5.7 | 5.6 | KYUSHU, JAPAN | 111010000 |
| 94121120035 | 36.901 | 67.163 | 19 | 6.0 | 6.3 | HINDU KUSH REGION | 111010000 |

Appendix 1 (continued)

| EventID | Lat | Lon | Z | Mb | Ms | Location | Key 123456789 |
|---|---|---|---|---|---|---|---|
| 94121211720 | 39.126 | 71.621 | 33 | 5.2 | 4.6 | TAJIK SSR | 111010000 |
| 94122171400 | -1.116 | 97.487 | 15 | 6.2 | 5.8 | SOUTHWEST OF SUMATERA | 111010010 |
| 94122181405 | 40.306 | 43.130 | 59 | 4.5 | | TURKEY-USSR BORDER REGION | 111010000 |
| 94123163643 | 10.241 | -60.758 | 36 | 5.8 | 5.8 | TRINIDAD | 111010010 |
| 94123202018 | 33.501 | 47.384 | 33 | 4.4 | | WESTERN IRAN | 111010000 |
| 94124063736 | -17.047 | 168.265 | 206 | 5.8 | | VANUATU ISLANDS | 101010010 |
| 94124114721 | 51.518 | -168.518 | 33 | 5.5 | 4.7 | FOX ISLANDS, ALEUTIAN ISLANDS | 101010010 |
| 94125051449 | 64.578 | -17.482 | 9 | 5.7 | 5.2 | ICELAND | 101010010 |
| 94125111853 | 37.648 | 72.040 | 33 | 4.5 | | TAJIK SSR | 101010000 |
| 94126042439 | 40.109 | 73.611 | 33 | 4.7 | | KIRGHIZ SSR | 101010010 |
| 94126182037 | -59.982 | -18.550 | 10 | 5.4 | 5.7 | SOUTHWESTERN ATLANTIC OCEAN | 101010010 |
| 94126223926 | -4.681 | 153.099 | 49 | 5.8 | 5.5 | NEW IRELAND REGION | 101010010 |
| 94127142444 | 30.329 | 50.586 | 54 | 4.7 | | IRAN | 101010000 |
| 94128034825 | -56.381 | 147.096 | 10 | 5.2 | 5.1 | WEST OF MACQUARIE ISLAND | 101010010 |
| 94129091411 | 40.263 | 78.938 | 46 | 4.8 | 4.7 | SOUTHERN XINJIANG, CHINA | 101010010 |
| 94129123637 | -2.060 | 99.731 | 28 | 6.0 | 5.5 | SOUTHERN SUMATERA | 101010010 |
| 94130014903 | -19.613 | -69.792 | 52 | 5.8 | | NORTHERN CHILE | 101010010 |
| 94130062653 | 5.234 | 125.971 | 111 | 4.6 | | MINDANAO, PHILIPPINE ISLANDS | 101010010 |
| 94130181912 | 13.433 | 120.603 | 70 | 5.7 | | MINDORO, PHILIPPINE ISLANDS | 101010000 |
| 94131081815 | -2.008 | 99.770 | 21 | 6.0 | 6.3 | SOUTHERN SUMATERA | 101010010 |
| 94131114111 | 37.471 | 72.327 | 130 | 4.2 | | TAJIK SSR | 101010000 |
| 94131211433 | -2.056 | 99.669 | 28 | 5.9 | 5.9 | SOUTHERN SUMATERA | 101010010 |
| 94133201227 | 7.972 | 123.189 | 33 | 5.6 | 5.6 | MINDANAO, PHILIPPINE ISLANDS | 101010010 |
| 94134223434 | 15.207 | 42.055 | 10 | 5.0 | 4.7 | WESTERN ARABIAN PENINSULA | 101010010 |
| 94135034457 | -48.993 | 73.666 | 10 | 5.8 | 5.7 | KERGUELEN ISLANDS REGION | 101010010 |
| 94137094613 | -1.902 | 99.618 | 33 | 5.7 | 5.6 | SOUTHERN SUMATERA | 101010010 |
| 94138035400 | 44.727 | 149.401 | 26 | 6.0 | 5.9 | KURIL ISLANDS | 101010010 |
| 94138165609 | 29.038 | 142.295 | 33 | 5.3 | 5.1 | SOUTH OF HONSHU, JAPAN | 101010010 |
| 94138171852 | 41.133 | 43.982 | 10 | 4.5 | | TURKEY-USSR BORDER REGION | 101010000 |
| 94139234143 | -8.204 | 124.813 | 33 | 5.4 | | TIMOR | 101010010 |
| 94140164000 | 25.099 | 128.829 | 37 | 5.7 | 5.1 | RYUKYU ISLANDS | 101010010 |
| 94142191233 | 12.405 | 57.834 | 10 | 4.5 | 4.7 | ARABIAN SEA | 101010000 |
| 94143014142 | 18.165 | -100.527 | 55 | 6.0 | | GUERRERO, MEXICO | 101010010 |
| 94143053601 | 24.166 | 122.535 | 20 | 5.7 | 6.0 | TAIWAN REGION | 101010000 |
| 94143064616 | 35.559 | 24.727 | 76 | 6.0 | | CRETE | 101010000 |
| 94143150448 | 14.657 | 54.465 | 10 | 4.5 | | ARABIAN SEA | 101010000 |
| 94143151657 | 24.065 | 122.560 | 26 | 6.0 | 5.8 | TAIWAN REGION | 101010010 |
| 94144020536 | 38.664 | 26.542 | 17 | 5.0 | 5.3 | AEGEAN SEA | 101010010 |
| 94144040042 | 23.959 | 122.448 | 16 | 6.2 | 6.7 | TAIWAN REGION | 101010010 |
| 94144211319 | 56.170 | 161.169 | 95 | 5.9 | | NEAR EAST COAST OF KAMCHATKA | 101010010 |
| 94145040341 | -4.199 | 135.489 | 33 | 6.0 | 6.4 | WEST IRIAN REGION | 101010010 |
| 94145074258 | 40.232 | 63.134 | 33 | 5.2 | | UZBEK SSR | 101010010 |
| 94145111515 | 35.560 | 71.344 | 33 | 4.2 | 4.4 | PAKISTAN | 101010000 |
| 94145163653 | -1.962 | 138.805 | 28 | 5.5 | 5.1 | NEAR N. COAST OF WEST IRIAN | 101010000 |
| 94145184219 | 7.646 | 94.279 | 25 | 5.7 | 5.5 | NICOBAR ISLANDS REGION | 101010000 |
| 94146034627 | 39.805 | 69.833 | 33 | 4.7 | | TAJIK SSR | 101010000 |
| 94146082652 | 35.305 | -4.103 | 10 | 5.7 | 5.8 | STRAIT OF GIBRALTAR | 101010000 |
| 94146233542 | 14.768 | 54.842 | 10 | 5.0 | | ARABIAN SEA | 101010000 |
| 94147024952 | 15.119 | 57.771 | 10 | 4.6 | | ARABIAN SEA | 101010000 |
| 94147044911 | 37.049 | 72.498 | 150 | 4.5 | | TAJIK SSR | 101010000 |
| 94148080432 | 35.406 | 136.134 | 49 | 5.1 | 4.4 | SOUTHERN HONSHU, JAPAN | 101010010 |
| 94148090350 | 37.750 | 72.737 | 33 | 4.3 | | TAJIK SSR | 101010000 |
| 94149141150 | 20.556 | 94.160 | 36 | 6.2 | 6.2 | BURMA | 101000010 |
| 94151174155 | 7.414 | -72.033 | 12 | 6.3 | 5.6 | NORTHERN COLOMBIA | 101000010 |
| 94152113308 | 38.307 | 39.463 | 10 | 4.3 | | TURKEY | 101000000 |
| 94153181734 | -10.477 | 112.835 | 18 | 5.7 | 7.2 | SOUTH OF JAVA | 101000010 |
| 94154112506 | 3.524 | -78.778 | 9 | 5.9 | 5.1 | SOUTH OF PANAMA | 101000010 |
| 94154155311 | 36.817 | 71.346 | 33 | 4.7 | | AFGHANISTAN-USSR BORDER REGION | 101000000 |
| 94154210659 | -10.362 | 112.892 | 26 | 6.1 | 6.4 | SOUTH OF JAVA | 101000010 |
| 94154224021 | 28.736 | 70.070 | 33 | 5.9 | 5.6 | PAKISTAN | 101000010 |

Appendix 1 (continued)

| EventID | Lat | Lon | Z | Mb | Ms | Location | Key 123456789 |
|---|---|---|---|---|---|---|---|
| 94155005750 | -10.777 | 113.366 | 11 | 6.0 | 6.3 | SOUTH OF JAVA | 101000010 |
| 94155103856 | 36.821 | 54.747 | 33 | 4.6 | | IRAN | 101000000 |
| 94155113636 | -10.831 | 113.225 | 34 | 5.6 | 5.1 | SOUTH OF JAVA | 101000010 |
| 94155200934 | -10.826 | 113.199 | 30 | 5.7 | 5.1 | SOUTH OF JAVA | 101000010 |
| 94156010930 | 24.511 | 121.905 | 11 | 6.1 | 6.6 | TAIWAN | 101000010 |
| 94156014502 | -10.349 | 113.398 | 26 | 5.8 | | SOUTH OF JAVA | 101000000 |
| 94156165408 | 29.601 | 52.313 | 33 | 4.5 | | SOUTHERN IRAN | 101000000 |
| 94157080238 | 36.333 | 71.413 | 33 | 4.7 | | AFGHANISTAN-USSR BORDER REGION | 101000000 |
| 94157090300 | 28.598 | 129.099 | 60 | 5.8 | | RYUKYU ISLANDS | 101000010 |
| 94157204740 | 2.917 | -76.057 | 12 | 6.4 | 6.6 | COLOMBIA | 101000010 |
| 94157222223 | 38.849 | 71.581 | 33 | 4.5 | | AFGHANISTAN-USSR BORDER REGION | 101000000 |
| 94158183142 | -5.792 | 104.436 | 42 | 5.7 | | SOUTHERN SUMATERA | 101000010 |
| 94160003316 | -13.841 | -67.553 | 631 | 7.0 | | NORTHERN BOLIVIA | 101000010 |
| 94160011517 | -14.365 | -68.439 | 650 | 6.1 | | PERU-BOLIVIA BORDER REGION | 101000000 |
| 94160162222 | 13.259 | 124.281 | 76 | 5.8 | | LUZON, PHILIPPINE ISLANDS | 101000010 |
| 94160203650 | 36.945 | 71.325 | 87 | 5.4 | | AFGHANISTAN-USSR BORDER REGION | 101000010 |
| 94161030044 | 38.560 | 70.629 | 33 | 5.4 | 4.6 | AFGHANISTAN-USSR BORDER REGION | 101000010 |
| 94161062557 | 41.527 | 88.710 | 0 | 5.8 | | SOUTHERN XINJIANG, CHINA | 101000010 |
| 94161213950 | 27.995 | 140.700 | 28 | 5.4 | 5.0 | BONIN ISLANDS REGION | 101000000 |
| 94162093756 | 29.070 | 52.537 | 18 | 4.8 | 4.2 | SOUTHERN IRAN | 101000010 |
| 94162161903 | 36.223 | 70.229 | 133 | 4.7 | | HINDU KUSH REGION | 101000010 |
| 94164100749 | 29.162 | 52.625 | 33 | 4.2 | | SOUTHERN IRAN | 101000000 |
| 94164210409 | -10.285 | 113.491 | 24 | 5.7 | 5.6 | SOUTH OF JAVA | 101000010 |
| 94166092257 | -10.335 | 113.660 | 20 | 6.0 | 6.1 | SOUTH OF JAVA | 101000010 |
| 94166165301 | 37.596 | 30.075 | 8 | 4.4 | | TURKEY | 101000000 |
| 94167101246 | -7.391 | 128.125 | 109 | 6.0 | | BANDA SEA | 101000010 |
| 94167184128 | -15.250 | -70.294 | 200 | 5.6 | | SOUTHERN PERU | 101000000 |
| 94169032515 | -42.963 | 171.658 | 14 | 6.2 | 7.1 | SOUTH ISLAND, NEW ZEALAND | 100000010 |
| 94169124200 | 28.971 | 52.673 | 11 | 5.1 | | SOUTHERN IRAN | 101000010 |
| 94169223819 | -10.150 | 113.632 | 46 | 5.6 | 5.0 | SOUTH OF JAVA | 101000010 |
| 94170134351 | -43.273 | 171.611 | 10 | 5.7 | 5.9 | SOUTH ISLAND, NEW ZEALAND | 101000010 |
| 94171090902 | 28.968 | 52.614 | 9 | 5.9 | 5.7 | SOUTHERN IRAN | 101001010 |
| 94171104434 | 29.131 | 52.388 | 33 | 4.5 | | SOUTHERN IRAN | 101001000 |
| 94172041552 | 29.021 | 52.596 | 41 | 4.7 | | SOUTHERN IRAN | 011001010 |
| 94172031754 | 29.151 | 52.554 | 33 | 4.4 | 4.5 | SOUTHERN IRAN | 001001000 |
| 94173065858 | 28.754 | 53.051 | 10 | 4.3 | | SOUTHERN IRAN | 111001000 |
| 94174201128 | 37.697 | 37.077 | 10 | 4.2 | | TURKEY | 111001000 |
| 94175013236 | 30.252 | 52.006 | 33 | 4.0 | | IRAN | 111001000 |
| 94176050046 | 41.777 | 43.697 | 33 | 4.4 | | TURKEY-USSR BORDER REGION | 111100000 |
| 94176083806 | 43.883 | 147.213 | 66 | 5.3 | | KURIL ISLANDS | 111100000 |
| 94176104416 | 39.386 | 72.707 | 33 | 4.7 | | KIRGHIZ SSR | 111100000 |
| 94178120303 | -16.122 | 67.484 | 10 | 5.1 | 4.5 | MID-INDIAN RISE | 111100100 |
| 94180182233 | 32.567 | 93.673 | 10 | 5.9 | 5.6 | TIBET | 111100110 |
| 94181092321 | 36.326 | 71.130 | 227 | 6.1 | | AFGHANISTAN-USSR BORDER REGION | 111100110 |
| 94181095509 | 40.941 | 50.609 | 33 | 4.9 | | CASPIAN SEA | 111100100 |
| 94182101241 | 40.232 | 53.383 | 41 | 6.0 | 5.2 | TURKMEN SSR | 111100110 |
| 94182130555 | 27.645 | 56.514 | 44 | 5.0 | 4.2 | SOUTHERN IRAN | 111100110 |
| 94182195004 | 40.219 | 53.391 | 44 | 5.6 | | TURKMEN SSR | 111100110 |
| 94182200231 | 38.267 | 38.824 | 10 | 4.7 | | TURKEY | 111100110 |
| 94183091443 | -5.763 | 131.103 | 88 | 5.9 | | BANDA SEA | 111100110 |
| 94183204532 | 36.714 | 68.707 | 33 | 4.8 | | HINDU KUSH REGION | 111100110 |
| 94183210726 | 36.743 | 68.650 | 57 | 4.7 | | HINDU KUSH REGION | 111100110 |
| 94184142641 | 28.742 | 34.573 | 15 | 4.3 | | ARAB REPUBLIC OF EGYPT | 111100110 |
| 94184214444 | -48.219 | 31.542 | 10 | 5.2 | 4.8 | SOUTH OF AFRICA | 111100100 |
| 94185213641 | 14.888 | -97.322 | 15 | 6.1 | 6.1 | OFF COAST OF OAXACA, MEXICO | 111100110 |
| 94186100922 | 10.432 | 125.322 | 29 | 5.5 | 5.5 | LEYTE, PHILIPPINE ISLANDS | 111100110 |
| 94187091310 | 5.983 | 125.929 | 151 | 5.7 | | MINDANAO, PHILIPPINE ISLANDS | 111100110 |
| 94187121925 | 37.024 | 71.645 | 33 | 4.8 | | AFGHANISTAN-USSR BORDER REGION | 111100110 |
| 94188193126 | 44.359 | 79.130 | 33 | 4.4 | | EASTERN KAZAKH SSR | 111100110 |
| 94189171014 | 0.256 | 66.740 | 10 | 5.1 | 4.8 | CARLSBERG RIDGE | 111100110 |

Appendix 1 (continued)

| EventID | Lat | Lon | Z | Mb | Ms | Location | Key 123456789 |
|---|---|---|---|---|---|---|---|
| 94190155758 | -37.217 | -95.101 | 26 | 5.4 | 5.1 | SOUTHERN PACIFIC OCEAN | 111100110 |
| 94191231406 | 36.478 | 70.150 | 230 | 4.8 | | HINDU KUSH REGION | 111100110 |
| 94192205737 | 37.541 | 54.474 | 29 | 4.8 | 4.3 | IRAN-USSR BORDER REGION | 111100110 |
| 94193001216 | 37.774 | 54.611 | 33 | 4.6 | | IRAN-USSR BORDER REGION | 111100100 |
| 94193043505 | 36.411 | 71.056 | 248 | 4.6 | | AFGHANISTAN-USSR BORDER REGION | 111100110 |
| 94194002514 | -16.644 | 167.469 | 33 | 5.4 | 5.1 | VANUATU ISLANDS | 111100110 |
| 94194023556 | -16.620 | 167.518 | 33 | 6.4 | 7.3 | VANUATU ISLANDS | 111100110 |
| 94194052343 | 29.875 | 51.195 | 33 | 4.5 | | SOUTHERN IRAN | 111100100 |
| 94194114523 | -7.532 | 127.770 | 159 | 6.5 | | BANDA SEA | 111100110 |
| 94195000924 | -16.582 | 167.452 | 20 | 5.6 | 5.9 | VANUATU ISLANDS | 111100110 |
| 94195201351 | 28.070 | 55.489 | 33 | 4.6 | | SOUTHERN IRAN | 111100100 |
| 94197180505 | -4.619 | 125.615 | 443 | 5.8 | | BANDA SEA | 111100100 |
| 94199154416 | 38.713 | 20.435 | 10 | 4.8 | | GREECE | 111000100 |
| 94199163359 | -9.591 | 112.939 | 33 | 5.6 | 5.0 | SOUTH OF JAVA | 111000110 |
| 94200040549 | 37.563 | 71.958 | 33 | 4.8 | | AFGHANISTAN-USSR BORDER REGION | 111000100 |
| 94200115944 | -23.438 | -175.470 | 50 | 5.3 | 5.7 | TONGA ISLANDS REGION | 111000110 |
| 94202183631 | 42.340 | 132.865 | 471 | 6.5 | | NEAR E. COAST OF EASTERN USSR | 111000100 |
| 94203165748 | -7.777 | 158.417 | 19 | 5.9 | 5.9 | SOLOMON ISLANDS | 111000100 |
| 94204070814 | 37.438 | 54.413 | 31 | 4.9 | | IRAN-USSR BORDER REGION | 111000100 |
| 94204205759 | 31.068 | 86.549 | 16 | 5.1 | 5.0 | TIBET | 111000110 |
| 94205054710 | 40.402 | 63.680 | 33 | 4.1 | | UZBEK SSR | 111000100 |
| 94205144748 | 37.006 | 71.662 | 120 | 5.6 | | AFGHANISTAN-USSR BORDER REGION | 111000110 |
| 94205175540 | -16.966 | 167.574 | 21 | 5.9 | 6.5 | VANUATU ISLANDS | 111000110 |
| 94205215727 | -10.654 | 113.269 | 34 | 6.0 | | SOUTH OF JAVA | 111000110 |
| 94206220022 | -56.362 | -27.365 | 81 | 6.3 | | SOUTH SANDWICH ISLANDS REGION | 111000100 |
| 94207014633 | -10.263 | 113.590 | 33 | 5.7 | | SOUTH OF JAVA | 111000110 |
| 94207180141 | 28.481 | 52.122 | 33 | 4.2 | | SOUTHERN IRAN | 111000100 |
| 94208133937 | 36.438 | 71.198 | 129 | 4.5 | | AFGHANISTAN-USSR BORDER REGION | 111000110 |
| 94209080301 | -47.278 | 100.224 | 10 | 5.3 | 5.7 | SOUTHEAST INDIAN RISE | 111000110 |
| 94210001745 | 52.398 | -168.333 | 11 | 6.0 | 5.6 | FOX ISLANDS, ALEUTIAN ISLANDS | 111000110 |
| 94210075328 | -16.984 | 167.739 | 14 | 5.7 | 5.8 | VANUATU ISLANDS | 111000110 |
| 94210220627 | 36.417 | 71.087 | 118 | 4.5 | | AFGHANISTAN-USSR BORDER REGION | 111000110 |
| 94211103745 | 37.493 | 36.189 | 10 | 4.7 | | TURKEY | 111000110 |
| 94211212125 | 40.890 | 142.596 | 57 | 5.1 | | NEAR EAST COAST OF HONSHU, JAPAN | 111000100 |
| 94212051539 | 32.558 | 48.369 | 43 | 5.3 | 5.3 | WESTERN IRAN | 111000110 |
| 94214141752 | 52.428 | 158.044 | 145 | 6.0 | | NEAR EAST COAST OF KAMCHATKA | 111000110 |
| 94215145957 | 21.514 | 93.981 | 34 | 5.7 | 5.1 | BURMA | 111000110 |
| 94216221537 | -6.338 | 131.575 | 33 | 6.2 | 5.6 | TANIMBAR ISLANDS REGION | 111000110 |
| 94217111910 | 26.651 | 92.522 | 33 | 4.8 | | EASTERN INDIA | 111000110 |
| 94218210214 | 26.991 | 54.363 | 16 | 5.3 | | SOUTHERN IRAN | 111000110 |
| 94219063254 | 27.106 | 54.469 | 44 | 4.7 | | SOUTHERN IRAN | 111000110 |
| 94220210831 | 24.721 | 95.200 | 122 | 6.0 | | BURMA | 111000110 |
| 94222021115 | 26.951 | 54.352 | 44 | 4.8 | 4.4 | SOUTHERN IRAN | 111000110 |
| 94222145749 | -58.756 | -25.538 | 33 | 5.6 | 5.0 | SOUTH SANDWICH ISLANDS REGION | 111000100 |
| 94223064632 | 27.035 | 54.469 | 25 | 5.2 | 4.5 | SOUTHERN IRAN | 111000110 |
| 94223204208 | -21.600 | -173.768 | 31 | 5.9 | 5.4 | TONGA ISLANDS | 111000110 |
| 94224205805 | 37.171 | 69.878 | 33 | 4.2 | | AFGHANISTAN-USSR BORDER REGION | 111000100 |
| 94226004620 | 44.709 | 150.103 | 17 | 6.0 | 5.9 | KURIL ISLANDS REGION | 111000110 |
| 94226013112 | 44.694 | 150.011 | 19 | 6.2 | 6.1 | KURIL ISLANDS REGION | 111000110 |
| 94226090652 | 38.794 | 142.075 | 44 | 5.4 | 5.3 | NEAR EAST COAST OF HONSHU, JAPAN | 111000110 |
| 94227061539 | 16.751 | -60.739 | 33 | 5.1 | 5.0 | LEEWARD ISLANDS | 111000110 |
| 94228100932 | 37.842 | 142.462 | 20 | 5.9 | 5.2 | OFF EAST COAST OF HONSHU, JAPAN | 111000110 |
| 94229071129 | 36.606 | 71.129 | 145 | 4.4 | | AFGHANISTAN-USSR BORDER REGION | 111000110 |
| 94230004547 | -7.433 | 31.751 | 25 | 6.0 | 5.7 | LAKE TANGANYIKA REGION | 111000110 |
| 94230011305 | 35.520 | -0.106 | 9 | 5.7 | 5.9 | ALGERIA | 111000110 |
| 94230044257 | 44.767 | 150.158 | 15 | 6.2 | 6.5 | KURIL ISLANDS REGION | 111000110 |
| 94230122947 | 39.217 | 72.097 | 33 | 4.1 | | KIRGHIZ SSR | 111000100 |
| 94231100251 | -26.642 | -63.421 | 564 | 6.4 | | SANTIAGO DEL ESTERO PROV., ARG. | 111000110 |
| 94231210245 | 17.974 | 96.415 | 12 | 5.6 | 5.6 | BURMA | 111000110 |
| 94232022111 | 44.606 | 149.325 | 23 | 6.0 | 5.2 | KURIL ISLANDS | 111000110 |

Appendix 1 (continued)

| EventID | Lat | Lon | Z | Mb | Ms | Location | Key 123456789 |
|---|---|---|---|---|---|---|---|
| 94232043850 | 44.656 | 149.176 | 24 | 6.2 | 6.1 | KURIL ISLANDS | 111000110 |
| 94233020633 | 37.891 | 69.944 | 33 | 4.3 | | AFGHANISTAN-USSR BORDER REGION | 011000110 |
| 94233155559 | 56.761 | 117.900 | 12 | 5.8 | 5.8 | EAST OF LAKE BAIKAL | 011000110 |
| 94234124116 | 70.922 | -6.103 | 10 | 5.3 | 4.9 | JAN MAYEN ISLAND REGION | 011000110 |
| 94234172637 | -11.509 | 166.452 | 142 | 6.2 | | SANTA CRUZ ISLANDS | 011000110 |
| 94235120543 | 36.542 | 70.396 | 33 | 4.8 | | HINDU KUSH REGION | 011000100 |
| 94235141831 | 40.041 | 78.818 | 33 | 5.0 | 5.0 | SOUTHERN XINJIANG, CHINA | 010000110 |
| 94236012826 | 52.302 | 160.336 | 32 | 5.4 | 4.7 | OFF EAST COAST OF KAMCHATKA | 010000100 |
| 94236151740 | -25.076 | -13.594 | 10 | 5.3 | 4.8 | SOUTH ATLANTIC RIDGE | 010000110 |
| 94237012446 | 42.771 | 145.049 | 72 | 5.4 | | HOKKAIDO, JAPAN REGION | 010000100 |
| 94238033814 | 33.120 | 56.052 | 33 | 4.4 | | IRAN | 010000100 |
| 94240183720 | 44.783 | 150.061 | 19 | 6.1 | 6.6 | KURIL ISLANDS REGION | 010000110 |
| 94241173620 | -0.404 | -19.172 | 10 | 5.5 | 5.3 | CENTRAL MID-ATLANTIC RIDGE | 010000100 |
| 94242061335 | 44.737 | 150.117 | 51 | 6.2 | 5.6 | KURIL ISLANDS REGION | 010000110 |
| 94242194246 | -6.965 | 124.111 | 596 | 5.9 | | BANDA SEA | 010000100 |
| 94243090725 | 43.719 | 146.013 | 76 | 6.0 | | KURIL ISLANDS | 010000110 |
| 94244151553 | 40.402 | -125.680 | 10 | 6.6 | 7.0 | OFF COAST OF NORTHERN CALIFORNIA | 010000110 |
| 94244161240 | 41.183 | 21.196 | 14 | 5.8 | | YUGOSLAVIA | 010000110 |
| 94245232940 | 33.529 | 48.861 | 49 | 4.4 | | WESTERN IRAN | 010000110 |
| 94246090253 | -31.422 | -111.028 | 7 | 5.8 | 5.4 | EASTER ISLAND REGION | 010000110 |
| 94246174641 | -21.212 | 173.640 | 33 | 5.8 | 6.2 | VANUATU ISLANDS REGION | 010000110 |
| 94247022802 | 37.471 | 69.971 | 33 | 4.9 | | AFGHANISTAN-USSR BORDER REGION | 010000110 |
| 94247071503 | 36.517 | 70.445 | 194 | 4.9 | | HINDU KUSH REGION | 010000100 |
| 94247145034 | 35.941 | 100.080 | 11 | 5.3 | 4.4 | QINGHAI PROVINCE, CHINA | 010000110 |
| 94248052615 | 29.419 | 51.283 | 33 | 5.0 | | SOUTHERN IRAN | 010000110 |
| 94248191317 | 41.905 | 46.231 | 62 | 4.7 | | EASTERN CAUCASUS | 010000110 |
| 94248221347 | 46.782 | 155.226 | 12 | 5.9 | | KURIL ISLANDS REGION | 010000110 |
| 94250135625 | 38.491 | 90.345 | 33 | 5.1 | 4.7 | SOUTHERN XINJIANG, CHINA | 010000110 |
| 94251092057 | 37.125 | 69.949 | 33 | 4.9 | | AFGHANISTAN-USSR BORDER REGION | 010000110 |
| 94251133336 | 28.030 | 61.837 | 77 | 5.1 | | SOUTHERN IRAN | 010000110 |
| 94252135004 | 36.739 | 70.297 | 33 | 4.8 | | HINDU KUSH REGION | 010000100 |
| 94253045410 | 7.552 | 126.599 | 79 | 5.6 | | MINDANAO, PHILIPPINE ISLANDS | 010000100 |
| 94254013203 | 19.586 | 99.516 | 33 | 5.1 | 4.6 | SOUTHEAST ASIA | 010000110 |
| 94255062954 | -31.103 | -71.706 | 40 | 5.9 | 5.7 | NEAR COAST OF CENTRAL CHILE | 010000110 |
| 94255113014 | -8.910 | 106.476 | 33 | 5.9 | 5.2 | SOUTH OF JAVA | 010000100 |
| 94256042801 | 29.287 | 129.910 | 34 | 5.8 | 6.2 | RYUKYU ISLANDS | 010000110 |
| 94256100132 | 7.054 | -76.678 | 14 | 5.8 | 5.6 | NORTHERN COLOMBIA | 010000110 |
| 94259062018 | 22.528 | 118.711 | 13 | 6.5 | 6.7 | TAIWAN REGION | 010000110 |
| 94260022437 | 37.885 | 41.584 | 9 | 5.1 | | TURKEY | 010000110 |
| 94260085753 | 26.450 | 55.601 | 33 | 4.7 | | SOUTHERN IRAN | 010000110 |
| 94261102715 | 38.563 | 71.733 | 33 | 4.6 | 3.9 | AFGHANISTAN-USSR BORDER REGION | 010000100 |
| 94262152342 | 42.631 | 43.049 | 33 | 4.4 | | WESTERN CAUCASUS | 010000110 |
| 94263055146 | 32.501 | 48.770 | 33 | 5.0 | 4.4 | WESTERN IRAN | 010000110 |
| 94264085323 | 42.465 | 43.535 | 33 | 4.4 | | WESTERN CAUCASUS | 010000110 |
| 94266023755 | 37.184 | 142.123 | 25 | 5.4 | 5.0 | OFF EAST COAST OF HONSHU, JAPAN | 010000100 |
| 94266075938 | -3.379 | 148.537 | 33 | 5.7 | 6.0 | BISMARCK SEA | 010000110 |
| 94270143253 | 31.661 | 49.176 | 42 | 4.5 | | WESTERN IRAN | 010000110 |
| 94273025616 | 36.412 | 71.067 | 242 | 4.7 | | AFGHANISTAN-USSR BORDER REGION | 010000110 |
| 94273025716 | 37.551 | 75.025 | 33 | 5.0 | | TAJIK-XINJIANG BORDER REGION | 010000100 |
| 94274082514 | 27.149 | 57.548 | 46 | 5.0 | | SOUTHERN IRAN | 110001110 |
| 94274140420 | 13.116 | 50.416 | 10 | 4.9 | 4.4 | EASTERN GULF OF ADEN | 110001110 |
| 94274163520 | -17.745 | 167.682 | 17 | 5.9 | 6.5 | VANUATU ISLANDS | 110001110 |
| 94274174637 | -17.768 | 167.830 | 33 | 5.8 | 6.3 | VANUATU ISLANDS | 110001100 |
| 94275162016 | 38.554 | 73.888 | 125 | 4.7 | | TAJIK-XINJIANG BORDER REGION | 100001010 |
| 94276022245 | 32.763 | 48.880 | 67 | 4.6 | | WESTERN IRAN | 110001100 |
| 94277120940 | -6.218 | 104.891 | 24 | 5.6 | 4.7 | SUNDA STRAIT | 100001100 |
| 94277132255 | 43.773 | 147.321 | 14 | 7.3 | 8.1 | KURIL ISLANDS | 100001100 |
| 94277152415 | 43.526 | 147.908 | 20 | 6.3 | | KURIL ISLANDS | 101001100 |
| 94277160102 | 43.706 | 147.991 | 16 | 6.3 | | KURIL ISLANDS | 101001100 |
| 94277191628 | 43.774 | 147.504 | 35 | 6.0 | 5.6 | KURIL ISLANDS | 101001100 |

Appendix 1 (continued)

| EventID | Lat | Lon | Z | Mb | Ms | Location | Key 123456789 |
|---|---|---|---|---|---|---|---|
| 94278040047 | 43.398 | 148.078 | 40 | 5.8 | 5.6 | KURIL ISLANDS REGION | 101001110 |
| 94278203948 | 43.954 | 147.336 | 40 | 6.2 | 5.5 | KURIL ISLANDS | 101001110 |
| 94279074635 | 43.239 | 148.061 | 33 | 5.3 | 5.6 | KURIL ISLANDS REGION | 101001000 |
| 94279154214 | -56.628 | -141.923 | 10 | 5.8 | 5.2 | SOUTH PACIFIC CORDILLERA | 101001110 |
| 94280023609 | 43.614 | 147.289 | 52 | 6.1 | | KURIL ISLANDS | 101001110 |
| 94280032558 | 41.662 | 88.753 | 0 | 6.0 | | SOUTHERN XINJIANG, CHINA | 101001110 |
| 94280070052 | 43.117 | 146.866 | 55 | 5.5 | | KURIL ISLANDS | 101001010 |
| 94280152403 | 42.877 | 146.063 | 24 | 6.0 | 5.2 | OFF COAST OF HOKKAIDO, JAPAN | 101001110 |
| 94281052826 | 43.319 | 146.676 | 26 | 5.6 | 5.0 | KURIL ISLANDS | 101001000 |
| 94281095434 | 43.873 | 148.171 | 9 | 5.9 | | KURIL ISLANDS REGION | 101001110 |
| 94281214407 | -1.258 | 127.980 | 17 | 6.4 | 6.8 | HALMAHERA | 101001110 |
| 94282075539 | 43.905 | 147.916 | 33 | 6.5 | 7.1 | KURIL ISLANDS | 101001110 |
| 94282122422 | 43.883 | 147.341 | 46 | 5.8 | 5.5 | KURIL ISLANDS | 101001110 |
| 94282190843 | 39.907 | 77.117 | 40 | 4.9 | 4.5 | SOUTHERN XINJIANG, CHINA | 101001010 |
| 94283210653 | 51.484 | -173.897 | 33 | 5.6 | 5.2 | ANDREANOF ISLANDS, ALEUTIAN IS. | 101001110 |
| 94284013720 | -32.100 | -71.447 | 47 | 5.7 | 5.4 | NEAR COAST OF CENTRAL CHILE | 101001100 |
| 94284203117 | 33.558 | 45.678 | 18 | 4.7 | | IRAN-IRAQ BORDER REGION | 101001110 |
| 94285060249 | 13.765 | 124.538 | 27 | 5.5 | 5.7 | LUZON, PHILIPPINE ISLANDS | 101001010 |
| 94285064339 | 13.773 | 124.529 | 16 | 5.8 | 6.1 | LUZON, PHILIPPINE ISLANDS | 101001110 |
| 94285074401 | 42.371 | 44.430 | 10 | 4.3 | | WESTERN CAUCASUS | 101001100 |
| 94285103322 | 51.605 | -173.770 | 33 | 5.1 | 4.8 | ANDREANOF ISLANDS, ALEUTIAN IS. | 101001000 |
| 94286050424 | -1.212 | 127.912 | 11 | 6.1 | 6.3 | HALMAHERA | 101001110 |
| 94286231957 | 40.381 | 52.975 | 33 | 4.3 | | TURKMEN SSR | 101001100 |
| 94286233127 | 45.493 | 21.004 | 10 | 4.7 | | ROMANIA | 101001000 |
| 94288003925 | -3.804 | 152.148 | 9 | 5.6 | 6.1 | NEW IRELAND REGION | 101001100 |
| 94289051000 | 45.749 | 149.167 | 117 | 6.4 | | KURIL ISLANDS | 101001100 |
| 94289100952 | 38.089 | 56.703 | 33 | 4.5 | | IRAN-USSR BORDER REGION | 101001100 |
| 94291171250 | 43.576 | 147.097 | 60 | 6.2 | | KURIL ISLANDS | 101001100 |
| 94293011516 | -39.187 | -70.811 | 162 | 5.8 | | ARGENTINA | 101001100 |
| 94294050621 | 36.391 | 69.708 | 47 | 5.4 | 5.3 | HINDU KUSH REGION | 101001100 |
| 94294114627 | 38.250 | 56.955 | 33 | 4.9 | | IRAN-USSR BORDER REGION | 101001100 |
| 94297192627 | 43.084 | 147.096 | 57 | 5.7 | | KURIL ISLANDS | 101001100 |
| 94298005434 | 36.359 | 70.957 | 239 | 5.9 | | HINDU KUSH REGION | 101001100 |
| 94298133026 | 43.771 | 147.698 | 35 | 5.5 | 4.8 | KURIL ISLANDS | 101001100 |
| 94300131911 | 31.430 | 49.409 | 33 | 4.6 | | WESTERN IRAN | 101001100 |
| 94300174558 | 43.515 | -127.427 | 20 | 5.6 | 6.0 | OFF COAST OF OREGON | 101001100 |
| 94300222028 | -25.778 | 179.339 | 519 | 5.9 | | SOUTH OF FIJI ISLANDS | 101001100 |
| 94301091120 | 14.537 | -103.755 | 33 | 5.2 | 5.5 | OFF COAST OF GUERRERO, MEXICO | 101001100 |
| 94303060627 | -28.032 | 26.738 | 5 | 5.6 | 4.7 | REPUBLIC OF SOUTH AFRICA | 101000100 |
| 94303081129 | -6.183 | 129.446 | 264 | 5.6 | | BANDA SEA | 101000100 |
| 94304114813 | 3.019 | 96.192 | 29 | 5.7 | 6.2 | NORTHERN SUMATERA | 101000100 |
| 94304225926 | 9.037 | -83.323 | 56 | 5.6 | | COSTA RICA | 101000100 |
| 94305080802 | -1.432 | 67.947 | 10 | 5.0 | 5.2 | CARLSBERG RIDGE | 101000100 |
| 94306014355 | 5.099 | 118.643 | 55 | 5.7 | | KALIMANTAN | 101000100 |
| 94306123101 | 38.152 | 48.315 | 10 | 5.0 | | N.W. IRAN-USSR BORDER REGION | 101000100 |
| 94307114333 | 28.260 | 52.203 | 33 | 4.9 | 4.4 | SOUTHERN IRAN | 101000100 |
| 94308011320 | -9.379 | -71.334 | 591 | 5.8 | | PERU-BRAZIL BORDER REGION | 101000100 |
| 94309021603 | -57.193 | 157.858 | 25 | 6.1 | 6.1 | MACQUARIE ISLANDS REGION | 101000100 |
| 94309120528 | -9.386 | -71.335 | 597 | 5.7 | | PERU-BRAZIL BORDER REGION | 101000100 |
| 94312053122 | 43.271 | 86.960 | 33 | 5.0 | | NORTHERN XINJIANG, CHINA | 101000100 |
| 94313182102 | 43.556 | 147.144 | 54 | 6.2 | 5.2 | KURIL ISLANDS | 101000100 |
| 94315084829 | -15.626 | -72.535 | 121 | 5.6 | | SOUTHERN PERU | 101000100 |
| 94317065600 | 36.910 | 29.060 | 10 | 4.9 | 5.0 | TURKEY | 101000100 |
| 94318191530 | 13.525 | 121.067 | 32 | 6.1 | 7.1 | MINDORO, PHILIPPINE ISLANDS | 101000100 |
| 94319201811 | -5.589 | 110.186 | 561 | 6.2 | | JAVA SEA | 101000100 |
| 94323021801 | 27.818 | 56.887 | 33 | 4.6 | | SOUTHERN IRAN | 101000100 |
| 94324025701 | 14.769 | 55.609 | 10 | 5.0 | | ARABIAN SEA | 101000100 |
| 94324025715 | -9.794 | 159.712 | 24 | 5.8 | 5.5 | SOLOMON ISLANDS | 101000100 |
| 94324143102 | 35.335 | 39.557 | 29 | 5.1 | 4.9 | JORDAN - SYRIA REGION | 101000100 |
| 94324165905 | -2.001 | 135.932 | 16 | 5.8 | 6.3 | WEST IRIAN REGION | 101000100 |

Appendix 1 (continued)

| EventID | Lat | Lon | Z | Mb | Ms | Location | Key 123456789 |
|---|---|---|---|---|---|---|---|
| 94324183434 | 4.330 | 97.591 | 153 | 5.7 | | NORTHERN SUMATERA | 101000100 |
| 94325022130 | -14.976 | 167.243 | 126 | 5.6 | | VANUATU ISLANDS | 101000100 |
| 94325081634 | 25.540 | 96.657 | 14 | 5.6 | 5.9 | BURMA | 101000100 |
| 94325185516 | 35.902 | 51.884 | 33 | 4.5 | | IRAN | 101000100 |
| 94326111157 | 43.961 | 147.293 | 49 | 5.6 | 5.1 | KURIL ISLANDS | 101000100 |
| 94328034636 | 37.484 | 72.276 | 33 | 5.2 | | TAJIK SSR | 101000100 |
| 94330061110 | -20.126 | 169.126 | 36 | 5.8 | 5.4 | VANUATU ISLANDS | 101000100 |
| 94330151047 | 71.946 | -4.846 | 10 | 4.6 | | JAN MAYEN ISLAND REGION | 101000100 |
| 94331211841 | 37.747 | 67.788 | 33 | 4.6 | | AFGHANISTAN-USSR BORDER REGION | 101000100 |
| 94333143028 | 38.707 | 20.484 | 21 | 4.9 | 4.8 | GREECE | 101000100 |
| 94335061101 | -7.639 | 128.173 | 84 | 5.6 | | BANDA SEA | 101000100 |
| 94337013551 | 37.643 | 49.349 | 33 | 4.8 | | CASPIAN SEA | 101000100 |
| 94337060251 | 32.624 | 47.307 | 81 | 4.6 | | IRAN-IRAQ BORDER REGION | 101000100 |
| 94339162009 | -8.576 | 159.833 | 49 | 5.8 | 5.1 | SOLOMON ISLANDS | 101000100 |
| 94340014047 | 40.632 | 27.750 | 10 | 0.0 | | TURKEY | 101000100 |
| 94340090607 | -15.316 | -75.294 | 27 | 5.3 | 5.0 | NEAR COAST OF PERU | 101000100 |
| 94341033754 | -23.422 | -66.639 | 235 | 5.6 | | JUJUY PROVINCE, ARGENTINA | 111000100 |
| 94341215210 | 30.928 | 51.145 | 28 | 4.9 | | IRAN | 011000100 |
| 94342104755 | 36.450 | 70.927 | 200 | 5.1 | | HINDU KUSH REGION | 011000100 |
| 94342125438 | 28.961 | 52.580 | 33 | 5.0 | | SOUTHERN IRAN | 011000100 |
| 94344033931 | -23.534 | -70.591 | 37 | 5.8 | 5.6 | NEAR COAST OF NORTHERN CHILE | 011000100 |
| 94344121601 | 27.914 | 64.985 | 57 | 5.2 | | PAKISTAN | 011000100 |
| 94344161738 | 18.136 | -101.384 | 48 | 6.6 | 6.2 | GUERRERO, MEXICO | 011000100 |
| 94345022546 | -5.829 | 104.661 | 51 | 5.7 | | SOUTHERN SUMATERA | 011000100 |
| 94346074155 | -17.477 | -69.598 | 148 | 5.9 | | PERU-BOLIVIA BORDER REGION | 010000100 |
| 94346125254 | 36.397 | 70.811 | 166 | 5.2 | | HINDU KUSH REGION | 010000100 |
| 94346131406 | 42.501 | 43.402 | 33 | 4.4 | | WESTERN CAUCASUS | 010000100 |
| 94346145253 | -9.975 | 119.199 | 26 | 5.9 | 5.1 | SUMBA ISLAND REGION | 010000100 |
| 94346151203 | 38.175 | 73.021 | 121 | 5.0 | | TAJIK-XINJIANG BORDER REGION | 010000100 |
| 94348072853 | -9.519 | 159.411 | 16 | 5.8 | 5.9 | SOLOMON ISLANDS | 010000100 |
| 94348204353 | 35.104 | 58.633 | 33 | 5.3 | | IRAN | 010000100 |
| 94349112022 | -37.282 | 177.523 | 33 | 5.9 | 6.4 | OFF E. COAST OF N. ISLAND, N.Z. | 010000100 |
| 94349232448 | 28.956 | 52.641 | 33 | 4.7 | | SOUTHERN IRAN | 010000100 |
| 94352163815 | 35.277 | 39.745 | 10 | 4.6 | | JORDAN - SYRIA REGION | 010000100 |
| 94352203832 | -17.838 | -178.703 | 545 | 5.6 | | FIJI ISLANDS REGION | 010000100 |
| 94353145958 | 40.934 | 47.816 | 33 | 4.6 | | EASTERN CAUCASUS | 010000100 |
| 94358235147 | 38.588 | 73.897 | 33 | 5.3 | | TAJIK-XINJIANG BORDER REGION | 010000100 |
| 94360144801 | 36.469 | 71.244 | 226 | 5.1 | | AFGHANISTAN-USSR BORDER REGION | 010000100 |
| 94361173250 | -31.965 | 179.860 | 212 | 6.0 | | KERMADEC ISLANDS REGION | 010000100 |
| 94362121923 | 40.525 | 143.419 | 27 | 6.4 | 7.5 | OFF EAST COAST OF HONSHU, JAPAN | 010000100 |
| 94362205225 | 40.094 | 142.687 | 22 | 5.9 | 5.9 | NEAR EAST COAST OF HONSHU, JAPAN | 010000100 |
| 94362223746 | 40.375 | 143.636 | 11 | 5.9 | 6.0 | OFF EAST COAST OF HONSHU, JAPAN | 010000100 |
| 94363160118 | 35.655 | 80.663 | 33 | 5.5 | | KASHMIR-TIBET BORDER REGION | 010000100 |
| 94364065616 | 38.179 | 39.670 | 10 | 4.7 | | TURKEY | 010000100 |
| 94365025720 | 20.524 | 109.330 | 33 | 5.7 | 5.3 | EASTERN CHINA | 010000100 |
| 94365135023 | 40.217 | 142.546 | 43 | 5.7 | 5.6 | NEAR EAST COAST OF HONSHU, JAPAN | 010000100 |
| 95001065954 | 40.635 | 143.585 | 10 | 5.7 | 6.2 | OFF EAST COAST OF HONSHU, JAPAN | 010000100 |
| 95001085108 | 30.543 | 50.378 | 33 | 4.9 | 4.4 | IRAN | 010000100 |
| 95003025457 | -56.211 | -27.205 | 136 | 5.4 | | SOUTH SANDWICH ISLANDS REGION | 010000110 |
| 95003161159 | -57.698 | -65.958 | 33 | 6.1 | 5.6 | DRAKE PASSAGE | 010000110 |
| 95003225144 | 34.901 | 23.622 | 33 | 4.8 | | CRETE | 010000110 |
| 95004022211 | 27.444 | 56.693 | 33 | 4.6 | | SOUTHERN IRAN | 010000110 |
| 95004085150 | 9.822 | 56.514 | 21 | 4.8 | | CARLSBERG RIDGE | 010000110 |
| 95005124601 | 59.650 | 56.440 | 10 | 4.7 | | URAL MOUNTAINS REGION | 010000110 |
| 95005233007 | -22.036 | 168.838 | 29 | 5.5 | 5.4 | NEW CALEDONIA | 010000110 |
| 95006215932 | 9.169 | 126.195 | 61 | 5.7 | | MINDANAO, PHILIPPINE ISLANDS | 010000110 |
| 95006223737 | 40.227 | 142.242 | 57 | 6.7 | | NEAR EAST COAST OF HONSHU, JAPAN | 010000110 |
| 95007023608 | 40.264 | 142.411 | 48 | 6.2 | 5.6 | NEAR EAST COAST OF HONSHU, JAPAN | 010000110 |
| 95007203047 | 37.920 | 19.949 | 10 | 4.7 | 4.4 | IONIAN SEA | 010000110 |
| 95008092219 | -8.444 | -74.289 | 149 | 5.1 | | PERU-BRAZIL BORDER REGION | 010000100 |

Appendix 1 (continued)

| EventID | Lat | Lon | Z | Mb | Ms | Location | Key 123456789 |
|---|---|---|---|---|---|---|---|
| 95009180017 | 35.864 | 141.345 | 33 | 5.6 | 5.7 | NEAR EAST COAST OF HONSHU, JAPAN | 010000100 |
| 95010100951 | 20.040 | 109.153 | 33 | 5.2 | 5.5 | EASTERN CHINA | 010000100 |
| 95012102646 | 43.986 | 147.088 | 33 | 6.2 | 5.4 | KURIL ISLANDS | 010000110 |
| 95013031259 | 43.102 | 147.070 | 33 | 5.8 | 5.2 | KURIL ISLANDS | 010000100 |
| 95015024018 | 27.519 | 128.443 | 47 | 5.7 | 5.4 | RYUKYU ISLANDS | 011000000 |
| 95015235926 | -5.264 | 152.025 | 66 | 5.7 | 5.9 | NEW BRITAIN REGION | 001000000 |
| 95016181449 | 51.241 | 179.172 | 33 | 5.5 | 6.0 | RAT ISLANDS, ALEUTIAN ISLANDS | 001000000 |
| 95016204651 | 34.549 | 135.002 | 16 | 6.4 | 6.8 | NEAR S. COAST OF SOUTHERN HONSHU | 001000000 |
| 95017165412 | -20.870 | -179.225 | 637 | 6.0 | | FIJI ISLANDS REGION | 001000000 |
| 95018143858 | 36.608 | 71.233 | 214 | 4.5 | | AFGHANISTAN-USSR BORDER REGION | 001001000 |
| 95019030023 | 43.326 | 147.010 | 40 | 5.5 | 5.1 | KURIL ISLANDS | 001001000 |
| 95019095534 | -7.345 | 128.271 | 170 | 5.8 | | BANDA SEA | 001001000 |
| 95019150503 | 5.075 | -72.918 | 18 | 6.4 | 6.6 | COLOMBIA | 001001000 |
| 95020005522 | -10.958 | 162.156 | 28 | 5.6 | 5.5 | SOLOMON ISLANDS | 001001000 |
| 95020033546 | 43.261 | 146.821 | 61 | 5.7 | | KURIL ISLANDS | 001001000 |
| 95020154901 | 1.142 | 126.107 | 51 | 5.7 | 5.4 | MOLUCCA PASSAGE | 001001000 |
| 95021001611 | 47.126 | 152.806 | 33 | 4.9 | | KURIL ISLANDS | 001001000 |
| 95021030231 | 29.040 | 52.073 | 33 | 4.6 | | SOUTHERN IRAN | 001001000 |
| 95021065633 | 40.565 | 143.633 | 32 | 5.2 | 5.4 | OFF EAST COAST OF HONSHU, JAPAN | 001001000 |
| 95021073023 | 2.529 | 126.905 | 47 | 6.1 | 6.1 | MOLUCCA PASSAGE | 001001000 |
| 95021084729 | 43.335 | 146.717 | 63 | 6.5 | | KURIL ISLANDS | 001001000 |
| 95022104127 | 5.126 | -72.966 | 22 | 5.6 | 5.1 | COLOMBIA | 001001000 |
| 95024041426 | 27.640 | 55.652 | 33 | 4.9 | | SOUTHERN IRAN | 001001000 |
| 95024065857 | 27.300 | 55.454 | 33 | 4.5 | | SOUTHERN IRAN | 001001000 |
| 95024223635 | -5.933 | 154.493 | 33 | 5.7 | 6.2 | SOLOMON ISLANDS | 001001000 |
| 95026070044 | 36.080 | 71.219 | 106 | 5.2 | | AFGHANISTAN-USSR BORDER REGION | 001001000 |
| 95027183451 | -2.332 | 138.883 | 47 | 5.6 | 5.1 | WEST IRIAN | 001001000 |
| 95027201653 | -4.456 | 134.462 | 33 | 6.2 | 6.8 | WEST IRIAN REGION | 001001000 |
| 95027210753 | 27.954 | 57.012 | 33 | 4.8 | | SOUTHERN IRAN | 001001000 |
| 95028103727 | 43.922 | 148.163 | 33 | 5.2 | 5.2 | KURIL ISLANDS REGION | 001001000 |
| 95029012011 | 36.978 | 71.552 | 107 | 5.2 | | AFGHANISTAN-USSR BORDER REGION | 001001000 |
| 95029045337 | 29.234 | 141.202 | 67 | 5.6 | | SOUTH OF HONSHU, JAPAN | 001001000 |
| 95030223630 | 36.421 | 71.450 | 54 | 4.6 | | AFGHANISTAN-USSR BORDER REGION | 001001000 |
| 95032142644 | -42.432 | -18.449 | 10 | 5.4 | 5.1 | SOUTH ATLANTIC RIDGE | 001001000 |
| 95033123358 | -1.268 | 127.567 | 33 | 5.5 | | HALMAHERA | 001001000 |
| 95033125353 | 10.755 | -42.557 | 10 | 5.6 | 5.4 | NORTH ATLANTIC RIDGE | 001001000 |
| 95033193449 | 39.214 | 67.407 | 33 | 4.6 | | SOUTHEASTERN UZBEK SSR | 001001000 |
| 95034023134 | -62.706 | 155.895 | 10 | 5.6 | 6.3 | BALLENY ISLANDS REGION | 001001000 |
| 95034154054 | -3.416 | 135.538 | 35 | 5.3 | 4.9 | WEST IRIAN REGION | 001001000 |
| 95034222909 | 34.219 | 25.194 | 33 | 4.8 | | CRETE | 001001000 |
| 95036203710 | 6.849 | -82.675 | 10 | 5.8 | 5.4 | SOUTH OF PANAMA | 001001000 |
| 95036225110 | -37.714 | 178.769 | 59 | 6.4 | | OFF E. COAST OF N. ISLAND, N.Z. | 001001000 |
| 95037104357 | -37.799 | 178.816 | 33 | 5.7 | 5.8 | OFF E. COAST OF N. ISLAND, N.Z. | 001001000 |
| 95037135135 | 41.124 | 142.188 | 71 | 5.6 | | HOKKAIDO, JAPAN REGION | 001001000 |
| 95037211547 | 28.942 | 34.748 | 5 | 0.0 | | ARAB REPUBLIC OF EGYPT | 001001000 |
| 95039184025 | 4.162 | -76.644 | 69 | 6.3 | | COLOMBIA | 001001000 |
| 95041014504 | -37.968 | 178.472 | 33 | 5.8 | 6.4 | OFF E. COAST OF N. ISLAND, N.Z. | 001001000 |
| 95041074918 | 36.196 | 69.070 | 33 | 4.8 | | HINDU KUSH REGION | 001001000 |
| 95041202703 | -19.770 | -68.544 | 164 | 5.4 | | CHILE-BOLIVIA BORDER REGION | 001001000 |
| 95042224533 | 12.607 | -81.603 | 11 | 5.3 | 5.2 | CARIBBEAN SEA | 001001000 |
| 95043010207 | -5.796 | -76.135 | 22 | 5.7 | 5.1 | NORTHERN PERU | 001001000 |
| 95044001147 | -37.541 | 178.543 | 28 | 5.6 | 6.2 | OFF E. COAST OF N. ISLAND, N.Z. | 001001000 |
| 95044084339 | -1.306 | 127.420 | 33 | 6.1 | 6.2 | HALMAHERA | 001001000 |
| 95044122955 | -1.383 | 127.449 | 33 | 5.8 | 6.0 | HALMAHERA | 001001000 |
| 95044131634 | 40.707 | 22.563 | 10 | 4.8 | | GREECE | 001001000 |
| 95044150426 | -1.351 | 127.522 | 33 | 6.2 | 6.8 | HALMAHERA | 001001000 |
| 95045111319 | 37.742 | 42.698 | 10 | 4.8 | 4.2 | TURKEY | 001001000 |
| 95045155356 | -23.290 | -67.702 | 156 | 5.7 | | CHILE-ARGENTINA BORDER REGION | 001001000 |
| 95045204741 | 43.991 | 148.098 | 37 | 5.9 | 5.6 | KURIL ISLANDS REGION | 001001000 |
| 95046130520 | 29.105 | 51.167 | 33 | 4.7 | | SOUTHERN IRAN | 001001000 |

Appendix 1 (continued)

| EventID | Lat | Lon | Z | Mb | Ms | Location | Key 123456789 |
|---|---|---|---|---|---|---|---|
| 95047145252 | 52.191 | -30.216 | 10 | 5.1 | 4.8 | NORTH ATLANTIC RIDGE | 001001000 |
| 95048024424 | 27.606 | 92.298 | 35 | 5.2 | 5.1 | INDIA-CHINA BORDER REGION | 001001000 |
| 95049132906 | 46.667 | 145.894 | 355 | 5.6 | | SEA OF OKHOTSK | 001001000 |
| 95050001748 | 5.206 | 126.225 | 104 | 5.9 | | MINDANAO, PHILIPPINE ISLANDS | 001001000 |
| 95050040316 | 40.560 | -125.527 | 10 | 6.1 | 6.8 | OFF COAST OF NORTHERN CALIFORNIA | 001001000 |
| 95050044550 | 43.098 | 146.842 | 33 | 5.8 | 5.8 | KURIL ISLANDS | 001001000 |
| 95051025912 | -27.835 | 76.213 | 10 | 5.3 | 5.6 | MID-INDIAN RISE | 001001000 |
| 95051041224 | 39.255 | 71.054 | 27 | 5.4 | | TAJIK SSR | 001001000 |
| 95051080733 | 41.225 | 72.498 | 33 | 5.0 | 4.5 | KIRGHIZ SSR | 001001000 |
| 95052020950 | 45.942 | 151.553 | 33 | 5.8 | 5.9 | KURIL ISLANDS | 001001000 |
| 95054050125 | 39.663 | 143.688 | 33 | 5.5 | 6.0 | OFF EAST COAST OF HONSHU, JAPAN | 001001000 |
| 95054051902 | 24.136 | 121.600 | 44 | 5.8 | 6.2 | TAIWAN | 001001000 |
| 95054210302 | 35.039 | 32.266 | 15 | 5.8 | 5.7 | CYPRUS | 001001000 |
| 95054211036 | 35.089 | 32.274 | 10 | 4.8 | | CYPRUS | 001001000 |
| 95054214031 | 35.005 | 32.270 | 10 | 5.2 | | CYPRUS | 001001000 |
| 95056060930 | -26.670 | -112.621 | 10 | 5.4 | 5.1 | EASTER ISLAND REGION | 001001000 |
| 95056094224 | 39.977 | 77.480 | 33 | 4.8 | | SOUTHERN XINJIANG, CHINA | 001001000 |
| 95056110531 | 36.654 | 71.006 | 175 | 4.8 | | AFGHANISTAN-USSR BORDER REGION | 001001000 |
| 95056215429 | -18.235 | -178.091 | 568 | 5.6 | | FIJI ISLANDS REGION | 001001000 |
| 95057150341 | 1.302 | 97.873 | 33 | 5.0 | 4.7 | NORTHERN SUMATERA | 001001000 |
| 95059102410 | 38.149 | 73.120 | 88 | 4.2 | | TAJIK-XINJIANG BORDER REGION | 001001000 |
| 95059211209 | 6.935 | -81.805 | 21 | 5.2 | 5.5 | SOUTH OF PANAMA | 001001010 |
| 95062120210 | -6.472 | 154.987 | 35 | 5.8 | 5.6 | SOLOMON ISLANDS | 001001010 |
| 95062135122 | 34.620 | 45.177 | 33 | 4.6 | | IRAN-IRAQ BORDER REGION | 001001010 |
| 95062211237 | -14.617 | -175.627 | 22 | 5.6 | 5.7 | SAMOA ISLANDS REGION | 001001010 |
| 95065184342 | 2.662 | 118.218 | 33 | 5.5 | 5.8 | CELEBES SEA | 001001010 |
| 95067034559 | 16.555 | -59.574 | 15 | 6.3 | 6.2 | LEEWARD ISLANDS | 001001010 |
| 95068183657 | 20.943 | 122.001 | 42 | 5.1 | 5.3 | PHILIPPINE ISLANDS REGION | 001001000 |
| 95069052222 | 46.075 | 143.540 | 350 | 5.4 | | SAKHALIN ISLAND | 001001000 |
| 95070152110 | 44.008 | 148.132 | 33 | 6.0 | 5.7 | KURIL ISLANDS | 001001010 |
| 95071044045 | 40.187 | 143.489 | 33 | 5.1 | 5.1 | OFF EAST COAST OF HONSHU, JAPAN | 001001000 |
| 95071082300 | 17.911 | 73.422 | 33 | 4.7 | | INDIA | 001001000 |
| 95071120943 | -5.330 | 146.695 | 233 | 5.6 | | EAST PAPUA NEW GUINEA REGION | 001001000 |
| 95072103150 | -2.820 | 134.330 | 33 | 5.5 | 5.7 | WEST IRIAN REGION | 001001000 |
| 95073004322 | 6.859 | -73.128 | 158 | 4.8 | | NORTHERN COLOMBIA | 001001000 |
| 95073033233 | -37.892 | -73.331 | 33 | 5.2 | | NEAR COAST OF CENTRAL CHILE | 001001000 |
| 95073102730 | 2.999 | 95.867 | 30 | 5.0 | 5.3 | OFF W COAST OF NORTHERN SUMATERA | 001001000 |
| 95073173350 | 54.793 | -161.295 | 33 | 6.1 | 5.9 | ALASKA PENINSULA | 001001000 |
| 95075032704 | 30.311 | 67.248 | 25 | 4.8 | 4.2 | PAKISTAN | 101001010 |
| 95076021840 | -13.142 | 166.676 | 33 | 5.7 | 5.2 | VANUATU ISLANDS | 111001010 |
| 95077180237 | 42.502 | 87.179 | 21 | 5.2 | | NORTHERN XINJIANG, CHINA | 111000010 |
| 95078165815 | 36.509 | 70.920 | 201 | 4.7 | | HINDU KUSH REGION | 111000010 |
| 95078174140 | 43.985 | 147.175 | 33 | 4.7 | 4.0 | KURIL ISLANDS | 111000010 |
| 95078183405 | -4.270 | 135.061 | 33 | 5.6 | 6.3 | WEST IRIAN REGION | 111000010 |
| 95078235314 | -4.148 | 135.087 | 33 | 6.3 | 7.1 | WEST IRIAN REGION | 111000010 |
| 95081062836 | 30.185 | 51.065 | 33 | 4.7 | | IRAN | 111000010 |
| 95082091821 | -36.263 | -72.943 | 43 | 5.2 | 5.5 | NEAR COAST OF CENTRAL CHILE | 111000010 |
| 95084224428 | -11.050 | 166.111 | 77 | 5.9 | | SANTA CRUZ ISLANDS | 111000010 |
| 95085021616 | -55.855 | -28.208 | 77 | 6.1 | 5.9 | SOUTH SANDWICH ISLANDS REGION | 111000010 |
| 95089181715 | 34.479 | 24.853 | 10 | 4.9 | | CRETE | 111000010 |
| 95090140140 | 38.150 | 135.058 | 365 | 6.0 | | SEA OF JAPAN | 111000010 |
| 95091034933 | 37.924 | 139.177 | 11 | 5.8 | | HONSHU, JAPAN | 111000010 |
| 95091044814 | 31.195 | 45.934 | 33 | 4.6 | | IRAQ | 111000010 |
| 95091055020 | 52.279 | 159.133 | 47 | 5.9 | 5.6 | OFF EAST COAST OF KAMCHATKA | 111000010 |
| 95093115443 | 24.083 | 122.250 | 33 | 5.7 | 5.5 | TAIWAN REGION | 111000010 |
| 95093200815 | 29.638 | 51.052 | 33 | 4.3 | | SOUTHERN IRAN | 111000010 |
| 95094152952 | 28.212 | 71.593 | 21 | 4.8 | 3.9 | INDIA-PAKISTAN BORDER REG. | 111000010 |
| 95097220658 | -15.187 | -173.594 | 31 | 6.7 | 8.0 | TONGA ISLANDS | 111000010 |
| 95098012007 | -15.227 | -173.521 | 33 | 5.9 | 6.1 | TONGA ISLANDS | 111000010 |
| 95098174518 | 21.804 | 142.632 | 319 | 6.3 | | MARIANA ISLANDS REGION | 111000010 |

Appendix 1 (continued)

| EventID | Lat | Lon | Z | Mb | Ms | Location | Key 123456789 |
|---|---|---|---|---|---|---|---|
| 95104003254 | 30.244 | -103.325 | 5 | 5.7 | 5.6 | WEST TEXAS | 111000010 |
| 95106132348 | -9.759 | 159.514 | 24 | 5.6 | 5.7 | SOLOMON ISLANDS | 111000010 |
| 95107011420 | -8.585 | 156.613 | 36 | 5.8 | 6.0 | SOLOMON ISLANDS | 111000010 |
| 95107071435 | 33.778 | -38.600 | 10 | 5.8 | 5.8 | NORTH ATLANTIC RIDGE | 111000010 |
| 95107232808 | 45.904 | 151.288 | 34 | 6.1 | 6.3 | KURIL ISLANDS | 111000010 |
| 95108034939 | -2.088 | 140.449 | 36 | 5.9 | 5.7 | NEAR N. COAST OF WEST IRIAN | 111000010 |
| 95108061240 | 31.812 | 49.283 | 33 | 4.7 | | WESTERN IRAN | 111000010 |
| 95109035005 | 44.027 | 148.204 | 33 | 5.9 | 5.5 | KURIL ISLANDS | 111000010 |
| 95110084510 | 6.288 | 126.828 | 85 | 6.2 | | MINDANAO, PHILIPPINE ISLANDS | 111000010 |
| 95110204910 | 45.901 | 151.253 | 33 | 5.7 | 5.0 | KURIL ISLANDS | 111000010 |
| 95111000956 | 11.999 | 125.699 | 33 | 6.1 | 6.9 | SAMAR, PHILIPPINE ISLANDS | 111000010 |
| 95111003447 | 12.064 | 125.931 | 23 | 6.2 | 7.3 | SAMAR, PHILIPPINE ISLANDS | 111000010 |
| 95111051700 | 12.142 | 125.948 | 23 | 5.6 | 6.9 | SAMAR, PHILIPPINE ISLANDS | 111000010 |
| 95111080256 | 43.756 | 7.567 | 25 | 4.9 | | NEAR SOUTH COAST OF FRANCE | 111000010 |
| 95111170317 | 11.997 | 125.877 | 33 | 5.2 | 5.2 | SAMAR, PHILIPPINE ISLANDS | 111000010 |
| 95112002149 | 30.912 | 49.843 | 33 | 5.0 | 4.9 | WESTERN IRAN | 111000000 |
| 95113025554 | 51.340 | 179.713 | 16 | 6.1 | 6.4 | RAT ISLANDS, ALEUTIAN ISLANDS | 111000000 |
| 95113050803 | 12.377 | 125.364 | 33 | 6.0 | 6.6 | SAMAR, PHILIPPINE ISLANDS | 111000000 |
| 95113235540 | 5.255 | -72.475 | 33 | 5.3 | 4.7 | COLOMBIA | 111000000 |
| 95115061502 | -5.855 | 147.302 | 33 | 5.6 | 5.7 | EAST PAPUA NEW GUINEA REGION | 111000010 |
| 95117124438 | 1.199 | -84.929 | 10 | 5.3 | 6.0 | OFF COAST OF ECUADOR | 111000010 |
| 95118163000 | 44.058 | 148.055 | 29 | 6.6 | 6.9 | KURIL ISLANDS | 111000010 |
| 95118170843 | 44.090 | 148.122 | 33 | 6.2 | 6.2 | KURIL ISLANDS | 111000010 |
| 95118174413 | -1.892 | 55.532 | 10 | 5.3 | | SOUTH INDIAN OCEAN | 111000010 |
| 95119094400 | 11.766 | 126.044 | 33 | 5.4 | 6.0 | PHILIPPINE ISLANDS REGION | 111000010 |
| 95122060605 | -3.854 | -76.958 | 103 | 6.5 | | NORTHERN PERU | 111000010 |
| 95122114811 | 43.824 | 84.607 | 33 | 5.5 | 5.3 | NORTHERN XINJIANG, CHINA | 111000010 |
| 95123024952 | 28.440 | 52.744 | 33 | 4.7 | | SOUTHERN IRAN | 111000010 |
| 95124003412 | 40.673 | 23.466 | 28 | 5.1 | 5.1 | GREECE | 111000010 |
| 95124021851 | 1.857 | 128.488 | 55 | 6.0 | 6.0 | HALMAHERA | 111000010 |
| 95124160331 | 35.023 | 27.748 | 33 | 4.9 | 4.3 | DODECANESE ISLANDS | 111000010 |
| 95125035347 | 12.622 | 125.314 | 33 | 6.2 | 7.0 | SAMAR, PHILIPPINE ISLANDS | 111000010 |
| 95125091729 | 13.856 | 51.464 | 10 | 5.0 | 4.4 | EASTERN GULF OF ADEN | 111000010 |
| 95125130139 | -10.165 | 118.809 | 33 | 5.7 | 5.4 | SOUTH OF SUMBAWA ISLAND | 111000010 |
| 95125224805 | -18.465 | 168.681 | 123 | 5.8 | | VANUATU ISLANDS | 111000010 |
| 95126015907 | 25.007 | 95.335 | 122 | 6.4 | | BURMA-INDIA BORDER REGION | 111000010 |
| 95128174025 | 43.884 | 148.413 | 34 | 5.7 | 5.2 | KURIL ISLANDS REGION | 111000010 |
| 95129011437 | 40.820 | 20.664 | 10 | 4.8 | 4.2 | GREECE-ALBANIA BORDER REGION | 111000010 |
| 95129095420 | 25.260 | 95.136 | 92 | 5.2 | | BURMA-INDIA BORDER REGION | 111000010 |
| 95133072041 | 40.750 | 50.635 | 33 | 4.8 | | CASPIAN SEA | 111000010 |
| 95133084712 | 40.144 | 21.684 | 13 | 6.2 | 6.5 | GREECE | 111000010 |
| 95133105834 | 40.058 | 21.552 | 10 | 4.9 | | GREECE | 111000010 |
| 95133114328 | 40.138 | 21.644 | 10 | 5.0 | | GREECE | 111000010 |
| 95133210054 | -5.215 | 108.917 | 554 | 5.7 | | JAVA SEA | 111000010 |
| 95134024658 | 40.138 | 21.540 | 10 | 4.7 | | GREECE | 111000010 |
| 95134044701 | 40.124 | 70.691 | 33 | 4.8 | 4.0 | TAJIK SSR | 111000010 |
| 95134113321 | -8.396 | 125.083 | 33 | 6.1 | 6.9 | TIMOR | 111000010 |
| 95134223347 | 39.957 | 77.610 | 33 | 5.0 | 4.3 | SOUTHERN XINJIANG, CHINA | 111000010 |
| 95135001652 | 38.407 | 49.390 | 27 | 4.8 | | CASPIAN SEA | 111000010 |
| 95135040558 | 41.665 | 88.821 | 0 | 6.1 | | SOUTHERN XINJIANG, CHINA | 111000010 |
| 95135041355 | 40.047 | 21.619 | 10 | 5.1 | | GREECE | 111000010 |
| 95135152654 | -56.061 | -27.770 | 100 | 5.4 | | SOUTH SANDWICH ISLANDS REGION | 111000000 |
| 95135202149 | 13.126 | 49.523 | 10 | 4.9 | | EASTERN GULF OF ADEN | 111000000 |
| 95136033503 | 36.485 | 70.896 | 190 | 5.7 | | HINDU KUSH REGION | 111000000 |
| 95136201245 | -23.014 | 169.893 | 33 | 6.8 | 7.7 | LOYALTY ISLANDS REGION | 111000000 |
| 95136214808 | 17.800 | 96.550 | 33 | 5.8 | | BURMA | 111000000 |
| 95136230040 | 40.034 | 21.574 | 10 | 4.8 | | GREECE | 111000000 |
| 95137022929 | -6.290 | 147.398 | 71 | 5.6 | | EAST PAPUA NEW GUINEA REGION | 111000000 |
| 95137041424 | 40.160 | 21.597 | 10 | 5.3 | 5.0 | GREECE | 111000000 |
| 95137094507 | 39.998 | 21.536 | 10 | 5.0 | 4.7 | GREECE | 111000000 |

Appendix 1 (continued)

| EventID | Lat | Lon | Z | Mb | Ms | Location | Key 123456789 |
|---|---|---|---|---|---|---|---|
| 95137112351 | -23.028 | 170.079 | 33 | 5.7 | 6.5 | LOYALTY ISLANDS REGION | 111000000 |
| 95138000626 | -0.950 | -21.985 | 10 | 6.2 | 6.1 | CENTRAL MID-ATLANTIC RIDGE | 111000000 |
| 95138143114 | 44.324 | 147.581 | 104 | 5.7 | | KURIL ISLANDS | 111000000 |
| 95139064849 | 40.043 | 21.580 | 10 | 5.1 | 5.0 | GREECE | 111000000 |
| 95139214451 | 39.996 | 21.595 | 10 | 4.6 | | GREECE | 111000000 |
| 95140134502 | -56.009 | -27.727 | 100 | 5.5 | | SOUTH SANDWICH ISLANDS REGION | 111000000 |
| 95142034504 | -22.771 | 169.931 | 33 | 5.8 | 6.1 | LOYALTY ISLANDS REGION | 111000000 |
| 95142040255 | -9.683 | 151.475 | 33 | 5.7 | 6.1 | DENTRECASTEAUX ISLANDS REGION | 111000000 |
| 95143221011 | -56.097 | -3.150 | 10 | 5.3 | 6.6 | SOUTH ATLANTIC RIDGE | 111000010 |
| 95144202125 | 12.204 | 125.707 | 33 | 5.4 | 5.7 | SAMAR, PHILIPPINE ISLANDS | 111000010 |
| 95146031110 | 12.134 | 57.931 | 10 | 5.3 | 5.4 | ARABIAN SEA | 111000010 |
| 95147130355 | 52.563 | 142.814 | 33 | 6.6 | 7.6 | SAKHALIN ISLAND | 111000010 |
| 95147201529 | -19.694 | 168.985 | 33 | 5.6 | 4.8 | VANUATU ISLANDS | 111000010 |
| 95147212128 | 39.041 | 49.056 | 10 | 4.7 | | CASPIAN SEA | 111000010 |
| 95148195912 | -29.048 | -71.098 | 42 | 5.6 | 5.1 | NEAR COAST OF CENTRAL CHILE | 101000010 |
| 95149140232 | 32.352 | 141.601 | 33 | 5.1 | 4.6 | SOUTH OF HONSHU, JAPAN | 110001000 |
| 95149072946 | -10.144 | 163.734 | 33 | 5.8 | 6.4 | SOLOMON ISLANDS | 010001000 |
| 95151135120 | 30.204 | 67.933 | 33 | 5.3 | 4.9 | PAKISTAN | 111001000 |
| 95151160840 | 18.949 | -107.434 | 33 | 5.4 | 6.1 | OFF COAST OF JALISCO, MEXICO | 111001000 |
| 95151204411 | 28.194 | 53.264 | 33 | 5.0 | 4.0 | SOUTHERN IRAN | 111001000 |
| 95153232906 | 3.289 | 96.358 | 33 | 5.0 | | NORTHERN SUMATERA | 111001000 |
| 95154115731 | 2.977 | 96.210 | 30 | 5.2 | 4.6 | NORTHERN SUMATERA | 111001000 |
| 95154200832 | 35.848 | 53.049 | 33 | 4.0 | | IRAN | 111001000 |
| 95156202017 | 18.402 | 120.858 | 47 | 5.4 | 5.4 | LUZON, PHILIPPINE ISLANDS | 111001000 |
| 95157000304 | 26.568 | 67.167 | 33 | 4.6 | 4.2 | PAKISTAN | 111001000 |
| 95158005347 | 51.325 | -179.326 | 30 | 5.2 | 4.7 | ANDREANOF ISLANDS, ALEUTIAN IS. | 111001000 |
| 95158230947 | 32.504 | 48.745 | 33 | 5.0 | 4.4 | WESTERN IRAN | 111001000 |
| 95162192050 | 11.711 | 125.867 | 33 | 5.0 | 5.4 | SAMAR, PHILIPPINE ISLANDS | 111001000 |
| 95162215549 | 32.556 | 69.618 | 33 | 5.1 | 5.6 | PAKISTAN | 111001000 |
| 95163033548 | -8.308 | -75.913 | 34 | 5.7 | 5.0 | PERU | 111001000 |
| 95163144759 | 39.169 | 95.365 | 33 | 5.2 | 4.5 | GANSU PROVINCE, CHINA | 111001000 |
| 95165054233 | 36.286 | 58.515 | 33 | 4.4 | 4.1 | IRAN | 111001000 |
| 95165111149 | 12.204 | -88.349 | 39 | 5.6 | 6.0 | OFF COAST OF CENTRAL AMERICA | 111001000 |
| 95165121159 | 42.388 | 21.421 | 10 | 5.1 | | YUGOSLAVIA | 111001000 |
| 95166001548 | 38.401 | 22.269 | 14 | 6.0 | 6.5 | GREECE | 111001000 |
| 95166003100 | 38.395 | 22.430 | 10 | 5.3 | 6.0 | GREECE | 111001000 |
| 95166183729 | 38.668 | 69.964 | 33 | 4.6 | | TAJIK SSR | 111001001 |
| 95168013711 | -8.255 | 123.020 | 38 | 5.2 | 5.4 | FLORES ISLAND REGION | 111001001 |
| 95170005744 | 44.031 | 150.473 | 33 | 5.3 | 4.8 | KURIL ISLANDS REGION | 111001001 |
| 95172152851 | -61.621 | 154.714 | 10 | 5.6 | 6.7 | BALLENY ISLANDS REGION | 111001001 |
| 95172163305 | -11.546 | -77.564 | 70 | 5.5 | | NEAR COAST OF PERU | 111001001 |
| 95173010121 | 50.325 | 89.915 | 33 | 5.5 | 5.3 | USSR-MONGOLIA BORDER REGION | 111001001 |
| 95175065806 | -3.979 | 153.945 | 386 | 6.2 | | NEW IRELAND REGION | 011001001 |
| 95176021041 | -3.281 | 150.365 | 45 | 5.5 | 6.3 | NEW IRELAND REGION | 011001001 |
| 95176065905 | 24.599 | 121.713 | 47 | 5.8 | 5.7 | TAIWAN | 011001001 |
| 95177034142 | -55.361 | -27.843 | 33 | 5.4 | 5.1 | SOUTH SANDWICH ISLANDS REGION | 111001001 |
| 95177211255 | 36.327 | 51.060 | 33 | 4.1 | | IRAN | 111001001 |
| 95177212649 | 7.106 | -34.331 | 10 | 4.9 | 5.3 | CENTRAL MID-ATLANTIC RIDGE | 111001001 |
| 95177232735 | 39.852 | 48.310 | 33 | 4.4 | | N.W. IRAN-USSR BORDER REGION | 111001001 |
| 95178004642 | 39.837 | 48.324 | 33 | 4.5 | | N.W. IRAN-USSR BORDER REGION | 111001001 |
| 95178040929 | -55.365 | -27.980 | 33 | 5.3 | 5.2 | SOUTH SANDWICH ISLANDS REGION | 111001001 |
| 95178100958 | 18.847 | -81.730 | 10 | 5.7 | 5.6 | CARIBBEAN SEA | 111001001 |
| 95178211256 | -17.228 | 66.829 | 10 | 5.0 | 6.3 | MASCARENE ISLANDS REGION | 111001001 |
| 95179211449 | -1.617 | 127.365 | 33 | 5.6 | 5.4 | HALMAHERA | 111001001 |
| 95180074509 | 48.784 | 154.459 | 62 | 5.9 | | KURIL ISLANDS | 111001001 |
| 95180122403 | -19.464 | 169.241 | 144 | 6.2 | | VANUATU ISLANDS | 111001001 |
| 95180230231 | 51.923 | 103.075 | 33 | 5.6 | 5.5 | LAKE BAIKAL REGION | 111001001 |
| 95181115856 | 24.621 | -110.264 | 10 | 5.8 | 6.3 | BAJA CALIFORNIA | 111001001 |
| 95182041055 | 12.942 | 57.468 | 10 | 5.2 | | ARABIAN SEA | 111001001 |
| 95182235744 | -55.516 | -27.819 | 33 | 5.2 | 5.2 | SOUTH SANDWICH ISLANDS REGION | 111001001 |

Appendix 1 (continued)

| EventID | Lat | Lon | Z | Mb | Ms | Location | Key 123456789 |
|---|---|---|---|---|---|---|---|
| 95184195050 | -29.198 | -177.612 | 33 | 6.5 | 7.2 | KERMADEC ISLANDS | 111001001 |
| 95184215651 | -29.052 | -177.676 | 55 | 6.0 | | KERMADEC ISLANDS | 111001001 |
| 95188104004 | -53.561 | 9.186 | 10 | 5.4 | 5.2 | SOUTHWEST OF AFRICA | 111001001 |
| 95188211518 | 33.947 | 137.122 | 324 | 5.8 | | NEAR S. COAST OF HONSHU, JAPAN | 111001001 |
| 95189054256 | 39.640 | 143.353 | 40 | 5.7 | 5.5 | OFF EAST COAST OF HONSHU, JAPAN | 111001001 |
| 95189113905 | 4.329 | 62.417 | 10 | 5.5 | 5.1 | CARLSBERG RIDGE | 111001001 |
| 95189171528 | 53.646 | -163.546 | 33 | 5.8 | 5.7 | UNIMAK ISLAND REGION | 111001001 |
| 95189234947 | -24.153 | -176.478 | 51 | 5.7 | | SOUTH OF FIJI ISLANDS | 111001001 |
| 95190022945 | 37.330 | 71.823 | 121 | 5.0 | | AFGHANISTAN-USSR BORDER REGION | 111001001 |
| 95190203131 | 22.003 | 99.196 | 12 | 5.7 | 5.9 | BURMA-CHINA BORDER REGION | 111001001 |
| 95191024232 | 12.399 | 141.651 | 55 | 5.2 | 4.9 | SOUTH OF MARIANA ISLANDS | 111001001 |
| 95192214639 | 21.933 | 99.162 | 13 | 6.1 | 7.2 | BURMA-CHINA BORDER REGION | 111001001 |
| 95193154659 | -23.237 | 170.824 | 33 | 5.9 | 6.4 | LOYALTY ISLANDS REGION | 111001001 |
| 95193183849 | 12.316 | 125.037 | 33 | 5.8 | 5.6 | SAMAR, PHILIPPINE ISLANDS | 111001001 |
| 95194000023 | -23.308 | 170.636 | 33 | 5.6 | 5.7 | LOYALTY ISLANDS REGION | 111001001 |
| 95195140307 | 42.818 | 48.825 | 33 | 4.2 | | CASPIAN SEA | 111001001 |
| 95198231815 | 40.265 | 21.404 | 10 | 5.3 | 4.8 | GREECE | 111001001 |
| 95199143545 | -3.855 | 135.293 | 33 | 5.4 | 5.7 | WEST IRIAN REGION | 111001001 |
| 95200002417 | -22.685 | 169.736 | 32 | 5.8 | 5.6 | LOYALTY ISLANDS REGION | 111001001 |
| 95202224407 | 36.443 | 103.105 | 33 | 5.7 | 5.4 | GANSU PROVINCE, CHINA | 111001001 |
| 95205191321 | 55.597 | -35.059 | 10 | 5.4 | 5.2 | NORTH ATLANTIC OCEAN | 111000001 |
| 95206151326 | 10.694 | -41.211 | 10 | 5.4 | 5.5 | NORTH ATLANTIC RIDGE | 111000001 |
| 95206223923 | 44.120 | 148.446 | 33 | 5.5 | 4.7 | KURIL ISLANDS | 111000001 |
| 95207234202 | 2.562 | 127.692 | 66 | 5.9 | | MOLUCCA PASSAGE | 111000001 |
| 95208055117 | -12.578 | 79.237 | 10 | 6.2 | 5.9 | SOUTH INDIAN OCEAN | 111000001 |
| 95209142912 | -21.097 | -175.485 | 102 | 6.1 | | TONGA ISLANDS | 111000001 |
| 95210080125 | 4.210 | 126.698 | 51 | 5.5 | 5.3 | TALAUD ISLANDS | 111000001 |
| 95211051123 | -23.364 | -70.312 | 47 | 6.6 | 7.3 | NEAR COAST OF NORTHERN CHILE | 111000001 |
| 95211210550 | -23.317 | -70.590 | 33 | 5.6 | 5.6 | NEAR COAST OF NORTHERN CHILE | 111000001 |
| 95213021039 | 46.342 | 153.903 | 33 | 5.6 | 4.7 | KURIL ISLANDS | 111000001 |
| 95214001409 | -23.152 | -70.578 | 33 | 5.4 | 5.5 | NEAR COAST OF NORTHERN CHILE | 111000001 |
| 95214110539 | -23.100 | -70.405 | 33 | 5.2 | 5.1 | NEAR COAST OF NORTHERN CHILE | 111000001 |
| 95215015721 | -23.132 | -70.602 | 33 | 5.4 | 5.9 | NEAR COAST OF NORTHERN CHILE | 111000001 |
| 95215081853 | -28.346 | -69.198 | 104 | 5.9 | | CHILE-ARGENTINA BORDER REGION | 111000001 |
| 95219194424 | 4.081 | 143.680 | 10 | 5.5 | 5.7 | CAROLINE ISLANDS REGION | 111000001 |
| 95220003524 | 11.780 | 125.791 | 33 | 5.3 | 5.0 | SAMAR, PHILIPPINE ISLANDS | 111000001 |
| 95226043717 | -4.827 | 151.507 | 126 | 6.3 | 6.3 | NEW BRITAIN REGION | 111000001 |
| 95228102726 | -5.809 | 154.212 | 16 | 6.4 | 7.8 | SOLOMON ISLANDS | 111000001 |
| 95228162426 | -5.418 | 153.765 | 21 | 5.6 | 6.8 | NEW IRELAND REGION | 111000001 |
| 95228231028 | -5.782 | 154.256 | 74 | 6.1 | 7.2 | SOLOMON ISLANDS | 111000001 |
| 95229005957 | 41.587 | 88.782 | 0 | 6.0 | | SOUTHERN XINJIANG, CHINA | 111000001 |
| 95229100127 | -5.176 | 153.404 | 33 | 5.5 | 6.4 | NEW IRELAND REGION | 111000001 |
| 95229231419 | 36.465 | 71.156 | 239 | 5.4 | | AFGHANISTAN-USSR BORDER REGION | 111000001 |
| 95230021626 | -55.898 | -28.901 | 36 | 5.6 | 5.8 | SOUTH SANDWICH ISLANDS REGION | 111000001 |
| 95231214332 | 5.096 | -75.690 | 125 | 6.1 | | COLOMBIA | 001000001 |

Prof. Thomas Ahrens
Seismological Lab, 252-21
Division of Geological & Planetary Sciences
California Institute of Technology
Pasadena, CA 91125

Prof. Keiiti Aki
Center for Earth Sciences
University of Southern California
University Park
Los Angeles, CA 90089-0741

Prof. Shelton Alexander
Geosciences Department
403 Deike Building
The Pennsylvania State University
University Park, PA 16802

Prof. Charles B. Archambeau
University of Colorado
JSPC
Campus Box 583
Boulder, CO 80309

Dr. Thomas C. Bache, Jr.
Science Applications Int'l Corp.
10260 Campus Point Drive
San Diego, CA 92121 (2 copies)

Prof. Muawia Barazangi
Cornell University
Institute for the Study of the Continent
3126 SNEE Hall
Ithaca, NY 14853

Dr. Jeff Barker
Department of Geological Sciences
State University of New York
at Binghamton
Vestal, NY 13901

Dr. Douglas R. Baumgardt
ENSCO, Inc
5400 Port Royal Road
Springfield, VA 22151-2388

Dr. Susan Beck
Department of Geosciences
Building #77
University of Arizona
Tuscon, AZ 85721

Dr. T.J. Bennett
S-CUBED
A Division of Maxwell Laboratories
11800 Sunrise Valley Drive, Suite 1212
Reston, VA 22091

Dr. Robert Blandford
AFTAC/TT, Center for Seismic Studies
1300 North 17th Street
Suite 1450
Arlington, VA 22209-2308

Dr. Stephen Bratt
ARPA/NMRO
3701 North Fairfax Drive
Arlington, VA 22203-1714

Dale Breding
U.S. Department of Energy
Recipient, IS-20, GA-033
Office of Arms Control
Washington, DC 20585

Dr. Lawrence Burdick
C/O Barbara Wold
Dept of Biology
CA Inst. of Technology
Pasadena, CA 91125

Dr. Robert Burridge
Schlumberger-Doll Research Center
Old Quarry Road
Ridgefield, CT 06877

Dr. Jerry Carter
Center for Seismic Studies
1300 North 17th Street
Suite 1450
Arlington, VA 22209-2308

Dr. Martin Chapman
Department of Geological Sciences
Virginia Polytechnical Institute
21044 Derring Hall
Blacksburg, VA 24061

Mr Robert Cockerham
Arms Control & Disarmament Agency
320 21st Street North West
Room 5741
Washington, DC 20451,

Prof. Vernon F. Cormier
Department of Geology & Geophysics
U-45, Room 207
University of Connecticut
Storrs, CT 06268

Prof. Steven Day
Department of Geological Sciences
San Diego State University
San Diego, CA 92182

Dr. Zoltan Der
ENSCO, Inc.
5400 Port Royal Road
Springfield, VA 22151-2388

Dr. Stanley K. Dickinson
AFOSR/NM
110 Duncan Avenue
Suite B115
Bolling AFB, DC 20332-6448

Prof. Adam Dziewonski
Hoffman Laboratory, Harvard University
Dept. of Earth Atmos. & Planetary Sciences
20 Oxford Street
Cambridge, MA 02138

Prof. John Ebel
Department of Geology & Geophysics
Boston College
Chestnut Hill, MA 02167

Dr. Petr Firbas
Institute of Physics of the Earth
Masaryk University Brno
Jecna 29a
612 46 Brno, Czech Republic

Dr. Mark D. Fisk
Mission Research Corporation
735 State Street
P.O. Drawer 719
Santa Barbara, CA 93102

Prof. Donald Forsyth
Department of Geological Sciences
Brown University
Providence, RI 02912

Dr. Cliff Frolich
Institute of Geophysics
8701 North Mopac
Austin, TX 78759

Dr. Holly Given
IGPP, A-025
Scripps Institute of Oceanography
University of California, San Diego
La Jolla, CA 92093

Dr. Jeffrey W. Given
SAIC
10260 Campus Point Drive
San Diego, CA 92121

Dr. Indra N. Gupta
Multimax, Inc.
1441 McCormick Drive
Landover, MD 20785

Dan N. Hagedon
Pacific Northwest Laboratories
Battelle Boulevard
Richland, WA 99352

Dr. James Hannon
Lawrence Livermore National Laboratory
P.O. Box 808, L-205
Livermore, CA 94550

Prof. Danny Harvey
University of Colorado, JSPC
Campus Box 583
Boulder, CO 80309

Prof. Donald V. Helmberger
Division of Geological & Planetary Sciences
California Institute of Technology
Pasadena, CA 91125

Prof. Eugene Herrin
Geophysical Laboratory
Southern Methodist University
Dallas, TX 75275

Prof. Robert B. Herrmann
Department of Earth & Atmospheric Sciences
St. Louis University
St. Louis, MO 63156

Prof. Lane R. Johnson
Seismographic Station
University of California
Berkeley, CA 94720

Prof. Thomas H. Jordan
Department of Earth, Atmospheric &
Planetary Sciences
Massachusetts Institute of Technology
Cambridge, MA 02139

Prof. Alan Kafka
Department of Geology & Geophysics
Boston College
Chestnut Hill, MA 02167

U.S. Dept of Energy
Max Koontz, NN-20, GA-033
Office of Research and Develop.
1000 Independence Avenue
Washington, DC 20585

Dr. Richard LaCoss
MIT Lincoln Laboratory, M-200B
P.O. Box 73
Lexington, MA 02173-0073

Dr. Fred K. Lamb
University of Illinois at Urbana-Champaign
Department of Physics
1110 West Green Street
Urbana, IL 61801

Prof. Charles A. Langston
Geosciences Department
403 Deike Building
The Pennsylvania State University
University Park, PA 16802

Jim Lawson, Chief Geophysicist
Oklahoma Geological Survey
Oklahoma Geophysical Observatory
P.O. Box 8
Leonard, OK 74043-0008

Prof. Thorne Lay
Institute of Tectonics
Earth Science Board
University of California, Santa Cruz
Santa Cruz, CA 95064

Dr. William Leith
U.S. Geological Survey
Mail Stop 928
Reston, VA 22092

Mr. James F. Lewkowicz
Phillips Laboratory/GPE
29 Randolph Road
Hanscom AFB, MA 01731-3010( 2 copies)

Prof. L. Timothy Long
School of Geophysical Sciences
Georgia Institute of Technology
Atlanta, GA 30332

Dr. Randolph Martin, III
New England Research, Inc.
76 Olcott Drive
White River Junction, VT 05001

Dr. Robert Masse
Denver Federal Building
Box 25046, Mail Stop 967
Denver, CO 80225

Dr. Gary McCartor
Department of Physics
Southern Methodist University
Dallas, TX 75275

Prof. Thomas V. McEvilly
Seismographic Station
University of California
Berkeley, CA 94720

Dr. Art McGarr
U.S. Geological Survey
Mail Stop 977
U.S. Geological Survey
Menlo Park, CA 94025

Dr. Keith L. McLaughlin
S-CUBED
A Division of Maxwell Laboratory
P.O. Box 1620
La Jolla, CA 92038-1620

Stephen Miller & Dr. Alexander Florence
SRI International
333 Ravenswood Avenue
Box AF 116
Menlo Park, CA 94025-3493

Prof. Bernard Minster
IGPP, A-025
Scripps Institute of Oceanography
University of California, San Diego
La Jolla, CA 92093

Prof. Brian J. Mitchell
Department of Earth & Atmospheric Sciences
St. Louis University
St. Louis, MO 63156

Mr. Richard J. Morrow
USACDA/IVI
320 21st St. N.W.
Washington , DC 20451

Mr. Jack Murphy
S-CUBED
A Division of Maxwell Laboratory
11800 Sunrise Valley Drive, Suite 1212
Reston, VA 22091 (2 Copies)

Dr. Keith K. Nakanishi
Lawrence Livermore National Laboratory
L-025
P.O. Box 808
Livermore, CA 94550

Prof. John A. Orcutt
IGPP, A-025
Scripps Institute of Oceanography
University of California, San Diego
La Jolla, CA 92093

Prof. Jeffrey Park
Kline Geology Laboratory
P.O. Box 6666
New Haven, CT 06511-8130

Dr. Howard Patton
Lawrence Livermore National Laboratory
L-025
P.O. Box 808
Livermore, CA 94550

Dr. Frank Pilotte
HQ AFTAC/TT
1030 South Highway A1A
Patrick AFB, FL 32925-3002

Dr. Jay J. Pulli
Radix Systems, Inc.
6 Taft Court
Rockville, MD 20850

Dr. Robert Reinke
ATTN: FCTVTD
Field Command
Defense Nuclear Agency
Kirtland AFB, NM 87115

Prof. Paul G. Richards
Lamont-Doherty Earth Observatory
of Columbia University
Palisades, NY 10964

Mr. Wilmer Rivers
Teledyne Geotech
1300 17th St N #1450
Arlington, VA 22209-3803

Dr. Alan S. Ryall, Jr.
Lawrence Livermore National Laboratory
P.O. Box 808, L-205
Livermore, CA 94550

Dr.Chandan K. Saikia
Woodward Clyde- Consultants
566 El Dorado Street
Pasadena, CA 91101

Dr. Richard Sailor
TASC, Inc.
55 Walkers Brook Drive
Reading, MA 01867

Prof. Charles G. Sammis
Center for Earth Sciences
University of Southern California
University Park
Los Angeles, CA 90089-0741

Prof. Christopher H. Scholz
Lamont-Doherty Earth Observatory
of Columbia University
Palisades, NY 10964

Dr. Susan Schwartz
Institute of Tectonics
1156 High Street
Santa Cruz, CA 95064

Mr. Dogan Seber
Cornell University
Inst. for the Study of the Continent
3130 SNEE Hall
Ithaca, NY 14853-1504

Secretary of the Air Force
(SAFRD)
Washington, DC 20330

Office of the Secretary of Defense
DDR&E
Washington, DC 20330

Thomas J. Sereno, Jr.
Science Application Int'l Corp.
10260 Campus Point Drive
San Diego, CA 92121

Dr. Michael Shore
Defense Nuclear Agency/SPSS
6801 Telegraph Road
Alexandria, VA 22310

Dr. Robert Shumway
University of California Davis
Division of Statistics
Davis, CA 95616

Dr. Matthew Sibol
Virginia Tech
Seismological Observatory
4044 Derring Hall
Blacksburg, VA 24061-0420

Prof. David G. Simpson
IRIS, Inc.
1616 North Fort Myer Drive
Suite 1050
Arlington, VA 22209

Donald L. Springer
Lawrence Livermore National Laboratory
L-025
P.O. Box 808
Livermore, CA 94550

Dr. Jeffrey Stevens
S-CUBED
A Division of Maxwell Laboratory
P.O. Box 1620
La Jolla, CA 92038-1620

Prof. Brian Stump
Los Alamos National Laboratory
EES-3
Mail Stop C-335
Los Alamos, NM 87545

Prof. Jeremiah Sullivan
University of Illinois at Urbana-Champaign
Department of Physics
1110 West Green Street
Urbana, IL 61801

Prof. L. Sykes
Lamont-Doherty Earth Observatory
of Columbia University
Palisades, NY 10964

Dr. Steven R. Taylor
Los Alamos National Laboratory
P.O. Box 1663
Mail Stop C335
Los Alamos, NM 87545

Prof. Tuncay Taymaz
Istanbul Technical University
Dept. of Geophysical Engineering
Mining Faculty
Maslak-80626, Istanbul Turkey

Prof. Clifford Thurber
University of Wisconsin-Madison
Department of Geology & Geophysics
1215 West Dayton Street
Madison, WS 53706

Prof. M. Nafi Toksoz
Earth Resources Lab
Massachusetts Institute of Technology
42 Carleton Street
Cambridge, MA 02142

Dr. Larry Turnbull
CIA-OSWR/NED
Washington, DC 20505

Dr. Gregory van der Vink
IRIS, Inc.
1616 North Fort Myer Drive
Suite 1050
Arlington, VA 22209

Dr. Karl Veith
EG&G
2341 Jefferson Davis Highway
Suite 801
Arlington, VA 22202-3809

Prof. Terry C. Wallace
Department of Geosciences
Building #77
University of Arizona
Tuscon, AZ 85721

Dr. Thomas Weaver
Los Alamos National Laboratory
P.O. Box 1663
Mail Stop C335
Los Alamos, NM 87545

Dr. William Wortman
Mission Research Corporation
8560 Cinderbed Road
Suite 700
Newington, VA 22122

Prof. Francis T. Wu
Department of Geological Sciences
State University of New York
at Binghamton
Vestal, NY 13901

Prof Ru-Shan Wu
University of California, Santa Cruz
Earth Sciences Department
Santa Cruz, CA 95064

ARPA, OASB/Library
3701 North Fairfax Drive
Arlington, VA 22203-1714

HQ DNA
ATTN: Technical Library
Washington, DC 20305

TACTEC
Battelle Memorial Institute
505 King Avenue
Columbus, OH 43201 (Final Report)

Phillips Laboratory
ATTN: XPG
29 Randolph Road
Hanscom AFB, MA 01731-3010

Phillips Laboratory
ATTN: GPE
29 Randolph Road
Hanscom AFB, MA 01731-3010

Phillips Laboratory
ATTN: TSML
5 Wright Street
Hanscom AFB, MA 01731-3004

Phillips Laboratory
ATTN: PL/SUL
3550 Aberdeen Ave SE
Kirtland, NM 87117-5776 (2 copies)

Dr. Michel Bouchon
I.R.I.G.M.-B.P. 68
38402 St. Martin D'Heres
Cedex, FRANCE

Dr. Michel Campillo
Observatoire de Grenoble
I.R.I.G.M.-B.P. 53
38041 Grenoble, FRANCE

Prof. Hans-Peter Harjes
Institute for Geophysic
Ruhr University/Bochum
P.O. Box 102148
4630 Bochum 1, GERMANY

Prof. Eystein Husebye
IFJF
Jordskjelvstasjonen
Allegaten, 5007 BERGEN NORWAY

David Jepsen
Acting Head, Nuclear Monitoring Section
Bureau of Mineral Resources
Geology and Geophysics
G.P.O. Box 378, Canberra, AUSTRALIA

Ms. Eva Johannisson
Senior Research Officer
FOA
S-172 90 Sundbyberg, SWEDEN

Dr. Peter Marshall
Procurement Executive
Ministry of Defense
Blacknest, Brimpton
Reading FG7-FRS, UNITED KINGDOM

Dr. Bernard Massinon, Dr. Pierre Mechler
Societe Radiomana
27 rue Claude Bernard
75005 Paris, FRANCE (2 Copies)

Dr. Svein Mykkeltveit
NTNT/NORSAR
P.O. Box 51
N-2007 Kjeller, NORWAY (3 Copies)

Prof. Keith Priestley
University of Cambridge
Bullard Labs, Dept. of Earth Sciences
Madingley Rise, Madingley Road
Cambridge CB3 OEZ, ENGLAND

Dr. Jorg Schlittenhardt
Federal Institute for Geosciences & Nat'l Res.
Postfach 510153
D-30631 Hannover , GERMANY

Dr. Johannes Schweitzer
Institute of Geophysics
Ruhr University/Bochum
P.O. Box 1102148
4360 Bochum 1, GERMANY

Trust & Verify
VERTIC
Carrara House
20 Embankment Place
London WC2N 6NN, ENGLAND

Prof. Dr. M. Namik YALCIN
Dept. of Earth Sciences
P.O. Box 21,
41470
GEBZE-KOCAELI, TURKEY

Defense Technical Information Center
8725 John J. Kingman Road
Ft. Belvoir, VA 22060-6218 (2 copies)